Argonne National Laboratory

PHYSICS DIVISION
SUMMARY REPORT

Annual Review

1 April 1969—31 March 1970

Printed in the United States of America
Available from
Clearinghouse for Federal Scientific and Technical Information
National Bureau of Standards, U. S. Department of Commerce
Springfield, Virginia 22151
Price: Printed Copy $3.00; Microfiche $0.65

ANL-7728
Physics

ARGONNE NATIONAL LABORATORY
9700 South Cass Avenue
Argonne, Illinois 60439

PHYSICS DIVISION SUMMARY REPORT

Annual Review

1 April 1969—31 March 1970

Lowell M. Bollinger, Division Director

Preceding Summary Reports:

ANL-7641, April-September 1969
ANL-7698, October-December 1969
ANL-7699, January-March 1970

TABLE OF CONTENTS

I. EXPERIMENTAL NUCLEAR PHYSICS

INTRODUCTION

The over-all purpose of the program continues to be to obtain a much more complete understanding of the atomic nucleus. Consequently, most of the program consists of experimental and theoretical studies of the energies, quantum numbers, and lifetimes of nuclear energy levels and investigations of the mechanisms by which simple nuclear projectiles interact with nuclear targets. Experimenters and theorists work closely together so that new results in one area may suggest new approaches in another. An effort is made to stress work that can be done more advantageously at Argonne than elsewhere because of the special facilities available here. In view of the history and tradition of the Laboratory, it is natural that considerable emphasis is placed on studies of interactions between nuclei and neutrons; but this is balanced by a well diversified program of other nuclear investigations.

With a few exceptions, the program in experimental nuclear physics is most easily outlined by subdividing the work into various categories for which a major piece of equipment or an important experimental technique is the unifying factor. The current categories are:

(1) Studies of the neutron and of neutron-induced reactions at the reactor CP-5.
(2) Threshold photoneutron experiments at the electron Linac.
(3) Neutron and charged-particle reactions at the 4-MV Dynamitron.
(4) Charged-particle reactions at the tandem Van de Graaff accelerator.
(5) Charged-particle reactions at the 60-in. cyclotron.
(6) Various other nuclear experiments, including the γ- and β-ray spectroscopy of radioactive sources.

Some physicists restrict their efforts to the use of a single machine or technique, whereas others investigate related problems with several systems of apparatus.

A. RESEARCH AT THE REACTOR CP-5

The program of the Physics Division at the reactor CP-5 is devoted entirely to nuclear physics. The experiments now fall into two broad categories—experiments on the fundamental properties of the neutron and a variety of measurements with neutron-capture γ rays.

The experimental phase of the work at CP-5 was suspended early in 1969 because the reactor was shut down for extensive rehabilitation. Unfortunately, this long interruption of the experimental program will not result in a facility with greatly improved characteristics from the user's point of view, but the work was necessary to extend the life of the reactor. On the other hand, the shutdown has provided an opportunity to carry out several major improvements in the experimental systems at the reactor. These improvements are (1) a reworking of the thermal column used for coincidence and internal-conversion measurements on neutron-capture γ rays, (2) a refinement in the source-handling system of the bent-crystal spectrometer, and (3) the construction of a better neutron polarizer for fundamental experiments with neutrons.

During the period in which the reactor has been out of operation, the staff members involved in the research program have devoted their efforts to the developmental work outlined above and especially to the analysis of data collected earlier. When the reactor goes into operation again (expected in July 1970) the research program will be similar to that in the past, except for the absence of the fast chopper. The three experiments on fundamental properties of the neutron that were reported last year (asymmetries in the decay of polarized neutrons, parity violation in the strong interaction, and Delbrück scattering) are so important that they will be repeated under improved conditions. And neutron-capture γ-ray measurements will proceed with the highly developed and varied experimental systems at our disposal. The Argonne-developed average-resonance-capture method of nuclear spectroscopy is expected to play an increasingly important role in these spectroscopic studies.

1. FUNDAMENTAL EXPERIMENTS

a. Measurement of Spatial Asymmetries in the Decay of Polarized Neutrons

V. E. Krohn and G. R. Ringo

This experiment involves the measurement of three coefficients which are of importance to the theory of the weak interaction. The electron-asymmetry coefficient A leads to a value for G_A/G_V, the ratio of the beta-decay coupling constants. The neutrino-asymmetry coefficient B helps establish an upper limit on the coupling constants G_S and G_T. A nonzero result for the third coefficient D would indicate a violation of time-reversal invariance. More precise experimental measurements of any or all of these coefficients will provide more stringent tests of the theory of the weak interaction. This is particularly important because, in the case of neutron decay, the comparison of theory and experiment is free from the complications associated with nuclear structure. Hence the apparatus for this experiment is being rebuilt so that more precise data can be obtained when the reactor CP-5 resumes operation.

b. Search for Chemically Bound Neutrons

V. E. Krohn, G. J. Perlow, G. R. Ringo, and S. L. Ruby

During 1969 Grant and Cobble reported the very surprising and potentially important finding that thermal neutrons could be retained in a crystal in a "chemically bound" state for periods of minutes. This result was totally unexpected and inexplicable. In an attempt to confirm this result we used the Juggernaut reactor which provided neutron fluxes 10 to 1000 times the flux described in the report by Grant and Cobble. The results[1] showed no evidence for the reported effect, so no further work is planned.

[1] V. E. Krohn, G. J. Perlow, G. R. Ringo, and S. L. Ruby, Phys. Rev. Letters 23, 1475 (1969).

c. Parity Mixing in Nuclear States

R. E. Segel, E. L. Segel, J. V. Maher, and R. H. Siemssen

The experiment searching for the parity-violating alpha decay of the 8.87-MeV level in ^{16}N is a continuing one. Because the CP-5 reactor has been down during this period, no new data have been taken. The analysis of the data taken before the reactor shut down at the start of 1969 has been completed, and a tentative effect (which we consider to be an upper limit) has been found. It corresponds to an alpha width of 10^{-9} eV, which in turn corresponds to $F^2 \approx 2 \times 10^{-13}$. Several improvements are being made during this shutdown. A better procedure for depositing the ^{16}N source has been developed, and as a result it is expected that a truly carrier-free source will now be possible. Moreover, producing the activity in a gas containing fluorine will lead to a significantly greater yield. A new target chamber of a better design is being built. There will be two sources so that one can be counted while the other is being deposited. It is expected that the yield obtained with the new system will be at least an order of magnitude greater and that the quality of the spectra will be improved. We hope to be taking data shortly after the reactor starts operating again.

d. Elastic and Inelastic Scattering of Photons by Nuclei

H. E. Jackson and K. J. Wetzel

The scattering of 10.8-MeV photons by a range of nuclei is currently under study in a program of measurements using the internal-target facility of the CP-5 reactor. An external beam of photons is generated by means of the $^{14}N(n,\gamma)^{15}N$ reaction in an internal Melamine target. Radiation scattered from the beam by various external targets is detected in a Ge(Li) detector. In results already reported, Delbrück scattering (i.e., the scattering of photons by the nuclear Coulomb field) was detected and was found to agree

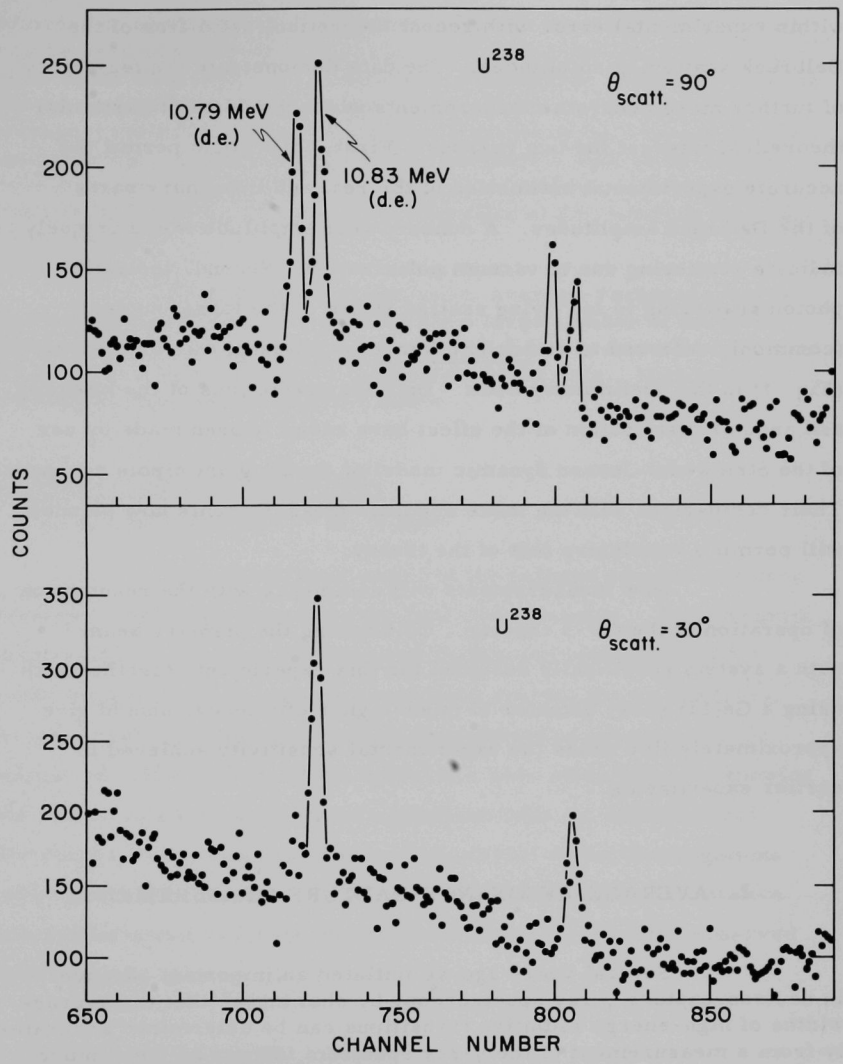

Fig. 1. Nuclear Raman scattering by ^{238}U. In these results for photons scattered from a beam of 10.8-MeV photons, the spectrum taken at $\theta = 30^{\circ}$ is dominated by strong elastic Delbrück scattering but at $\theta = 90^{\circ}$ an equally intense inelastic Raman peak corresponding to excitation of the 0.045-MeV level of ^{238}U is observed.

within experimental error with recent theoretical estimates of the Delbrück scattering amplitudes. The data demonstrate the feasibility of further more accurate measurements which would be of particular theoretical interest for two reasons. First, they would permit the accurate experimental estimation of the real and imaginary parts of the Delbrück amplitudes. A nonzero real amplitude would uniquely indicate scattering due to vacuum polarization. Second, inelastic photon scattering to low-lying excited states of the target nucleus (commonly referred to as nuclear Raman scattering) was also observed (Fig. 1) in the preliminary work. Detailed predictions of the intensity and angular distribution of the effect have recently been made by use of the Steinwedel-Jensen dynamic model of the E1 giant dipole resonance. Their comparison with the more accurate measurements now planned will permit a conclusive test of the theory.

New measurements will commence with the resumption of operation of the CP-5 reactor. Collimating the primary beam with a system specifically designed for this experiment, together with using a Ge(Li) γ-ray detector of much higher efficiency, should give approximately five times the experimental sensitivity achieved in earlier experiments.

2. AVERAGE-RESONANCE-CAPTURE MEASUREMENTS

Several years ago we initiated an important advance in neutron-capture γ-ray spectroscopy by showing[1,2] that the average widths of high-energy radiative transitions can be determined accurately from a measurement of the γ-ray spectrum formed by the capture of neutrons in a broad band of energy levels. The data obtained in this way are of interest from two points of view: (a) they provide

[1] L. M. Bollinger and G. E. Thomas, Phys. Rev. Letters 18, 1143 (1967).

[2] L. M. Bollinger and G. E. Thomas, Phys. Rev. Letters 21, 233 (1968).

information about the mechanisms of radiative capture,[1] and (b) they may be used to determine the parities and to set narrow limits on the spins of the final states.[2] A thorough investigation of its effectiveness and its applicability to a wide variety of nuclei has established the average-resonance-capture method as a standard technique of nuclear spectroscopy. This technique will be intensively applied to further measurements during 1970 in an effort to capitalize on the unique experimental system that has been developed at CP-5 during the past three years.

As was reported last year, average-resonance-capture measurements have been completed for a large number of nuclides. During the past year (while the reactor CP-5 has been out of operation) the effort has been devoted to an analysis of the data. Highlights of the results obtained are outlined below.

a. Model of the Capture Process

L. M. Bollinger and J. W. Tippie*

A mathematical model of the capture process has been developed and programmed for the IBM-360 computer. This program enables one to calculate the expected shapes and intensities of the γ-ray lines in average-resonance-capture spectra for an arbitrary target. Also, the expected random fluctuations in intensity can be calculated. The validity of the model has been established by showing that the calculations are in good agreement with the experimental line shapes and intensities observed in several of the investigations described in this section. Thus, the calculations allow quantitative information about radiation widths to be extracted from the observed spectra.

b. Radiative-Capture Mechanisms

L. M. Bollinger and G. E. Thomas

Although most of our effort during the past year has been devoted to the use of average-resonance-capture spectra to

---

*Applied Mathematics Division.

obtain spectroscopic information about final states, the data also provide some insight into the mechanisms responsible for radiative capture. The most important result of this kind is the general one that the average intensities of high-energy neutron-capture γ-ray transitions are a smooth function of γ-ray energy and that the random scatter in the intensities is determined principally by the Porter-Thomas distribution of partial radiation widths. These characteristics (established most quantitatively for transitions in ^{106}Pd, ^{156}Gd, ^{158}Gd, ^{166}Ho, ^{168}Er, and ^{196}Pt) suggest strongly that radiative capture in the typical heavy nucleus is a compound-nucleus reaction that is insensitive to the structure of the final state involved. This conclusion conflicts sharply with recently reported evidence (mainly obtained at the BNL fast chopper) that the structure of the final state does have an important effect on the intensity of high-energy neutron-capture γ rays.

The energy dependence of the average widths for E1 transitions in every nuclide studied is in qualitative agreement with what is expected from the giant-resonance model of the radiation process. That is, the width Γ_{ij} varies with γ-ray energy E_γ approximately as Γ_{ij}/E_γ^5, in contrast to the E_γ^3 dependence that results from phase-space considerations alone. This conclusion is likely to have a widespread influence on statistical calculations of γ-ray spectra.

c. States of ^{166}Ho

L. M. Bollinger and G. E. Thomas

The most extensive spectroscopic results obtained to date from average-resonance-capture measurements are those for ^{166}Ho. Although this nuclide had been intensively studied by other techniques, our measurements doubled the number of detected and identified states. These states have been analyzed in terms of a

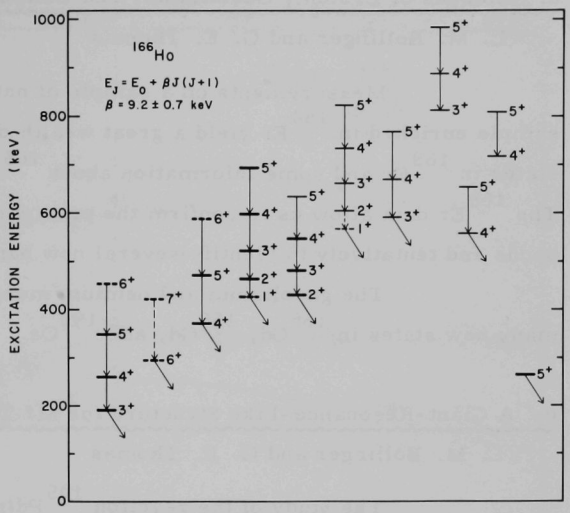

Fig. 2. Positive-parity rotational bands of ^{166}Ho. The states represented by heavy lines were observed and identified previously by Motz et al. (Ref. 1); the states represented by dashed lines are not populated by primary dipole (n, γ) transitions. The connecting vertical lines represent γ rays reported previously, and the diagonal lines identify states from which relatively strong transitions are observed.

rotational-band structure. All of the first 31 positive-parity states observed can be fitted into 11 rotational bands, and 5 bands involving negative-parity states were also identified—probably the largest number of rotational bands yet observed in a single nucleus. The positive-parity bands are shown in Fig. 2.

The energy differences of the states in the bands deduced from the average-resonance-capture data were compared with the low-energy γ rays reported previously.[1] The presence of the expected γ rays supports the validity of the band structure. This structure is well explained in terms of the collective model by assuming that ^{166}Ho consists of an odd neutron and odd proton that are independently coupled to a ^{164}Dy core. From the configuration assignments obtained in this way, we conclude that there is no significant difference in the average widths of radiative transitions to proton-excited and neutron-excited final states, in contradiction to the conclusion of Sheline et al.[2] that the transitions to proton-excited states are strongly inhibited.

[1] H. T. Motz et al., Phys. Rev. 155, 1265 (1967).

[2] R. K. Sheline et al., Phys. Rev. 143, 877 (1966).

d. Isotopes of Erbium, Gadolinium, and Osmium

L. M. Bollinger and G. E. Thomas

Measurements on a sample of natural erbium and a sample enriched in ^{164}Er yield a great wealth of information about states in ^{168}Er and some information about ^{165}Er, ^{167}Er, and ^{169}Er. The ^{168}Er data allow us to confirm the previously-reported rotational bands and tentatively to identify several new bands.

The gadolinium and osmium measurements reveal many new states in ^{165}Gd, ^{158}Gd, and ^{190}Os.

e. A Giant-Resonance-Like Structure for M1 Transitions

L. M. Bollinger and G. E. Thomas

The study of the reaction ^{105}Pd(n, γ)^{106}Pd has been completed. As was reported last year, this work demonstrated that the shape of the observed γ-ray lines depends greatly on the parity of the final state and hence that the parity can be determined from the observed shape. In this way the positive-parity states in ^{106}Pd were identified.

Since the literature contains almost no experimental information on the energy dependence of M1 transitions from highly excited states, the most interesting result from the study of ^{106}Pd is the finding that a plot of Γ_{M1}/E_γ^3 vs E_γ exhibits a giant-resonance-like peak at about 7.8 MeV. This is shown by the lower (dashed) curve of Fig. 3. The shape of the curve is similar to those calculated by Shapiro and Emery[1] from a two-quasiparticle model.

[1] C. S. Shapiro and G. T. Emery, Phys. Rev. Letters 23, 244 (1969).

f. Level Structures of ^{148}Sm and ^{150}Sm

D. J. Buss and R. K. Smither

The average-resonance-neutron-capture spectra of ^{147}Sm(n, γ)^{148}Sm and ^{149}Sm(n, γ)^{150}Sm obtained with the Argonne

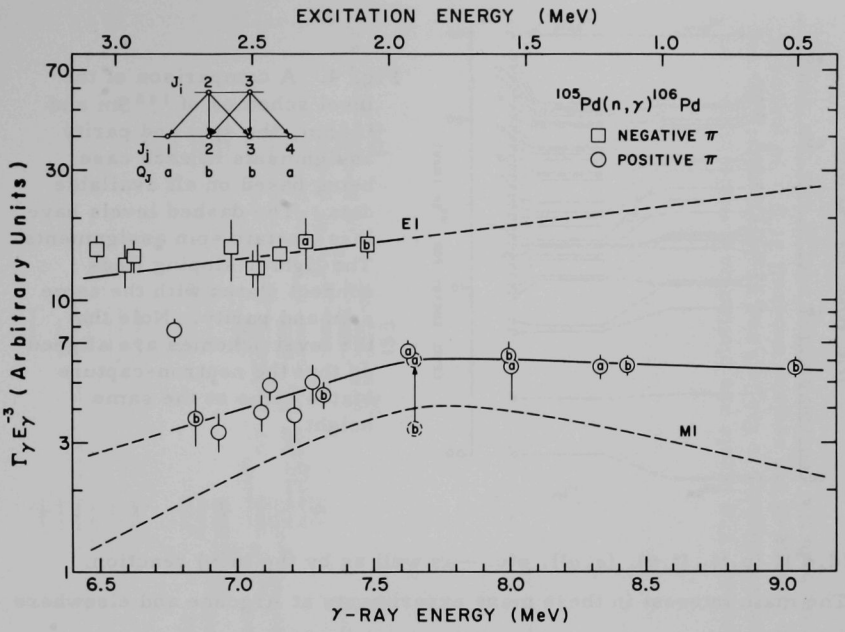

Fig. 3. Energy dependence of $\Gamma_\gamma E_\gamma^{-3}$ for the reaction $^{105}Pd(n,\gamma)^{106}Pd$. The letters a and b refer to states known to have J = 1 or 4 and J = 2 or 3, respectively. The indicated errors include both Porter-Thomas fluctuations and errors of measurement, and when no error bar is given it is smaller than the data point. The dashed line labeled M1 is a plot of $\Gamma_{M1} E_\gamma^{-3}$ vs E_γ.

in-pile (n, γ) facility have been used to develop and extend the level schemes of ^{148}Sm and ^{150}Sm. Information was obtained about the spin and parity assignments of 33 levels with excitation energies from 0 to 2.7 MeV in ^{148}Sm and 47 levels from 0 to 2.5 MeV in ^{150}Sm. Unique spin and parity assignments were given for almost all the states below 2.2 MeV in both isotopes. In many cases in which previous experiments gave conflicting indications, the new data led to definite spin assignments.

The level schemes of the even-N samarium isotopes (Fig. 4) have been investigated by many charged-particle reactions—(d, p)

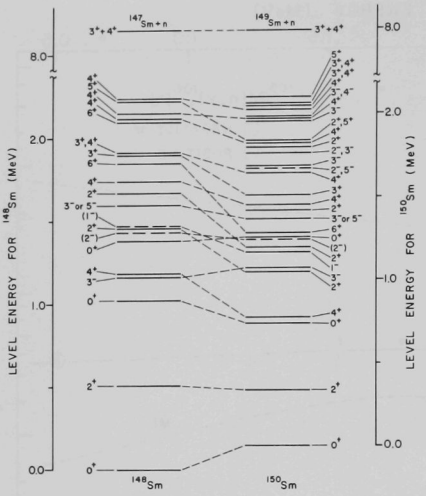

Fig. 4. A comparison of the level schemes of ^{148}Sm and ^{150}Sm, the spin and parity assignments in each case being based on all available data. The dashed levels have less-certain spin assignments. The lighter sloping lines connect states with the same spin and parity. Note that the level schemes are aligned so that the neutron-capture states come at the same height.

(d,d'), (p,t), (t,p), (α,α'), etc. —as well as by the (n,γ) reaction. The main interest in these many experiments at Argonne and elsewhere is in seeking to understand how the energy levels change in the transition region between the highly deformed nucleus ^{154}Sm (for which rotational features predominate) and the near-spherical nucleus ^{146}Sm (which has only two neutrons outside the closed neutron shell at N = 82). The character of the first few levels suggests that although the rotational level scheme becomes strongly distorted as the closed neutron shell is approached, the essential character of the levels does not. It will be interesting to see if this trend holds true for the higher excited states as well.

g. Energy Levels in the Odd-A Sm Isotopes

R. K. Smither, D. J. Buss, and D. L. Bushnell

The energy levels of the odd-A samarium isotopes (mass 145, 149, 151, 153, and 155) were investigated by use of the average-resonance-neutron-capture technique developed at Argonne.

Fig. 5. Energy levels in the odd-A samarium isotopes. The levels are plotted on a scale of neutron binding energies, with positive-parity states extended slightly to the left and negative-parity states to the right for easy identification. Note that the closing of the neutron subshell at N = 90 (between ^{151}Sm and ^{153}Sm) produces an interesting effect on both the neutron binding energy and the level structure.

This technique gives information about the spins and parities of levels that can be populated by primary (n, γ) transitions. When this information is combined with thermal (n, γ) data taken with Ge(Li) detectors and the Argonne bent-crystal spectrometer, unambiguous spin and parity assignments can be made for many of the energy levels in the odd-A isotopes, as seen in Fig. 5. The ground-state J^{π} values are: ^{145}Sm, $\frac{7}{2}^-$; ^{149}Sm, $\frac{7}{2}^-$, ^{151}Sm, $\frac{3}{2}^-$; ^{153}Sm, $\frac{3}{2}^+$; and ^{155}Sm, $\frac{3}{2}^-$. This removes the uncertainty with regard to the ^{151}Sm and ^{153}Sm isotopes. Of special interest is a new first excited state for ^{155}Sm at 6.6 keV with $J^{\pi} = \frac{1}{2}^-$ or $\frac{3}{2}^-$. Also, the negative-parity states appear to follow a consistent pattern from isotope to isotope. The neutron binding energies are found to be 6762.7, 5872.5, 5591.7, 5869.1, and 5814.2 keV for the isotopes of mass 145, 149, 151, 153, and 155, respectively. We plan to repeat the average-resonance-capture work with separated-isotope samples when the Argonne reactor begins operating later this year.

h. Level Schemes of ^{112}Cd and ^{114}Cd

R. K. Smither, D. J. Buss, and D. L. Bushnell

The average-resonance-neutron-capture technique is being used to make spin and parity assignments for the energy levels above 1.5 MeV in ^{112}Cd and in ^{114}Cd. Although the analysis is still in progress, the level scheme of ^{112}Cd is almost identical to that of ^{114}Cd for the levels below 3 MeV. The even-N cadmium isotopes have always attracted special interest from both experimenter and theorist because of special features of their level schemes (level spacings, enhanced E2 transitions, etc.) which strongly suggest a collective nature for their low-lying levels. The near-by tin isotopes, for example, also show some of these collective characteristics but to a much lesser degree. Further (n, γ) studies are planned when the Argonne reactor goes back to power. Ge(Li) detectors and the

bent-crystal spectrometer will be used in a detailed investigation of the gamma-ray branching ratios associated with the levels below 3 MeV. It will be interesting theoretically to see if the suggested similarities between the ^{112}Cd and ^{114}Cd level schemes are borne out by these γ-ray branching ratios.

3. THERMAL-NEUTRON-CAPTURE GAMMA RAYS

a. (n, γ) Studies with the Bent-Crystal Spectrometer and Ge-Diode Detector

(i) Modification of the Bent-Crystal Spectrometer

R. K. Smither, D. J. Buss, and D. L. Bushnell

A new thinner (1 mm) quartz crystal for the Argonne 7.7-m bent-crystal spectrometer is presently being cut and polished by Hilger and Watts of England. This new crystal, when bent and installed in the spectrometer, will double the energy resolution of the instrument. This is very important in the study of the (n, γ) spectrum for intermediate γ energies (0.4—2.0 MeV), where the spectra are extremely complex. The new crystal will also increase the sensitivity of the instrument at low γ energies ($E_\gamma < 30$ keV) by reducing the absorption of the diffracted γ beam in the quartz crystal.

During the reactor shutdown, the source-handling mechanism, which positions the (n, γ) source in the reactor, was modified so that the source could be moved laterally (perpendicular to the gamma beam). This will allow one to compensate for the source motions that result from temperature changes in the reactor. A monitoring system and servo mechanism is being designed to use the position-control mechanism to automatically stabilize the position of the source relative to the spectrometer. Such a system will greatly

improve the long-term stability of the spectrometer and greatly reduce the number of energy calibrations of the (n, γ) spectrum needed in order to monitor and correct for the temperature-induced source motions. Incorporated in this system will be the ability to visually check the position of the source in the reactor while the reactor is running. In addition, some temperature regulation of sensitive parts of the system will be used to improve thermal stability.

(ii) Level Scheme of ^{180}Hf

D. L. Bushnell, R. K. Smither, and D. J. Buss

The gamma-ray spectrum following thermal neutron capture in ^{179}Hf has been obtained with the precision capture-gamma-ray spectrometer equipped with a new, higher resolution Ge-diode detector. Analysis of the 1—2-MeV region of this spectrum together with improved bent-crystal data has led to the identification of sixteen levels above the ground-state band. Primary transitions to these levels have been observed in the average-neutron-resonance-capture

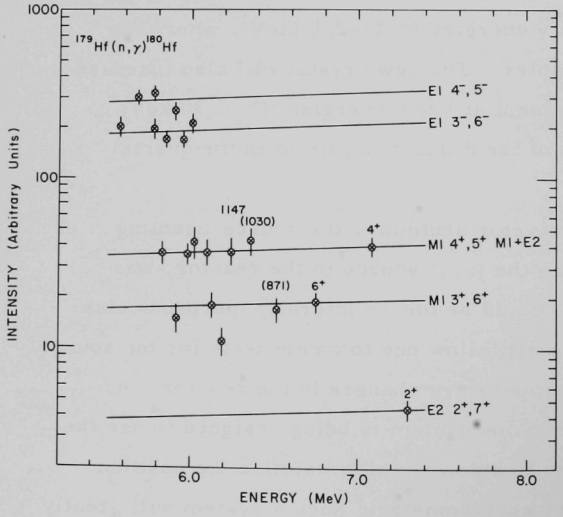

Fig. 6. A plot of I_γ/E_γ^6 as a function of E_γ for the ^{179}Hf(n, γ)^{180}Hf reaction from the average-resonance-capture experiment. The labels at the right indicate the multipolarity and the two possible J^π values associated with each group of γ transitions. The J^π labels on the individual points indicate previously-known values.

spectrum, and have led to tentative J^{π} values which are consistent with the thermal-capture data. The plot of $I_{\gamma}/E_{\gamma}^{6}$ vs E_{γ} (Fig. 6) shows how the gamma intensities separate into groups characterized by their values of J^{π}.

The level scheme of ^{180}Hf shows all of the expected rotational features of a strongly deformed nucleus: a K=0 ground-state band and a K=0 and a K=2 positive-parity excited-state band just above 1 MeV excitation (β and γ vibrational bands). What is new and still practically unexplained is the presence of negative-parity bands and additional positive-parity bands at about the same excitation energy. It was originally expected that these excited-state rotational bands would come at a slightly higher energy. It now appears that some changes in the theoretical calculations will be necessary.

(iii) Forbidden K x-Ray Transitions

R. K. Smither, M. S. Freedman,* and F. T. Porter*

Rosner and Bhalla, using a relativistic Hartree-Fock-Slater numerical program, have recently calculated the ratio of the K-L_I x-ray transition ($2s_{1/2} \rightarrow 1s_{1/2}$) to that of the K-$L_{III}$ transition ($2p_{3/2} \rightarrow 1s_{1/2}$). The K-$L_I$ transition is completely forbidden by calculations based on single-electron product wave functions so that a good measurement of the intensity of the K-L_I x ray would be an important check on these relativistic calculations. Preliminary results on Hf and Au, obtained by analysis of data taken earlier with the Argonne 7.7-m bent-crystal spectrometer, suggest that the Rosner and Bhalla calculations are high by at least a factor of two. Further measurements of the K-L_I, K-M_I, and K-N_I x rays in the high-Z elements are planned when the reactor goes back into operation. Although this is a slight diversion from the normal (n, γ) program, such measurements are possible only with high-sensitivity crystal-diffraction spectrometers such as the Argonne instrument.

---

*Chemistry Division.

b. Investigations of the Level Structure of Low-Lying Excited States of Selected Nuclides

H. H. Bolotin and D. A. McClure

This experimental program seeks to provide detailed information concerning the energies, radiative decay characteristics, and other pertinent parameters of the low-lying excited states of selected nuclides populated in thermal-neutron-capture gamma-ray reactions. Two types of experimental systems are used to unravel these complex spectra. The high-energy primary gamma-ray transitions that populate the low-lying states of the product nucleus from direct decay of the capture state are observed in an efficient pair-spectrometer arrangement at the high-sensitivity internal-target facility at the CP-5 reactor. These transitions establish the excitation energies of states up to ~1—2 MeV above the ground state. The low-energy secondary gamma-ray transitions among the low-lying excited states are studied by means of singles and coincidence gamma-ray spectroscopic techniques at the external-neutron-beam facility at CP-5. Here targets are placed in the external neutron beam (thermal flux $\approx 10^7$ neutrons $cm^{-2} sec^{-1}$). Singles and coincidence spectra are obtained entirely with the use of high-resolution Ge(Li) detectors in conjunction with a two-parameter magnetic-tape recording system in a 1024×1024-channel pulse-height array.

Two types of two-parameter Ge(Li)-Ge(Li) coincidence studies are performed: (a) "high-low" coincidences between high-energy primary transitions (~6—8 MeV) and low-energy secondary gamma rays (~30—2000 keV) and (b) "low-low" coincidences with both detectors set to view the low-energy transitions. These two sets of coincidence experiments provide the independent and complementary information necessary to delineate the level scheme and radiative decay properties of excited states up to ~1—2 MeV above the ground state. The efficacy of these detailed investigations has been repeatedly demonstrated over the last several years.

(i) Improvements in the External-Beam Coincidence Facility

H. H. Bolotin and D. A. McClure

Additional improvements in the external-beam coincidence facility, made concurrently with the rehabilitation of the CP-5 reactor, are: (a) modifications of the east thermal column to provide increased thermal-neutron flux, decreased background, and a higher Cd ratio, and (b) modification of the coincidence recording apparatus by expansion

to a three-dimensional pulse-height array of 2048 × 2048 × 256 channels. The larger dimensions are reserved to record expanded pulse-height regions of the coincidence γ-ray spectra while the smaller dimension will record the time-to-pulse-height information corresponding to each event. This timing information allows both after-the-fact time-resolution settings to improve the true-to-chance ratio of coincidence events and the ability to determine the lifetimes of low-lying excited states that fall in the time domain ($t_{1/2} \gtrsim 5 \times 10^{-9}$ sec) of the detection apparatus. In addition, the newer magnetic-tape storage is computer-compatible and is capable of recording $\sim 5 \times 10^{6}$ three-parameter events (as opposed to only $\sim 2.6 \times 10^{6}$ two-parameter events in the older system) on a single reel of tape. These characteristics will enable us to record data of greater statistical relevance and permit an order-of-magnitude increase in the speed of data analysis.

Several investigations, made feasible by the above improvements in the external-beam coincidence facility, will be initiated when the rehabilitation of the CP-5 reactor is completed.

(ii) Level Structure of Low-Lying Excited States of ^{187}W

H. H. Bolotin and D. A. McClure

The odd-A deformed tungsten isotopes are close to the edge of the deformed region where rotational characteristics are not expected to be as strongly manifested as in nuclei close to the center of the deformed region. Some (d, p) work and a limited amount of neutron-capture γ-ray spectroscopy concerned with the primary transitions following thermal-neutron capture had been reported earlier by other workers. Despite these efforts, many details of the level structure of ^{187}W were still unknown or poorly established. The present experimental investigation of the levels of this nuclide was undertaken in an effort to provide additional detailed level-structure information that could permit a more critical evaluation of the

applicability of the simple rotational model to the low-lying states in this nuclide and/or point up any systematic behavior reflecting the approach of ^{187}W to the edge of the deformed region.

This investigation concerned itself with the study of the low-lying ^{187}W states populated in the thermal-neutron-capture reaction ^{186}W(n,γ)^{187}W, and included studies of the primary and secondary transitions by means of singles and coincidence γ-ray techniques that made exclusive use of large-volume high-resolution Ge(Li) detectors. In this experiment, we recorded coincidences between the high-energy (4—5.5 MeV) and the subsequently emitted low-energy transitions, as well as among the low-energy cascade γ rays. The results of the present study established the excitation of 24 excited states up to an energy of 1217 keV in ^{187}W, several of which had not been reported earlier. Of more significance, a rather complete description of the radiative decay characteristics of these states has been deduced. Additional members of the two lowest rotational bands have been established.

These results have been compared with the simple rotor-plus-odd-particle model with the inclusion of Coriolis band mixing. The results of this comparison show a departure from the model prescriptions. These discrepancies arise principally from the unexpectedly high excitation energy of the 201.4-keV state assigned as the $\frac{7}{2}^-$ member of the rotational band built upon the $\frac{3}{2}^-$[512] ground-state Nilsson orbital. This behavior is analogous to that of the same state of the same band in ^{189}Os (an isotone of ^{187}W). These discrepancies in the model descriptions of ^{187}W and ^{189}Os may be indicative of (K + 2) vibrational mixing, the approach of the edge of the deformed region, or inaccuracies in the Nilsson wave functions in these "transitional" nuclides. This investigation is complete and ready to be submitted for publication.

4. THERMAL-NEUTRON BEAM FACILITY FOR MEASUREMENT OF INTERNAL-CONVERSION COEFFICIENTS OF CAPTURE-GAMMA TRANSITIONS

S. B. Burson and H. G. Miller

The experimental investigation of radiations accompanying neutron capture continues to be a fertile source of information about nuclear structure. An expanding body of high-precision data on transition energies exists, but the complexity of most spectra continues to be an imposing obstacle to interpretation of the results. The Argonne superconducting internal-conversion spectrometer promises to be a significant aid in overcoming this obstacle. The instrument provides a facility for the determination of internal-conversion coefficients as well as various coincidence relationships. Preliminary data, taken before the CP-5 Reactor was shut down in January 1969, verified the feasibility of the experimental technique.

These initial experiments were severely hampered by gamma rays and fast neutrons in the beam and by extraneous room background. The measurements emphasized the importance of having a neutron beam of high quality. We are therefore constructing a new facility (Fig. 7) with which a well-defined external beam of high intensity and purity can be brought out of the reactor. An aluminum moderator tank, filled with heavy water, is situated next to the reactor vessel. The tank measures approximately 23 in. square and is 18 in. thick. It replaces an equivalent volume of graphite in the reactor's reflector and has the effect of increasing the intensity of the transmitted thermal flux while at the same time substantially attenuating the fast component. The intense gamma-ray background from the reactor core is blocked by a D_2O-cooled bismuth shield which has the same vertical cross section as the moderator and is 8 in. thick. The central region of this shield is the effective source of neutrons from which the beam is formed. The defining collimator, composed of lead and natural lithium, is convergent toward the target.

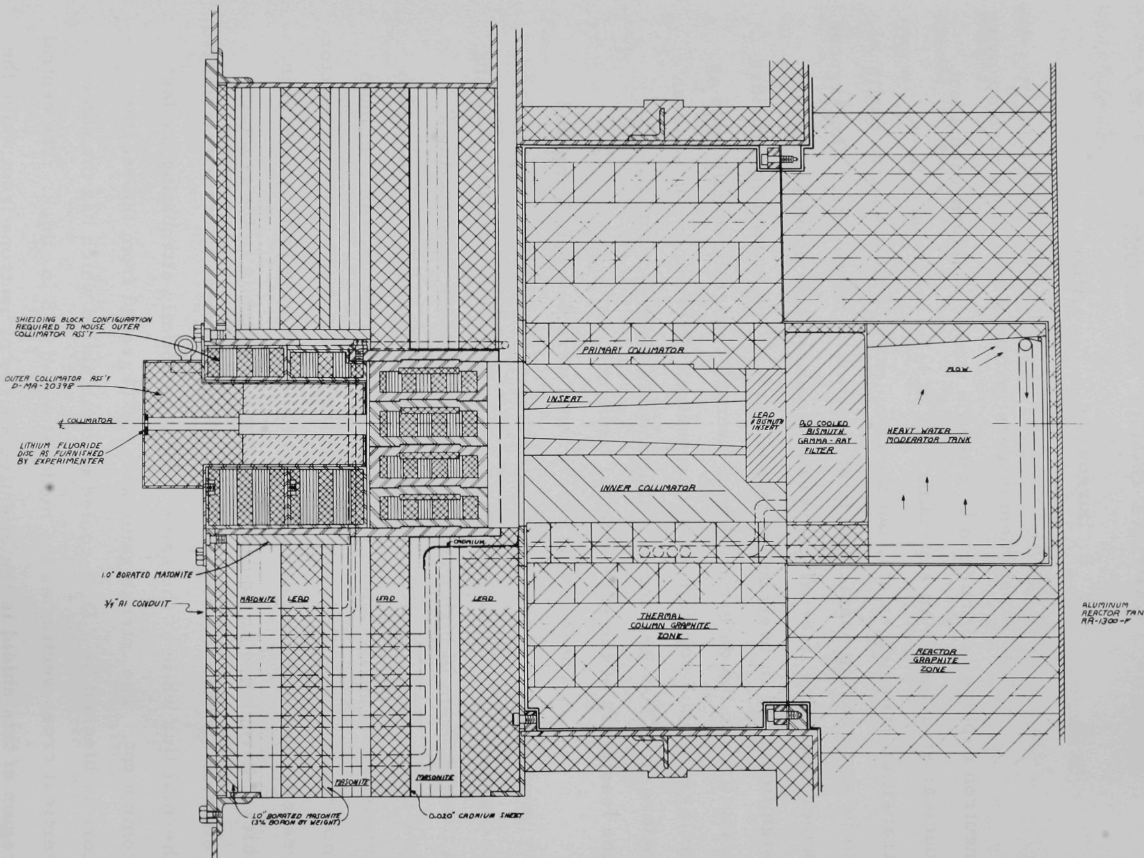

SHIELDING BLOCK CONFIGURATION REQUIRED TO HOUSE OUTER COLLIMATOR ASS'Y
OUTER COLLIMATOR ASS'Y D-MA-20398
℄ COLLIMATOR
LITHIUM FLUORIDE DISC AS FURNISHED BY EXPERIMENTER
1.0" BORATED MASONITE
3/4" Al CONDUIT
MASONITE
LEAD
LEAD
LEAD
MASONITE
MASONITE
CADMIUM
1.0" BORATED MASONITE (3% BORON BY WEIGHT)
0.020" CADMIUM SHEET
PRIMARY COLLIMATOR
INSERT
INNER COLLIMATOR
LEAD & BISMUTH INSERT
D₂O COOLED BISMUTH GAMMA-RAY FILTER
FLOW
HEAVY WATER MODERATOR TANK
THERMAL COLUMN GRAPHITE ZONE
REACTOR GRAPHITE ZONE
ALUMINUM REACTOR TANK RR-1300-F

The system is expected to produce a sharply-defined beam of thermal neutrons with a flux at the target of $1—5 \times 10^8$ neutrons/cm^2-sec—from 5 to 10 times the flux previously available at this beam hole. In addition, it will be substantially more free of fast neutrons and gamma rays. The increased intensity of the beam will make possible the study of many nuclides with low capture cross sections and at the same time will permit more exhaustive study of those already measured.

Fig. 7. Vertical section through the collimated thermal-neutron-beam facility located in the east thermal column of the Argonne CP-5 reactor.

B. PHOTONEUTRON EXPERIMENTS AT THE ANL LINAC

This new experimental program makes use of bremsstrahlung from the intense electron beam from the Linac operated by the Chemistry Division.

a. Threshold Photoneutron Studies

H. E. Jackson

A program of photoneutron experiments in which photoneutron spectra at threshold are observed with high resolution was undertaken during the past year, culminating several years of preparation. This class of experiments is of interest because it complements traditional (n, γ) measurements and in many cases extends experimentation to previously inaccessible classes of nuclei. In these experiments, targets of interest are bombarded with a bremsstrahlung beam from the new ANL high-intensity Linac, and established neutron time-of-flight techniques are used to determine the energy spectrum of photoneutrons. Because $E_\gamma / E_n \approx 100$, measuring neutron energy with 1% resolution measures the incident-photon energy with 0.01% resolution. Previously undetected fine structure near threshold in the (γ, n) cross section can be studied in detail. Both the (γ, n) and the (n, γ) reactions excite states just above the neutron binding, but because the photoneutron experiments involve the inverse reaction, a new set of physical parameters is available for study.

In initial measurements of photoneutrons from the Pb isotopes, the spectra were at least ten times as intense as those previously available—in spite of more stringent limitations on photon energy and sample thickness.

Initial measurements already begun will focus on three physical problems: (1) Determination of the strength of semi-direct capture, as proposed by Brown, through studies of the detailed shape of neutron resonances excited in the (γ, n) reaction. (2) Search for

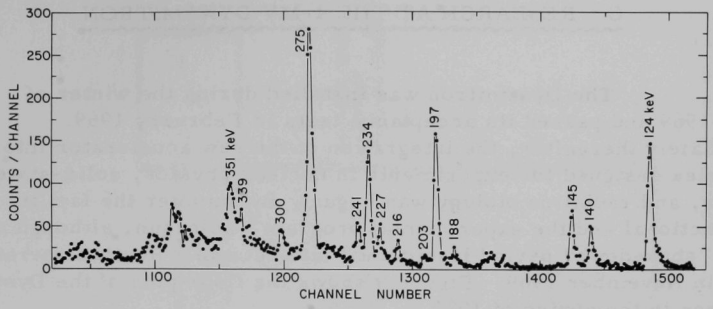

Fig. 8. Photoneutron spectrum for lead. The maximum bremsstrahlung energy (7.4 MeV) was chosen to permit excitation only of states in ^{207}Pb. Use of a thin target ($\frac{1}{8}$ in.) eliminated effects due to neutron scattering in the target material. The spectrum was obtained in 10 h.

correlations between neutron widths and ground-state radiative widths by comparison of parameters for (γ, n) and (n, γ) reactions in adjacent isotopes. The existence of such correlations indicates the dominance of a simple single-particle configuration in the neutron channel.

(3) Study of the systematic behavior of the electric- and magnetic-dipole strength function in medium-weight nuclei. To date measurements have been made with targets of ^{53}Cr, ^{138}Ba, ^{207}Pb, and ^{208}Pb. The spectrum for lead is shown in Fig. 8.

C. RESEARCH AT THE 4-MV DYNAMITRON

The Dynamitron was installed during the winter of 1968—1969 and passed its acceptance tests in February 1969. Immediately thereafter, the integration of the new accelerator into a complex designed for experiments in nuclear physics, solid-state physics, and radiation biology was begun. By summer the facility was functional and the experimental program was begun, although the initial "shakedown" period lasted until late autumn. Routine operation began in November 1969. Figure 9 shows the floor plan of the Dynamitron area in the spring of 1970.

Some charged-particle experiments are performed at the Dynamitron; these include measurements of lifetimes by the attenuated-Doppler-shift method and experiments on the channeling and blocking of energetic ions penetrating monocrystalline targets. However, the main justification for the accelerator and for the continuing development of its high-current capability is fast-neutron physics—in particular, studies of spontaneously fissioning isomers produced in neutron-induced reactions, of (p,n) reactions, of triple (elastic) scattering, and of resonance scattering by light nuclei. These are described in the following individual reports.

In addition to the nuclear and atomic physics experiments mentioned above, the Dynamitron is beginning to be used by other divisions in various areas of science and technology. These include experiments on radiation damage in materials, radiation biology, and neutron cross sections of interest to the reactor program.

Although routine operation of the Dynamitron has begun, we anticipate that a long effort will be required to develop the full capability of the system. A first step is the installation of a pulsed ion source, now nearing completion. Major improvements planned for the future are high-current beam lines, a high-current target for neutron generation, and possibly the development of a new high-current accelerator tube. The aim of these plans is to make the 4-MV Dynamitron a uniquely powerful tool for research with fast neutrons.

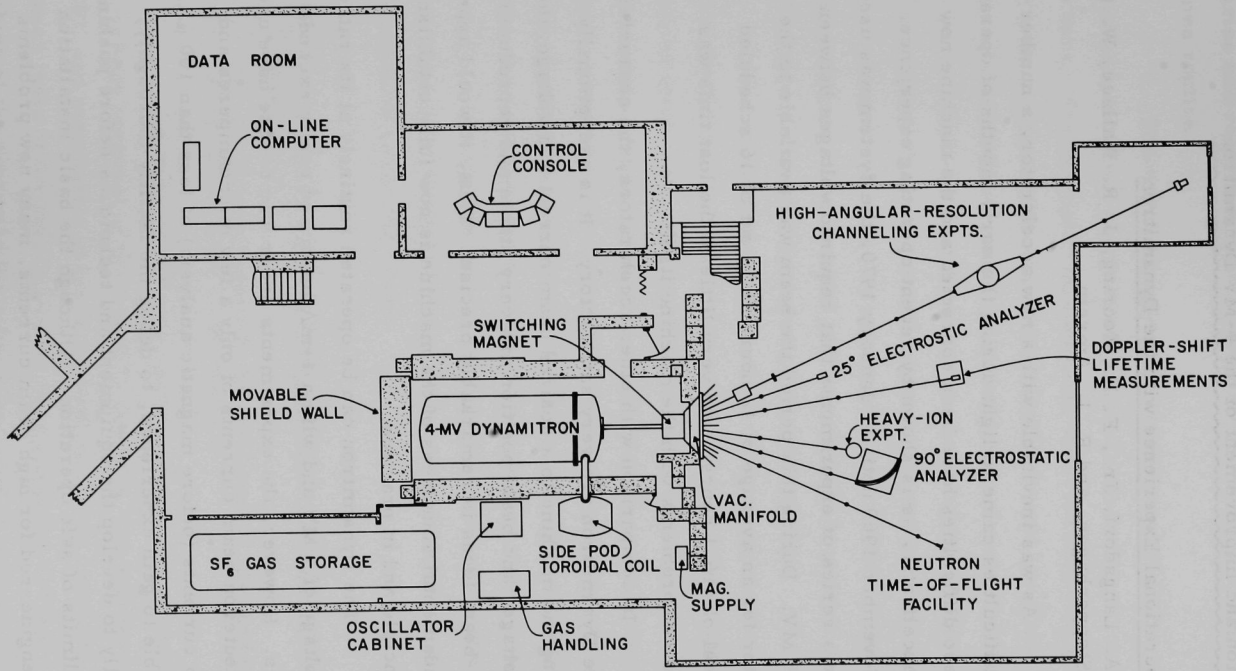

Fig. 9. Floor plan of the Dynamitron area, showing the relative positions and floor areas of the data room, control room, vault for the 4-MV accelerator, and the experimental room. The locations of the experiments now in progress are shown along with the beam lines serving them.

a. Operation and Improvement of the 4-MV Dynamitron

(i) Operational Experience with the Dynamitron

A. Langsdorf, Jr., F. P. Mooring, J. R. Wallace, W. G. Stoppenhagen, and R. L. Amrein

As was inevitable with a new accelerator, a number of technical difficulties came to light during the early months of operation. Most of these difficulties have been corrected and the machine now performs excellently, as is shown by recent operating experience. From 21 November 1969 until 19 January 1970, the system was used routinely in a series of experiments that required voltages between 3.5 and 4.5 MV. During this period the beam was available to the experimenter for an average of 12 hours daily out of 16 scheduled hours (a total of 416.1 hours), and very little of the lost time was due to technical problems with the machine itself.

In comparison with other accelerators, the characteristics of the Dynamitron are very satisfactory. It is exceptionally easy to bring the machine to a desired beam current and voltage; the current, voltage, and beam position are very stable and reproducible; and the ion-beam focus is remarkably precise. Thus, it would appear that the fundamental soundness of the machine is now fully established both in principle and in practice.

The Dynamitron can be operated routinely at its rated terminal voltage of 4 MV and with a 1-mA beam and easily exceeds these values. However, the experiments under way to date have used proton or deuteron beam currents of only a few microamperes and gross beam currents (before magnetic analysis) of less than 100 μA. It is desirable to gain experience, to debug the facility thoroughly, and gradually to develop the equipment and techniques before pushing toward the limits of safe operation. Although the basic installation is already engineered for high beam currents, many new problems

will arise and require solution before the use of large beam currents becomes routine.

The excellent operation record since 21 November appears to be a direct result of several accelerator improvements made here. For example, (a) insulating brackets supporting protective spark gaps inside the machine were redesigned and installed, (b) defects in electrical connections in the heating circuits for the filaments of the 94 vacuum-tube rectifiers in the column of the machine were identified and corrected, (c) difficulties in the operation of the Duoplasmatron were corrected by means of a design modification, and (d) arcing problems in the toroidal coil were traced to parasitic oscillations and should be eliminated by redesign of the coupling.

In addition to the work on the accelerator itself, the experimental area has been improved by better heating, lighting, and acoustical treatment. The experimental cable-tray system, the water-cooling system for beam-line components, and the beam-line support system have been extended. A system of lights and horns to warn of radiation hazards has been installed, and a radiation-detection system and interlocked access gates are under construction.

In view of our success to date in operating the machine and eliminating difficulties as they arise, we look forward with confidence to its effective use in the future.

(ii) Nanosecond Terminal Pulsing Equipment for the 4-MV Dynamitron

W. G. Stoppenhagen, F. P. Mooring, A. Langsdorf, Jr., A. J. Elwyn, and J. R. Wallace

A nanosecond beam-pulsing system to be used in the high-voltage terminal of the 4-MV Dynamitron was purchased from ORTEC and installation of the equipment is almost complete. Preliminary tests of the source system have indicated that the optical matching of the source to the accelerator tube is satisfactory. The

crossed-field analyzer has undergone preliminary tests. Several pressure-sensitive leaks in the source have delayed the testing under operating conditions. The initial planned uses of the pulsed-beam facility will be in (p,n) reaction studies, in studies of spontaneously fissioning isomers in neutron-induced reactions, and in triple-scattering measurements.

b. Planned Experimental Program at the Dynamitron

A. J. Elwyn, A. Langsdorf, Jr., J. E. Monahan, F. P. Mooring, and W. G. Stoppenhagen

The Dynamitron accelerator can provide charged-particle beams that are from 10—100 times more intense than those that were available at the 4-MV Van de Graaff machine. With the proper choice of neutron-producing target, neutron beams of well-defined energies from ~20 keV to 20 MeV can be expected. The increased intensities, together with the pulsed-beam facility that will shortly be available, should make feasible a number of "low-yield" measurements that can provide detailed information about nuclear structure and reactions. A brief description of a few proposed areas of research follows. Experiments in some of these areas are expected to begin before summer 1970.

Spontaneously Fissioning Isomers in Neutron-Induced Reactions. As mentioned in Sec. I.Cc, the pulsed-beam facility at the Dynamitron should prove useful in the study of the existence and properties of short-lived spontaneously fissioning isomeric states formed in reactions induced by neutrons. Under experimental conditions in which the effects of low-energy background neutrons can be understood and controlled, the excitation functions, half-lives, and isomer ratios for short-lived isomeric states formed in (n,γ) reactions, for example, should yield new and important information on the nuclear structure of heavy nuclei. Such experiments that will utilize both

solid-state detectors and gas scintillators for fission-fragment detection are being planned.

(p,n) Reaction Studies. In the proposed investigations of (p,n) reactions by use of the pulsed-beam facility at the Dynamitron, time-of-flight techniques with stilbene and liquid scintillators will be utilized in order to resolve the neutron groups that correspond to the formation of the residual nucleus in various final states. The targets will be elements with mass number between A = 40 and A = 90, and the measurements will be performed at those proton energies that selectively excite analog states in the "proton + target nucleus" compound system. In these cases, the neutron decay of the analog state is assumed to proceed through a sufficient number of $T_<$ compound states that a statistical mixture is formed. Under these conditions, the yields to the various final states can be determined by the use of statistical compound-nucleus theory with the important simplification that only those compound states that have the same spin and parity as the analog state are involved in the process. The technique, as has been pointed out by a number of authors,[1] can be utilized to test the assumptions of the theory as well as to determine the spins and parities of final states—at least in certain cases.

Triple (Elastic) Scattering. These measurements, which determine both the initial and final states of polarization of the neutrons, provide the basis for the design of a set of experiments to determine all of the S-matrix elements for reactions with spin-zero scatterers. Such complete information is of interest only in special cases; in general it seems more practical to select only a subset of experiments that bear directly on a specific question of interest. In one type of triple-scattering experiment, for example, the angle through which an initial polarization is rotated in the scattering process can be determined. It can be shown that a knowledge of this

[1] See, for example, M. H. Macfarlane, in Nuclear Isospin, edited by J. D. Anderson, S. D. Bloom, J. Cerny, and W. M. True (Academic Press, Inc., New York, 1969), p. 591.

rotation angle at scattering angles between 5 and 10^{o} (along with a measurement of both the polarization and differential-scattering cross section) allows the determination of the compound elastic-scattering cross section. Since compound-nucleus cross sections are directly related to neutron strength functions, such measurements might permit the investigation of possible structure in the strength function. The observation and identification of intermediate structure in a nuclear reaction is an important current area of research. It is planned to use the high direct currents available from the Dynamitron in an experimental program to measure the rotation angle for a number of zero-spin scatterers at scattering angles near 10^{o}.

c. Spontaneously Fissioning Isomers in Neutron-Induced Reactions

A. J. Elwyn and A. T. G. Ferguson*

The properties of the currently known short-lived spontaneously fissioning isomers have been determined for the most part from measurements in reactions induced by charged-particle beams. The present study, carried out while the first author was on assignment at AERE, Harwell, was a search for such isomers in neutron-induced reactions on various isotopes of U and Pu. The pulsed proton beam from the IBIS electrostatic accelerator at Harwell, England, was utilized to produce 0.55—2.2-MeV neutrons in pulses of between 1 and 2 nsec duration. Fission fragments from the bombardment of thin foils of the fissile samples were detected in a Si surface-barrier counter, and the time distribution of the pulses was measured relative to the proton beam pulse with a time-to-amplitude converter. Figure 10 shows the time distribution of the fission events from the bombardment of ^{239}Pu with 2.2-MeV neutrons. The time

*Nuclear Physics Division, Atomic Energy Research Establishment, Harwell, Berkshire, England. The experiment reported here was performed at the IBIS accelerator at Harwell.

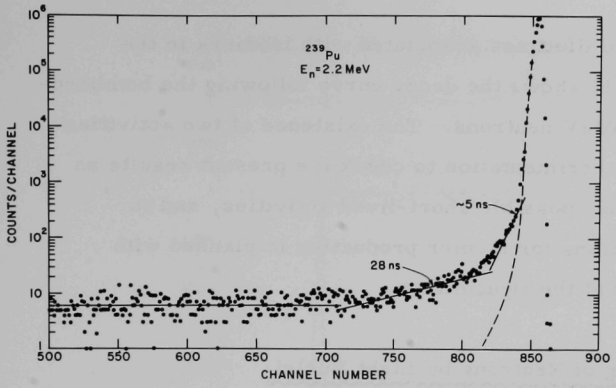

Fig. 10. Time distribution of the fission events from the 2.2-MeV neutron bombardment of ^{239}Pu. In this figure, time increases to the left. The dashed curve is representative of the shape of the distribution associated with prompt fission events. The solid curves are the results of numerical analysis of the events in the tail of the prompt peak (as shown on a larger scale in Fig. 11).

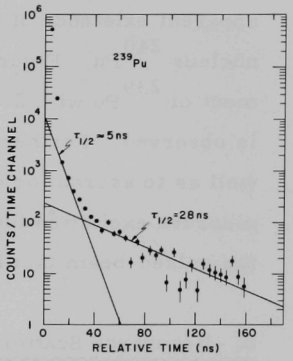

Fig. 11. Decay curve of the 2.2-MeV neutron bombardment of ^{239}Pu. The net counts (after background subtraction) are summed over 5 channels (so that the time channel has a width of 4.6 nsec) and the counts per time channel are plotted as a function of the time measured from the prompt fission peak.

distribution of the alpha particles in the $^{10}B(n,\alpha)^{7}Li$ reaction was also studied. On the basis of this test, it appeared possible to rule out the existence of short-lived activities arising from interaction between the fissile samples and any time-dependent population of low-energy background neutrons.

Short-lived activities with half-lives between 5 and 67 nsec were observed in the neutron-induced fission of ^{234}U, ^{235}U, and ^{239}Pu at 2.2 MeV incident-neutron energy, and preliminary results revealed an activity with a half-life of about 30 nsec at both 0.55 and 2.2 MeV with targets of ^{233}U. The observed activities are probably associated with the (n,γ) reactions on the targets listed, so that the data are consistent with the existence of fissioning isomers in ^{235}U, ^{236}U, ^{240}Pu and, tentatively, in ^{234}U. Of particular interest is the

apparent existence of two lifetimes associated with isomers in the nucleus ^{240}Pu. Figure 11 shows the decay curve following the bombardment of ^{239}Pu with 2.2-MeV neutrons. The existence of two activities is observed. Further experimentation to check the present results as well as to search for other possible short-lived activities, and to measure excitation functions for isomer production is planned with the pulsed-beam facility at the Dynamitron.

d. Resonance Scattering of Neutrons by Light Nuclei

J. L. Adams,* A. J. Elwyn, R. D. Koshel,* R. O. Lane,* A. Langsdorf, Jr., J. E. Monahan, F. P. Mooring, and C. E. Nelson*

The polarization and differential cross sections for neutrons scattered from ^{10}B, ^{11}B, and ^{12}C for energies in the interval 0.075—2.2 MeV were measured at Argonne several years ago. Recently we have analyzed these data to obtain spectroscopic information about the resonances excited in these reactions. In particular, an attempt has been made to interpret these spectra in terms of single-particle and particle-hole shell-model configurations. One report on this work has been published[1] and another is in preparation. Figure 12 shows the energy dependence of the differential cross section and of the polarization for the case of neutron scattering by ^{11}B. The solid curve is based on an R-matrix analysis of the data in terms of energy levels in ^{12}B at 3.39 MeV (3^-), 3.76 MeV (2^+), 4.30 MeV (1^-), 4.37 MeV (2^-), and 4.54 MeV (4^-). A simple shell-model calculation based on a δ-function residual interaction is consistent with the above ordering of spins and parities for states in ^{12}B.

---

*Ohio University, Athens, Ohio.

[1] R. O. Lane, R. D. Koshel, and J. E. Monahan, Phys. Rev. 188, 1618 (1969).

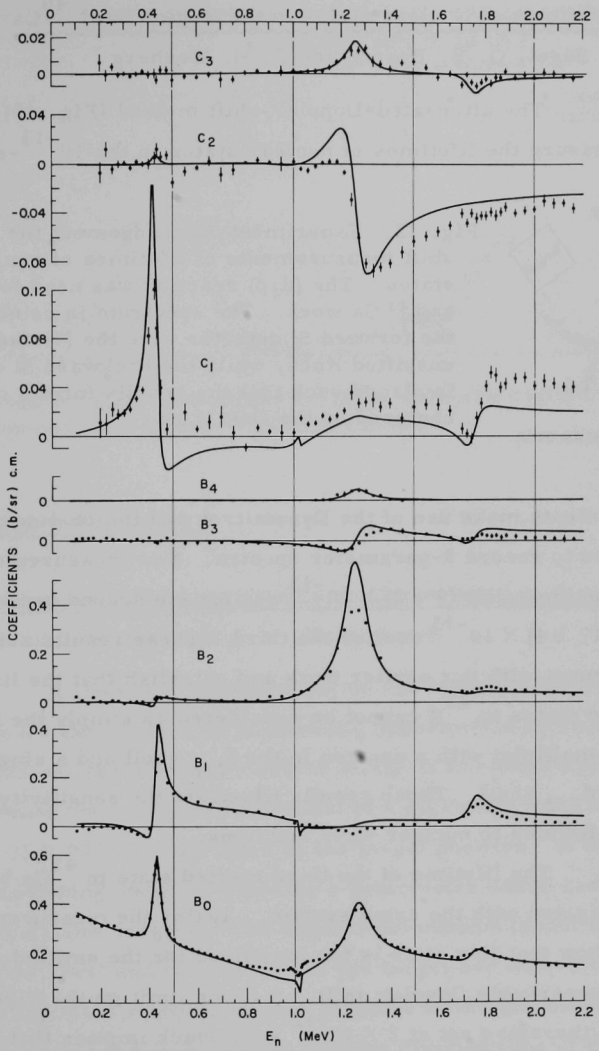

Fig. 12. Coefficients B_L in the Legendre-polynomial expansion of $\sigma(\theta)$ and C_L in the associated-Legendre-polynomial expansion of the product $\sigma(\theta)P(\theta)$ in the scattering of neutrons by ^{11}B, plotted as a function of neutron energy. The solid curve represents calculations based on a two-channel three-level R-matrix analysis.

e. The Lifetimes of Nuclear States in the Region Near ^{40}Ca

R. E. Segel, G. B. Beard, and G. H. Wedberg

The attenuated-Doppler-shift method (Fig. 13) is being used to measure the lifetimes of nuclear states in the 10^{-13}-sec region.

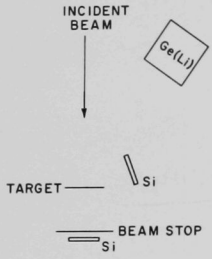

Fig. 13. Experimental arrangement for Doppler-shift measurements of lifetimes of nuclear excited states. The (d,p) reaction was used for the ^{40}K and ^{41}Ca work. The spectrum in coincidence with the forward Si detector gave the (virtually) unshifted lines, while the backward Si detector is placed such that the recoils form a cone centered on the Ge(Li) axis.

The experiments make use of the Dynamitron and the on-line computing system used to record 3-parameter spectra. New measurements on ^{40}K give the mean life $(9 \pm 2) \times 10^{-13}$ sec for the second excited state and $(17 \pm 4) \times 10^{-13}$ sec for the third. These results are in good agreement with our earlier work and establish that the first four excited states in ^{40}K cannot be considered as simply the four states of a multiplet with a neutron in the $f_{7/2}$ shell and a single proton hole in the $d_{3/2}$ shell. These results illustrate the sensitivity of radiative lifetimes to nuclear wave functions.

The lifetime of the third excited state in ^{41}Ca has been investigated with the same system. Again, the measurements (Fig. 14) show that this state is too long lived for the emitted γ rays to have an observable Doppler shift. A lower limit on the lifetime of the state is therefore set at 2×10^{-12} sec, which implies that the strength of the E2 transition to the ground state is less than 1/1500 of a single-particle unit. As far as is known, this is the slowest E2 transition that is not obviously violating some selection rule. While some inhibition of this transition is theoretically understood, this extreme inhibition is not predicted by any of the current theories.

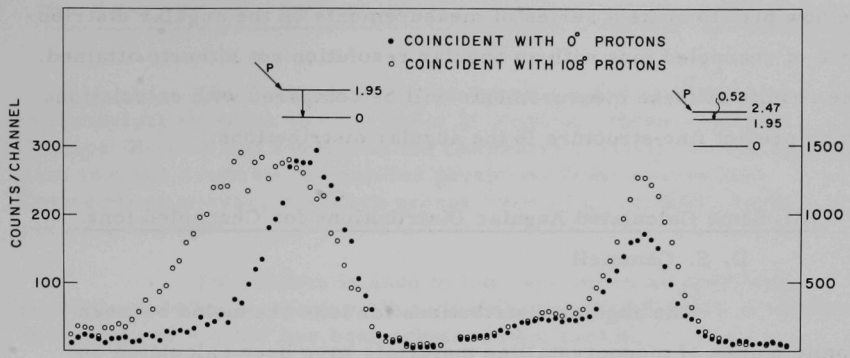

Fig. 14. Doppler-shift spectra for the first and third excited states in ^{41}Ca formed through the ^{40}Ca(d, p) reaction.

f. Channeling and Blocking

(i) An Apparatus for Experiments on Channeling and Blocking

D. S. Gemmell and J. N. Worthington

A beam line has been set up and tested at the 4-MeV Dynamitron for the purpose of performing experiments on channeling, blocking, and related effects. Careful design of the beam-collimating system permits the routine achievement of a maximum total angular divergence of 0.007° for the beam at the target position. A 28-in.-diameter scattering chamber contains a goniometer which carries the monocrystalline targets. The angular orientation (about three perpendicular axes) and the position of the target are determined by computer-controlled stepping motors attached to the goniometer. A movable detector for measuring the angular distributions of channeled ions is located in another smaller chamber about 7 m from the target. The motion (in a plane) of this detector is also computer-controlled. Before the accelerator was shut down for installation of a pulsed ion source, the apparatus was tested and found to operate quite satisfactorily.

We now plan to make a series of measurements on the angular distributions of channeled ions with an angular resolution not hitherto attained. The results of these measurements will be compared with calculations which predict fine-structure in the angular distributions.

(ii) Some Calculated Angular Distributions for Channeled Ions

D. S. Gemmell

The angular distributions for ions channeled between atomic planes of monocrystalline materials have been calculated on the Argonne CDC-3600 computer. The program numerically integrates the classical equations of motion for channeled particles. The form of the average interplanar potential experienced by the channeled ions makes the wavelength of the ion oscillations strongly amplitude dependent, and consequently the computed angular distributions contain marked fine structure. The dependence of this structure on such factors as particle energy, crystal thickness, temperature, etc. has been explored by use of the computer. The results show the structure to be quite sensitive to the detailed shape of the potential used. It is hoped that these calculations can be compared with the results of channeling experiments performed with good angular resolution.

D. RESEARCH AT THE TANDEM VAN DE GRAAFF ACCELERATOR

The FN tandem Van de Graaff accelerator provides the principal research tool for about 15 Argonne scientists in the Physics Division and several in the Chemistry Division. Also, running time is made available to qualified physicists from universities. During the past year, research groups from 14 universities made use of the system.

The tandem is used to full capacity on an operating schedule of 24 hours per day. A terminal voltage of 8.5 MV is obtained with ease and 9.0 MV has been achieved on occasion.

The research carried out at the tandem is very broad in scope, reflecting the diverse interests of the physicists involved. The general features of the work have not changed greatly during the past year, although there have been some significant changes in emphasis. Perhaps the most noteworthy of these is a series of experiments with the new split-pole magnetic spectrograph. This experimental system (developed by John Erskine) actually consists of two major parts—the spectrograph itself and the automatic plate reader. The large solid angle, good energy resolution, high precision, and ease of use of the spectrograph make it a very powerful research tool, and hence it is being used in a great variety of experiments carried out at the tandem. Almost as important as the spectrograph itself is the automatic plate reader, since it allows the experimenter to obtain information from the exposed nuclear emulsions while the experiment is still in progress. Also, the operation and maintenance of the reader cost substantially less than human scanning of the same plates.

The individual experiments carried out at the tandem are described below. However, since the detail of these descriptions and the great diversity of the work tend to obscure the more general features of the research, we first outline some of the basic ideas and trends of the program.

Heavy-Ion Scattering. Systematic studies of heavy-ion scattering involving various projectiles and targets are continuing. A careful analysis of the results is leading to deeper insight into the nucleus-nucleus interaction and thus to a better understanding of the relevance of the optical model for heavy-ion reactions. The picture emerging from these studies is that of a "black" nucleus with a very transparent surface region.

Transfer Reactions on Deformed Nuclei. Single-nucleon transfer reactions are the fundamental basis for understanding nuclear reactions and are the subject of continuing investigations. Some of

our recent experiments are linked to related studies of neutron-capture γ rays. This combination of techniques is particularly advantageous, because the capture γ rays provide general information about a very large number of states and nucleon-transfer reactions elucidate the structure of particular states. Two-nucleon-transfer (p,t) experiments on tungsten, platinum, and uranium isotopes are revealing interesting effects of strongly-populated excited 0^+ states. In view of the high density of states in heavy deformed nuclei, the good energy resolution of the new split-pole spectrograph is of special importance for these investigations.

Two-Body Spectra. Inasmuch as the basic microscopic description of nuclear processes involves the interaction between two nucleons, the study of two-particle spectra near closed-shell nuclei is of great importance for an understanding of nuclear structure. A number of experiments at Argonne have led to information on such features as the two-particle states in ^{210}Bi and the particle-hole configurations of ^{208}Bi, ^{40}Ca, and ^{48}Sc. During the last year, investigations of ^{34}Cl, ^{88}Y, ^{90}Nb, and ^{96}Nb have extended the study of two-particle interactions to additional orbitals and provided two-body matrix elements of considerable interest.

The Charge-Exchange (^{3}He,t) Reaction. Recent studies have revealed unexpected simplicities in the (^{3}He,t) reaction. These make the reaction useful for selecting proton-particle neutron-hole configurations, based on the target, and for giving a reasonably reliable measure of angular-momentum transfer. The ^{3}He beam of the Argonne tandem and particle detection with the new split-pole spectrograph and computer-controlled plate scanner have made possible a program of experiments utilizing this reaction on a variety of target nuclei. An informal conference on (^{3}He,t) reactions was organized by our staff members and held in Chicago in January 1970.

Isospin Violation in (d,α) Reactions. The reaction ^{12}C(d,α)^{10}*B$_{T=1}$ has been the subject of continuing investigation at Argonne. The early experimental results led to some interesting theoretical speculations regarding the origin of this isospin-violating process. More recent work on a ^{28}Si target indicates that the isospin-violating part of the reaction proceeds by way of a compound-nucleus process.

Giant-Resonance Investigations. A series of experiments on the dipole giant resonance by way of the (p,γ) reaction have been carried out at Argonne since 1962. A number of new effects, among them the constancy of the angular distributions over a fluctuating cross section, were established here. Most recently, the giant resonances in ^{36}Ar and ^{38}Ar were investigated. The resonance in ^{38}Ar exhibits the expected isospin splitting, but again the angular distributions are nearly constant, a still unexplained phenomenon.

1. TANDEM OPERATION AND EQUIPMENT

a. Operation of the Tandem Van de Graaff Accelerator

Jack R. Wallace

The FN tandem operated 5833 hours in the period from 1 April 1969 to 20 March 1970. Many different ions have been accelerated and used as bombarding particles for the various reactions studied by our experimentalists. These particles were $^{16}O^{+4,+5,+6}$, $^{18}O^{+4,+5}$, protons, deuterons, $^{3}He^{+2}$, $^{4}He^{+2}$, $^{6}Li^{+3}$, $^{7}Li^{+3}$, $^{14}N^{+4,+5}$, and $^{32}S^{+5,+7}$. Ion energies in excess of 50 MeV have been achieved.

The energy-control circuit has been improved and new functions added to it. Two new beam-switching magnets were installed. A second ion-source assembly has been constructed. The lithium-vapor charge-exchange ion source has been reworked for improved performance and greater ease of maintenance.

b. University Use of the 17-MeV Tandem

J. P. Schiffer and F. P. Mooring

The university community has continued its intense use of the Argonne tandem during the past year. The user groups generally fall into two categories. In the first category are those universities that have a continuing program of research which depends to a large extent on the use of the Argonne tandem. The second includes those institutions that use the tandem once or twice to extend measurements made in their own laboratories. Often the university groups will collaborate with local scientists.

During the past year, seventeen groups of scientists from fourteen universities have performed experiments at the Argonne tandem. Of these, eight have or had continuing programs. Three new universities have become regular users, and one has completed

its program. The experimental groups who have used the tandem during the past year are as follows.

1. University of Alberta

   $^{40}Ca(d,p)^{41}Ca$

   G. Roy and W. Saunders

2. Cleveland State University

   Conversion-Electron Spectra

   G. T. Wood

3. Columbia University

   Investigation of the Bohr Independence Hypothesis for Nuclear Reactions in the Continuum

   J. Miller

4. DePaul University

   $(^{3}He,t)$ Reactions on Nuclei with $A \approx 90$

   M. Stautberg

5. Florida State University

   Fragmentation of the Strength of "Antianalog States" in ^{89}Y and ^{90}Zr

   L. Parish

6. Illinois Institute of Technology

   Radiative-Capture Studies of the Giant Dipole Resonance

   E. Segel

7. Indiana University

   Scattering of Alpha Particles

   J. Kroepfl, R. Malmin, T. Marvin, L. Medskir, D. Plummer, P. Singh, D. Sink, W. T. Sloan, and G. Wedberg

   Elastic Scattering of Nitrogen Isotopes from Light Nuclei

   P. Singh and W. T. Sloan

8. University of Iowa

   $^{7}Li(^{7}Li,\alpha)^{10}Be$

   R. R. Carlson, N. Throop, and H. Wyborny

   Deuteron-Induced Reactions

   R. T. Carpenter, D. Spry, and F. Snyder

9. University of Kansas

(^{3}He,t) Reactions on Nuclei with A ≈ 90

R. C. Bearse

10. Kansas State University

J Dependence of Inelastic Scattering

J. C. Legg and D. R. Abraham

11. Purdue University

Multiple Coulomb Excitation and Reorientation Effect

R. P. Scharenberg, J. A. Thomson, Jr., R. Beyer, and W. Lutz

12. Rochester University

^{33}S(^{3}He,d)^{34}Cl

W. P. Alford

13. Western Michigan University

Properties of Nuclear Energy Levels

G. Hardie

(d,p) Reactions

E. Bernstein, J. Boss, and R. Shamu

14. Washington University

(^{3}He,d) and (^{4}He,t) Reactions on ^{100}Ru

D. G. Sarantites

c. Split-Pole Magnetic Spectrograph at the Tandem

J. R. Erskine

The new spectrograph has been fully operational since the summer of 1969, and in six months more than 1000 spectra have been recorded with the instrument. During some scheduling periods, more than a third of the useful beam time from the tandem has been devoted to spectrograph exposures.

The instrument (Fig. 15) has proved to be far easier to use than the older spectrograph and the higher energy resolution, larger solid angle, and lower background have enabled scientists to

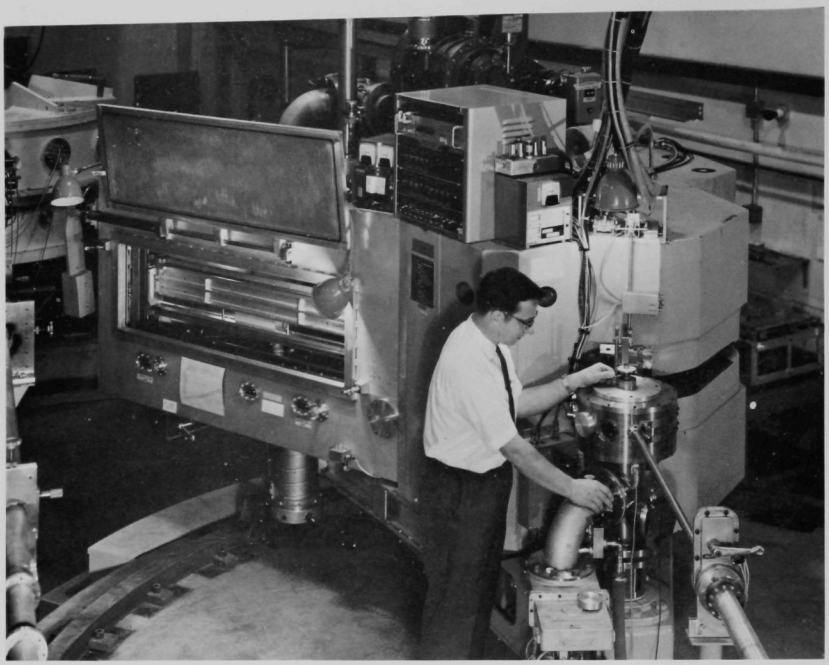

Fig. 15. Split-pole magnetic spectrograph for high-resolution studies of charged-particle nuclear reactions. The beam from the tandem Van de Graaff accelerator comes from the lower right and strikes targets located in the scattering chamber (the cylindrical unit being adjusted by the operator). Reaction products are momentum analyzed and focused by the precision magnetic field inside the spectrograph; a particle with higher momentum is less deflected and strikes the nuclear emulsion (or sometimes an electronic detector) farther to the left in the picture. The camera (shown with its vacuum-tight cover open, just to the left of the operator) holds the emulsion (or detector) at the focal surface of the spectrograph. The instrument can focus 95-MeV protons and can cover a 5-fold variation of energy in one exposure.

study many new reactions. The speed and ease of use of the new instrument, together with the fast emulsion processing made possible by the automatic plate scanner, have greatly simplified the taking of angular-distribution data. The difference between the new and the old

spectrographs in this respect results in an almost qualitative change in the kind of physics that is done routinely.

The new spectrograph competes very favorably with a multiple-gap spectrograph. The solid angle for each of the 25 gaps in a multiple-gap instrument is typically an order of magnitude smaller than the usual solid angle of the split-pole spectrograph. Since one normally is more interested in the forward angles, the total-solid-angle advantage of the multiple-gap spectrograph is no longer of major importance. With good current integration and/or a monitor detector system, there is no real difficulty in maintaining accurate normalization from one angle to the next. The split-pole has one important advantage in that the absolute energy calibration (consistently within 1 part in 2000) is considerably better than that in a typical multiple-gap spectrograph.

Most of the data are recorded on nuclear emulsions, but some (^{3}He,t) and (d,α) experiments have been performed with position-sensitive electronic detectors. Further increase in the use of active detectors, probably proportional counters, is anticipated.

d. Automatic Nuclear-Emulsion Scanner

J. R. Erskine and R. H. Vonderohe*

The scanner (Fig. 16) has been heavily used since the fall of 1969 to scan plates from the split-pole magnetic spectrograph. The machine is busy typically 35 hours each week. About 90% of all plates from the spectrograph are scanned by the machine.

The cost of hand scanning all the data from the spectrograph would be prohibitive. With our system, one operator can almost keep up with the copious output of the split-pole spectrograph. In a typical day the machine will scan 12 strips, each 10 in. × 1 cm, in $\frac{1}{2}$-mm steps along the length of each strip.

---

*Applied Mathematics Division.

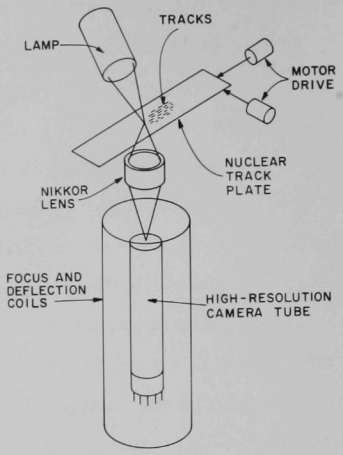

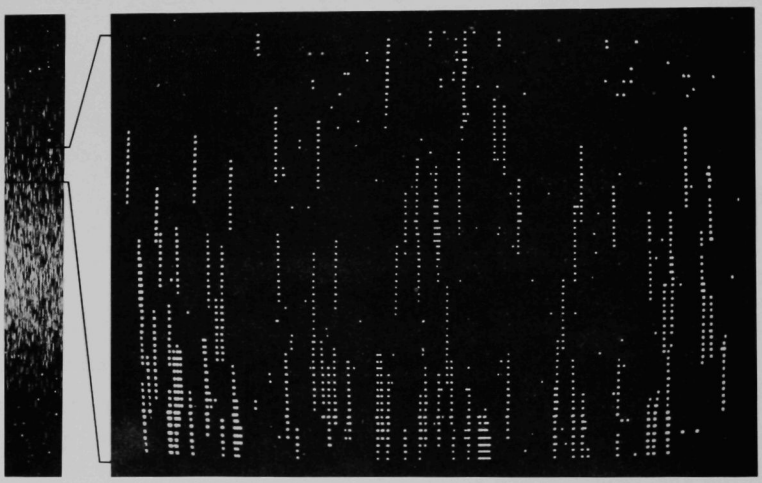

Fig. 16. Machine counting of tracks produced by nuclear particles striking a photographic emulsion. Above: Photograph of the system developed at Argonne and diagram of the scanning head. A digital computer processes the information from the camera tube to determine the number of tracks present. Below: Nuclear tracks as they appear in the emulsion (microphotograph at left) and on the display tube of the scanner (right). The tracks (about 100 microns long) appear as strings of dots on the display tube because a dot is produced each time the scan (from left to right) crosses a track and each subsequent scan line is 10 microns higher than its predecessor.

Many people—scientists, graduate students, technicians, and visitors—have learned to use the machine. The most reliable scanning is done by full-time operators, but any patient person can usually be taught to use the machine. The computer program is constantly being improved to make operation simpler and more reliable.

A new and more sensitive camera tube, which can tolerate a higher photocathode current, is now available. Plans are being made to install this new tube in the summer of 1970. The improvements in the tube will enable the machine either to scan twice as fast or to do better scanning of poor-quality plates.

e. Polarized-Ion Source

D. C. Hess and D. von Ehrenstein

Shortly after completion of the successful initial tests on the source (including acceleration of polarized nuclei through the tandem and measurement of the polarization of the accelerated beam by use of the regular tandem scattering chamber), the operation of the source had to be suspended because of lack of funds. We are continuing to do some work on the use of a resonant charge-exchange method to produce negative ions directly from the polarized atoms. This would eliminate the need to use the vapor of potassium (or some other alkali metal) as the charge-exchange medium, and thus would increase the safety of operation and maintenance since there would be no handling of alkalis.

In the resonant-charge-exchange method of ionization, an intense beam of unpolarized negative particles (supplied by direct extraction from a Duoplasmatron for tests, or by a high-intensity diode source for actual operation) is caused to interact with the polarized atomic beam so that some electrons will transfer from the negative ions to the un-ionized beam. The negative beam could be deuterium if the polarized beam is ordinary hydrogen and vice versa, so the

beams (after charge exchange) can be separated by energy or mass. This has the effect of supplying a sufficiently large current of slow electrons—something that cannot be done with a conventional electron beam because the required electron energy is so low that space charge restricts the electron current to too low a value to produce sufficient ion current. At present, it is planned to borrow the Duoplasmatron. If the system is successful, the high-intensity diode source will be needed to increase the ion current available.

f. Argonne 70-in. Scattering Chamber

J. L. Yntema and J. Bicek

The secondary angle-indicating system has been installed on all four arms. An automatic vacuum-protection system has been built, and progress has been made on the installation of a variety of interlocks to protect the instrument against operator errors. A new target changer which permits scanning of the target was constructed. A system was developed to allow each user to construct his own detector and target assemblies without need for complicated alignment procedure in order to make full use of the accuracy of the instrument.

g. Computer-Controlled Multiple-Detector Array for Heavy-Ion Studies

R. H. Siemssen, H. T. Fortune, J. W. Tippie,* and J. L. Yntema

Further work both on the hardware and on the software has been done to improve the system. It now consists of an array of six conjugate pairs of large-area detectors which are mounted on the four remotely controlled arms of the 60-in. scattering chamber at the tandem, as shown schematically in Fig. 17. Kinematic coincidences between the scattered and the recoiling ions are employed for the identification of the reaction products. For each angle setting of the

*Applied Mathematics Division.

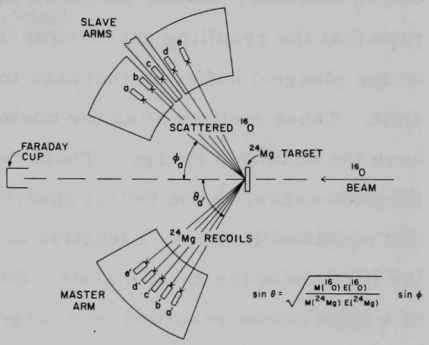

Fig. 17. Diagram showing the detector arrangement in an experiment on the scattering of ^{16}O on a ^{24}Mg target. When a ^{24}Mg nucleus recoils into detector a', the scattered ^{16}O is detected by a; and other pairs of recoil and scattered ions are detected in coincidence by b' and b, c' and c, etc. Although the computer moves each detector only over an arc of about 5°, the array of detectors covers the entire angular range of interest.

"master" arm which holds the recoil detectors, the computer calculates the kinematically correct settings of the slave arms holding the conjugate detectors and automatically positions the arms. Two-dimensional coincidence spectra of 64 × 128 channels each from the six coincident detector pairs are directly stored into the 64K external memory and subsequently analyzed with the light-pen facility.

h. Lifetimes of Excited Nuclear States by the Doppler-Shift Recoil-Distance Method

H. H. Bolotin

Determinations of the lifetimes of excited nuclear states having mean lives in the range from 10^{-9} to 10^{-12} sec fall between the ranges of applicability of Doppler-shift attenuation and electronic timing methods. The long-standing difficulty of measuring lifetimes within this range is ameliorated by the use of Doppler-shift recoil-distance "plungers."

In this method, a thin target is bombarded by α particles or heavier projectiles. The product nucleus recoils forward into vacuum at a velocity anywhere from ~0.7% to 3% of the velocity of light. The recoils are quickly stopped in a metal plunger placed close to the target. De-excitation γ rays are viewed in a high-resolution

Ge(Li) detector, usually placed in the forward direction. Gamma rays that the recoiling nuclei emit in flight (i.e., prior to impinging on the plunger) suffer an increase in energy due to the full Doppler shift. Those emitted after the nucleus has come to rest in the plunger have the unshifted energy. These two displaced peaks can be resolved (in most cases) by the Ge(Li) spectrometer. The ratio of the shifted and unshifted lines, as a function of target-to-plunger distance yields the lifetime of the excited state. Since virtually the entire spectrum of γ rays can be recorded on a large multichannel pulse-height analyzer, the lifetimes of all states that fall into the range $\sim 10^{-9} - 10^{-12}$ sec can be determined simultaneously. The plunger design must allow for distances of only a few thousandths of an inch to be measured to a precision of $\lesssim 0.1 \times 10^{-3}$ in. A set of these plungers has been designed and constructed to measure the lifetimes of nuclear states populated in charged-particle reactions and in Coulomb excitation by heavy ions. Successful preliminary studies prove the feasibility of such experiments at the tandem accelerator, although the available running time is limited.

A more precise plunger, now about to be tested, will define the recoil direction of the product nucleus more closely by means of charged-particle/γ-ray coincidence techniques. This plunger will initially be employed to study the lifetimes of states populated by means of Coulomb excitation by ^{16}O and heavier projectiles.

2. NUCLEAR STRUCTURE AND REACTION MECHANISMS IN THE 1p SHELL

a. Lifetime of the First Excited State in ^{8}Li

M. J. Throop,* G. C. Morrison, and D. H. Youngblood†

The attenuated-Doppler-shift technique has been utilized to measure the lifetime of the 981-keV state in ^{8}Li populated in the reaction D(^{7}Li,p)^{8}Li. After passage through a thin nickel window, the ^{7}Li beam (produced by the University of Iowa Van de Graaff) had an energy of 7.4 MeV. With a 20-cc Ge(Li) detector at 0° to the beam, the typical energy difference between the fully shifted gamma ray (from a D_2 gas target, 1.5—2.5 cm Hg) and the attenuated gamma (from a ZrD target, 110 or 140 $\mu g/cm^2$) was found to fall in the range 400 ± 150 eV, depending on experimental conditions. About 170 eV of this difference can be attributed to the difference in energy loss in the two targets. The ZrD targets were found to contain substantial amounts of oxygen with an O/Zr atomic ratio of 1.1. The calculations of energy loss and stopping power took such an oxygen content into account. The Doppler-shifted ^{8}Li peak located at 1016 keV was found to be significantly contaminated by the 2101 → 1080-keV transition in ^{18}F from the ^{12}C(^{7}Li,n) reaction. Corrections for the effect of the contaminant line were made for two separate groups of D_2 and ZrD measurements made under slightly different experimental conditions. The resulting net D_2-ZrD energy difference was 450 ± 200 eV, which leads to a deduced ^{8}Li lifetime of 10.6 ± 4.7 fsec. This lifetime is in agreement with a theoretical prediction of Kurath, and also that of Barker, although the large error limits preclude a detailed test of either prediction. A paper communicating these results is in the final stages of preparation.

---

*University of Iowa, Iowa City, Iowa.

†Texas A & M University, College Station, Texas.

b. ^{3}He-Induced Reactions in the 1p Shell

J. R. Comfort, H. T. Fortune, J. V. Maher, and B. Zeidman

Nuclei in the 1p shell are most interesting to study inasmuch as extensive model calculations exist for comparison with experimental data. In addition, previous studies of the high-excitation region of ^{12}C and ^{16}O with (^{3}He, p) reactions have shown the existence of several states not observed in other reactions. The character of these states is not well known. The present study aims to shed additional light on nuclei in the 1p shell. A 21-MeV ^{3}He beam and solid-state detectors were used to obtain data for (^{3}He, p) and (^{3}He, d) reactions on targets of ^{10}B, ^{12}C, and ^{14}N. Some (^{3}He, t) data were also acquired from the ^{10}B and ^{14}N targets. Some of the data have been analyzed already and are discussed below.

(i) ^{10}B(^{3}He, d)^{11}C Reaction

The spin of the 8.11-MeV level in ^{11}C (and its presumed mirror level at 8.57 MeV in ^{11}B) has long been assigned $J \leq \frac{5}{2}$. Data previously obtained at the Argonne cyclotron from the ^{12}C(^{3}He, α)^{11}C reaction showed that this level is populated by $\ell = 1$; this limits the spin to either $J = \frac{1}{2}$ or $\frac{3}{2}$ (with negative parity). The present data showed that the level is also populated by $\ell = 1$ in the (^{3}He, d) reaction. In view of the $J^{\pi} = 3^{+}$ assignment of the ^{10}B ground state, a unique assignment of $J^{\pi} = \frac{3}{2}^{-}$ is thus established for the 8.11-MeV state of ^{11}C. A paper reporting these results has been submitted for publication.

(ii) ^{12}C(^{3}He, p)^{14}N Reaction

Angular distributions have been extracted for levels up to an excitation energy of about 13 MeV. Those for levels with T = 1 should have shapes identical to angular distributions from the (t, p) reaction leading to their analog states, and should have cross sections about 1/6 those from the (t, p) reaction. Existing data show these expectations are well satisfied. Calculations of the two-particle transfer mechanism are proceeding in order to test wave functions obtained from model calculations.

(iii) $^{10}B(^{3}He,p)^{12}C$ and $^{14}N(^{3}He,p)^{16}O$ Reactions

The data obtained from these reactions cover excitation regions of about 15—25 MeV. Known levels in ^{12}C were confirmed. In ^{16}O, a level at about 22.7 MeV excitation, detected in the $^{14}N(d,\gamma)^{16}O$ reaction, was not observed. However, a level at 21.05 MeV excitation, previously detected in the $^{12}C(\alpha,\gamma)^{16}O$ reaction was observed. Analysis is continuing.

c. Spectroscopic Factors in the Mass-12 System

H. T. Fortune, J. E. Monahan, C. M. Vincent, and R. E. Segel

The $^{11}B(d,p)$ reaction leading to the low-lying states of ^{12}B has previously been studied in this laboratory. In a separate experiment, the excited states of ^{12}C in the 16—20-MeV region have been studied through the $^{11}B + p$ reaction. This region in ^{12}C contains the second through seventh analog states. What has been done now is to compare the two systems (Fig. 18) with the specific goal of comparing the spectroscopic factors extracted from the $^{11}B(d,p)^{12}B$ differential cross sections with the spectroscopic factors extracted from the proton widths of the analog states in ^{12}C.

A standard DWBA analysis of the (d,p) data has been done with particular care taken in choosing the potentials. The proton optical potential was taken from a p-shell optical potential, developed at Argonne, which fits the bulk of the nucleon-scattering data in the light nuclei. Since there is no well-established deuteron potential, several were tried, and it was shown that the spectroscopic factors are insensitive to the choice of deuteron potential. The final state is depicted as a nucleon moving in a Woods-Saxon well. For the $^{11}B + p$ system, R-

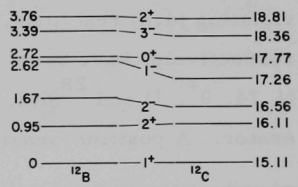

Fig. 18. Energy level diagram of ^{12}B and the ^{12}C analogs of these states.

matrix theory was used in order to connect the parameters of the analog states with the observed proton scattering widths. The proton-nucleus interaction was again represented by a Woods-Saxon well.

In both cases the well depth was varied in order to have the states with the appropriate nucleon angular momentum come at the observed energies. The same relative well depths were found for the two systems. For three of the states that were compared, the (d,p) spectroscopic factors were about 20% greater than those from the proton widths of the analog states, and the spread in values was only a few percent. On the other hand, poor agreement was found for the 2s states, for which the resonances are so broad (the width being on the order of half the energy) that resonance parameters start to lose physical meaning. If (as appears likely) we can find a number of other cases in which such comparison can be made, we will have a good method for checking the accuracy with which spectroscopic factors can be extracted from nucleon-transfer reactions.

d. Isospin-Violating (d,α) Reactions on ^{12}C and ^{28}Si

D. von Ehrenstein,* L. Meyer-Schützmeister, A. Richter,† and J. Stoltzfus

In order to test the validity of the recently proposed strong-absorption model of Noble[1] as a description of direct isospin-violating (d,α) reactions, angular distributions and excitation functions, respectively, have been measured for the reactions $^{12}C(d,\alpha)^{10}B$ (1.74, 0^+, 1) and $^{28}Si(d,\alpha)^{26}Al$ (0.23, 0^+, 1) using the tandem accelerator. A position-sensitive detector was placed in the focal plane of

---

*Now also at the Physics Department, Northern Illinois University, DeKalb, Illinois.

†On leave from the Max-Planck-Institut für Kernphysik, Heidelberg, Germany.

[1] J. V. Noble, Phys. Rev. Letters 22, 473 (1969).

the Enge split-pole spectrograph to count the α particles. In the (d,α) reaction on ^{12}C, the angular distributions at deuteron energies E_d = 14, 14.4, 14.8, 15.4, and 16 MeV (i.e., over the second large resonance-like maximum in the excitation function observed previously) all show a strong forward-peaked cross section and little cross section at backward angles. Although this would be in accordance with Noble's model, an alternative description of the angular distributions is sought in terms of two interfering compound states in ^{14}N, since recent measurements by Smith and Richards[2] indicate some contributions from the compound nucleus. No evidence of the proposed direct mechanism of the isospin-violating (d,α) reaction on ^{28}Si has been found. Excitation functions (Fig. 19) measured at $\theta_{lab} = 20^{\circ}$ and 22.5° between 12 and 17 MeV bombarding energy show structures due to fluctuations in the compound-nucleus cross section.

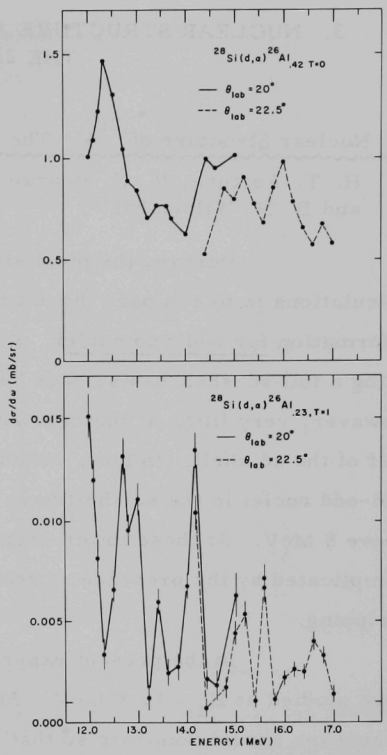

Fig. 19. Excitation functions for $^{28}Si(d,\alpha)^{26}Al$ reactions as observed at $\theta_{lab} = 20^{\circ}$ and 22.5°: (above) for the isospin-allowed reaction to the 3^+ T=0 second excited state and (below) for the isospin-forbidden reaction to the 0^+ T=1 first excited state.

[2] H. V. Smith, Jr., and H. T. Richards, Phys. Rev. Letters 23, 1409 (1969).

3. NUCLEAR STRUCTURE AND REACTION MECHANISMS IN THE 2s1d SHELL

a. Nuclear Structure of ^{20}F: The ^{19}F(d,p) Reaction

H. T. Fortune, R. C. Bearse, G. C. Morrison, J. L. Yntema, and B. H. Wildenthal*

Perhaps the most stringent test of theoretical shell-model calculations is to compare these calculations with experimental information for odd-odd nuclei. Recently, shell-model calculations, using a full sd-shell basis, have been extended through A = 22. However, very little is known about the odd-odd nuclei in the lower half of the sd shell. In fact, very few (d,p) reactions leading to odd-odd nuclei in the sd shell have been studied at bombarding energies above 8 MeV. At these lower energies, the analysis of the data is complicated by the presence of reaction mechanisms other than direct stripping.

In the present experiment, the ^{19}F(d,p)^{20}F reaction has been studied at E_d = 16.0 MeV. At this bombarding energy, direct processes should dominate so that states having large cross sections are expected to be populated mainly via direct stripping. The outgoing protons were detected in photographic emulsions in a Browne-Buechner split-pole magnetic spectrograph at 14 angles. Of the previously known 21 states below E_x = 4.3 MeV, angular distributions were obtained for all but three (those at E_x = 1.824, 2.871, and 3.176 MeV). Strong stripping angular distributions were observed for eight states—five dominantly ℓ=2 states at E_x = 0.657, 2.044, 2.196, 2.966, and 3.590 MeV (the last one having some ℓ=0 admixture) and three dominantly ℓ=0 states at E_x = 3.489, 3.531, and 4.089 MeV. The transition to the known 1^+ state at 1.056 MeV was weak, but was nevertheless dominated by ℓ=0 stripping. The state at E_x = 4.282 MeV, though weak,

*Michigan State University, East Lansing, Michigan.

TABLE I. Comparison of experimental and theoretical spectroscopic factors for $^{19}F(d,p)^{20}F$.

Experimental				Theoretical			
E_x	J^π	$(2J+1)S$		E_x	J^π	$(2J+1)S$	
		$\ell=0$	$\ell=2$			$\ell=0$	$\ell=2$
0	2^+		(0.055)	0	2^+		0.10
0.657	3^+		3.19	0.92	3^+		4.48
1.058	1^+	0.04		1.34	1^+	0.24	0.03
2.044	(2^+)		3.49	2.12	2^+		3.45
2.196	(3^+)		0.50	2.41	3^+		0.56
2.967	(3^+)		0.55	3.12	3^+		0.35
3.489	1^+	1.75	0.25	3.29	1^+	0.96	0.09
3.531	0^+	0.69		3.33	0^+	0.53	
3.590	$(2^+),(1^+)$	(0.24)	0.80	3.56	2^+		0.05
3.686	(3^+)		0.053	3.88	3^+		0.07
4.089	(1^+)	0.31	0.25	4.09	1^+	0.66	0.30
4.282	(2^+)	____	0.18	4.17	2^+	____	0.05
Sum		3.03	9.21			2.39	9.36

appeared to be dominated by $\ell = 2$. Table I shows that these ten states agree reasonably well in position and strength with the ten lowest states that recent shell-model calculations predict to have appreciable amounts of the configuration [^{19}F(g. s.)$\otimes$(1d or 2s neutron)]. The final report on this work is almost complete.

b. Study of the Low-Lying $T=\frac{3}{2}$ States in ^{21}Na

R. C. Bearse, J. C. Legg,* G. C. Morrison, and R. E. Segel

Analog states offer the opportunity to study low-lying levels of systems not readily accessible in other ways. To this end, we have been studying the $T=\frac{3}{2}$ states in $T_z = -\frac{1}{2}$ nuclei. Our previous studies[1] have shown that the rotational picture describes the low-lying

*Kansas State University, Manhattan, Kansas.

[1] G. C. Morrison, D. H. Youngblood, R. C. Bearse, and R. E. Segel, Phys. Rev. 174, 1366 (1968).

$T=\frac{3}{2}$ states in ^{25}Al. We have now extended this work to the mass-21 system. The gamma decays of the two lowest $T=\frac{3}{2}$ states in ^{21}Na at 8.97 and 9.22 MeV were studied as resonances in the ^{20}Ne(p, γ) reaction by use of a gas cell and a 30-cc Ge(Li) detector. For the lower resonance we find three branches: to the $\frac{3}{2}^+$ ground state (11%), to the $\frac{5}{2}^+$ first excited state (50%), and to the $\frac{7}{2}^+$ second excited state (39%). These results imply $J = \frac{5}{2}^+$ for the $T=\frac{3}{2}$ state. On the simple rotational model, transitions from states of the $K=\frac{1}{2}$ (Nilsson orbit #6) band are possible only to the ground-state $K=\frac{3}{2}$ (#7) band. A $J=\frac{5}{2}^+$, $K=\frac{1}{2}$ assignment for the lowest $T=\frac{3}{2}$ state fits the observed branching ratios. The second resonance decays predominantly to the ground state, and there is at most a 9% branch to the $\frac{1}{2}^+$ state at 2.41 MeV. The second resonance is assigned $J = \frac{1}{2}^+$, $K = \frac{1}{2}$. If the 2.41-MeV state is $K = \frac{1}{2}$ (#9), no transition to it is expected. On both resonances, transitions to higher excited states are obscured by background.

In conclusion, we find[2] that the rotational model which is so successful in fitting the low-lying $T=\frac{1}{2}$ states in ^{21}Na is equally successful in describing the low $T=\frac{3}{2}$ states.

[2] R. C. Bearse, J. C. Legg, G. C. Morrison, and R. E. Segel, Phys. Rev. C1, 608 (1970).

c. The ^{24,26}Mg(p, α)^{21,23}Na Reactions at 35 MeV

G. C. Morrison, R. C. Bearse, W. Pickles,* and E. Kashy*

Angular distributions of the ^{24,26}Mg(p, α) reactions, measured with 35-MeV protons from the MSU cyclotron, demonstrate that the (p, α) reaction at these energies is analogous to the direct (d, ^{3}He) reaction on an (N - 2) target; proton-hole states are strongly populated. In the ^{24}Mg(p, α) reaction, hole states of negative parity in ^{21}Na are observed at 2.80 (one member of a doublet) and 3.68 MeV. The j dependence of the (p, α) angular distribution fixes their spins and parities as $\frac{1}{2}^-$ and $\frac{3}{2}^-$, respectively, in agreement with theoretical

* Michigan State University, East Lansing, Michigan.

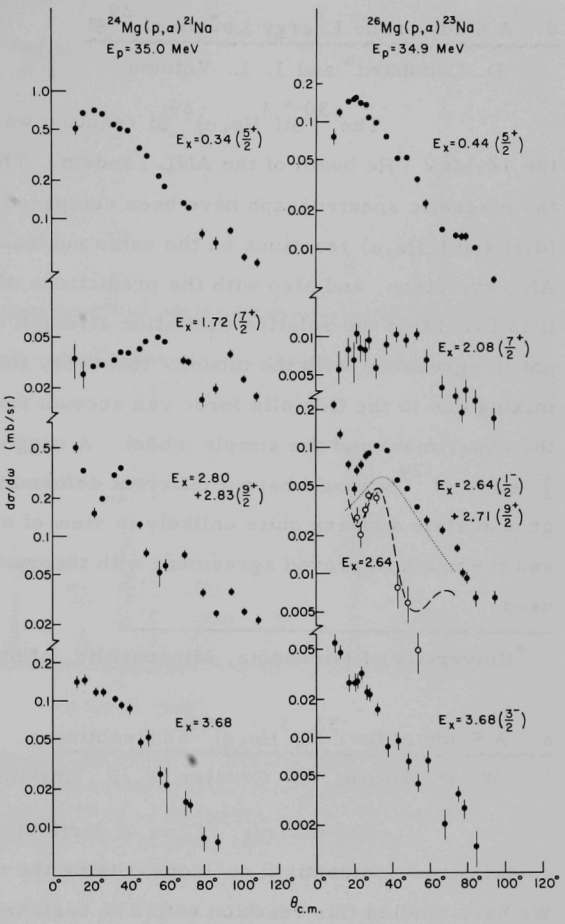

Fig. 20. Angular distributions of the ^{24,26}Mg(p,α)^{21,23}Na reactions to low-lying states in the residual nuclei.

expectations but contrary to a $\frac{3}{2}$ assignment for the mirror state of the lower at 2.79 MeV in ^{21}Ne. The ^{26}Mg(p,α) reaction to the negative-parity states at 2.64 MeV ($\frac{1}{2}^-$) and 3.68 MeV ($\frac{3}{2}^-$) in ^{23}Na confirms the j dependence. The angular distributions of the two reactions to corresponding states shown in Fig. 20 are very similar, although the cross sections of the reaction on ^{26}Mg are only 1/5 of those of the reaction on ^{24}Mg. Some reduction can be accounted for on the Nilsson model of these nuclei. Analysis of the results is being extended to higher excited states in both ^{21}Na and ^{23}Na.

d. A Study of the Energy Levels of ^{29}Si

D. Dehnhard* and J. L. Yntema

The ^{30}Si(^{3}He,α)^{29}Si reaction was investigated with the 12-MeV ^{3}He beam of the ANL Tandem. The results obtained with the magnetic spectrograph have been compared with those of the (d,t) and (^{3}He,α) reactions on the same nucleus with beams from the ANL cyclotron, and also with the predictions of the Nilsson model. It is found that the relative excitation strength of the $\frac{5}{2}^{+}$ levels is not in agreement with the model. However, indications are that band mixing due to the Coriolis force can account for discrepancies between the experiment and the simple model. A suggestion that the 4.90-MeV $\frac{5}{2}^{+}$ state of ^{29}Si would have a different deformation from the ^{29}Si ground state appears quite unlikely in view of our experimental results and the much improved agreement with theory when band mixing is used.

*University of Minnesota, Minneapolis, Minnesota.

e. A Study of the ^{33}S(^{3}He,d)^{34}Cl Reaction

W. P. Alford,* D. Crozier, J. R. Erskine, and J. P. Schiffer

The nucleus ^{34}Cl is of particular interest because it contains two nonidentical nucleons outside the closed subshell of ^{32}S. We have studied this reaction with 83% enriched ^{33}S, using the 14-MeV ^{3}He beam from the Argonne tandem Van de Graaff and detecting the deuterons in photographic emulsions placed in the focal plane of the Argonne split-pole magnetic spectrograph. The emulsions were scanned with a computer-controlled automatic plate scanner. The spectrum is shown in Fig. 21. Of particular interest in this nucleus are the odd-parity states belonging to the $d_{3/2}f_{7/2}$ configurations. When the data are completely analyzed, we hope to be able to identify these from the angular distributions.

*University of Rochester, Rochester, New York.

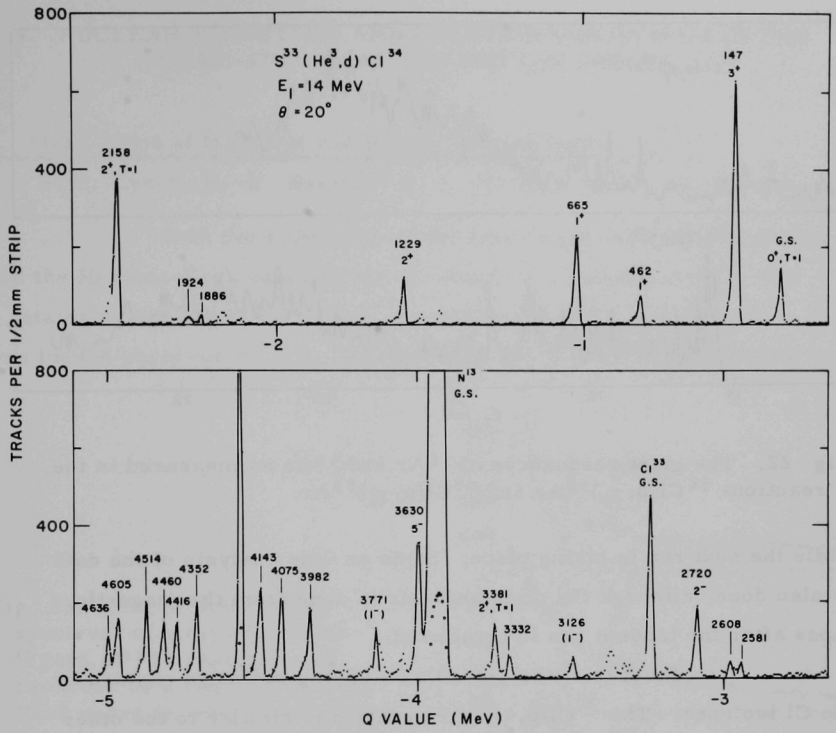

Fig. 21. Spectrum of deuterons from a ^{33}S target bombarded with a 14-MeV ^{3}He beam, as observed at 20°. Each deuteron peak corresponding to a level in ^{34}Cl is labeled with the measured excitation energy (keV) and its assigned spin and parity.

f. Giant Dipole Resonance

L. Meyer-Schützmeister, R. E. Segel, R. C. Bearse, J. V. Maher, Jr., E. L. Segel, and D. S. Gemmell

The program of studying the giant dipole resonance through radiative capture has been continuing. Large NaI crystals are used for the γ-ray detectors and extensive measurements of yield curves and angular distributions are made. The data taking is now computer controlled, with the program determining the length of the run, transferring the data to magnetic tape, and plotting the data

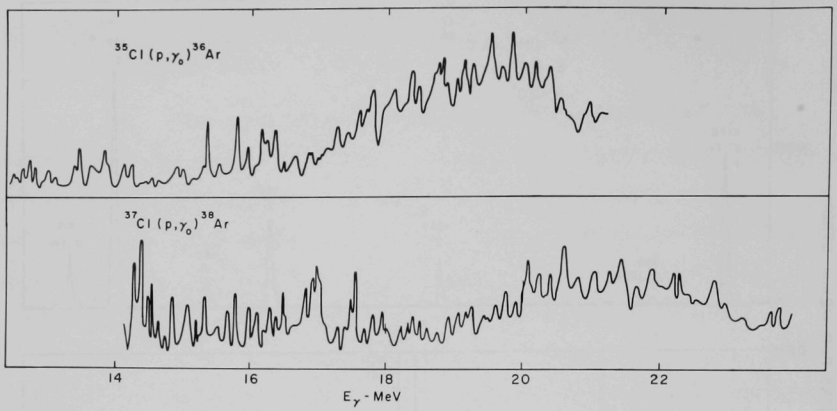

Fig. 22. The giant resonances of ^{36}Ar and ^{38}Ar as measured in the reactions $^{35}Cl(p,\gamma_0)^{36}Ar$ and $^{37}Cl(p,\gamma_0)^{38}Ar$.

while the next run is taking place. Some on-line analysis of the data is also done, although the main analysis is done from the magnetic tapes after the tandem run is completed.

Emphasis was placed on studying radiative capture by the Cl isotopes. The $^{35}Cl(p,\gamma)^{36}Ar$ reaction is similar to the other cases that we have studied in that the final nucleus has equal numbers of neutrons and protons and therefore the giant resonance has only one isospin component, namely T = 1. On the other hand, ^{38}Ar formed by $^{37}Cl(p,\gamma)$ has $T_z = 1$ and therefore the giant resonance should have T=1 and T=2 components of roughly equal strength. Comparison of the measured yield curves (Fig. 22) shows that the ^{38}Ar giant resonance is much broader than that of ^{36}Ar. This broadening is attributed to T splitting into two broad components. Our angular-distribution measurements show that in spite of this T splitting, the angular distributions from $^{37}Cl(p,\gamma)$ are just as invariant as those from $^{35}Cl(p,\gamma)$; i.e., the angular distributions continue to show little energy dependence even when the giant resonance is fragmented into components having different isospin.

4. NUCLEAR STRUCTURE AND REACTION MECHANISMS IN THE QUASI-SPHERICAL 1f2p AND 1g2d SHELLS

a. Mean Lives of the First and Second Excited States in ^{45}Ti

F. J. Lynch, K.-E. Nyström,* R. E. Holland, and R. D. Lawson

Both the rotational-model calculation of Malik and Scholz and the Hartree-Fock calculations of Johnstone predict excited $\frac{3}{2}^-$ and $\frac{5}{2}^-$ states within 200 keV of the $\frac{7}{2}^-$ ground state in ^{45}Ti. A doublet was indeed observed by Jett, Jones, Lind, and Ristinen within 40 keV

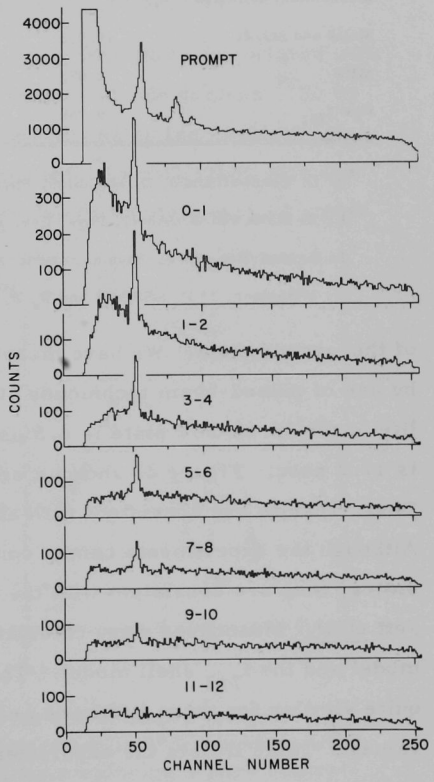

Fig. 23. Plot of pulse-height spectrum of γ rays from the ^{45}Sc(p,n)^{45}Ti reaction, as recorded by a Ge(Li) detector. Each curve is labeled with the time (μsec) measured from the end of the beam pulse. The γ-ray peak which persists in channel 51 is from the 37-keV metastable level in ^{45}Ti. The peak in channel 57 in the prompt pulse-height spectrum is from the 40-keV level of ^{45}Ti.

*Department of Physics, Institute of Technology, Otaniemi, Helsinki, Finland.

TABLE II. Electric-quadrupole and magnetic-dipole properties of the low-lying states in ^{45}Ti. The static moments are taken from a paper by Cornwell and McCullen.[a] The deformed calculation of Malik and Scholz[b] assumes $\beta = -0.35$, $g_R = Z/A$ and that the magnetic moment of the extra-core nucleons is 3/4 of its free-particle value. The shell-model calculations listed in the last two rows assume a pure $f_{7/2}$ configuration, a proton effective charge of 1.97 e and a neutron effective charge of 1.87 e. The gyromagnetic ratios of the shell-model particles are $g_p = 1.499$ nm and $g_n = 0.39$ nm. The row labeled MBZ gives the predictions obtained when the wave functions of McCullen et al.[c] are used; the last row is based on wave functions that are obtained when the interaction energies of Moinester et al.[d] are used.

	Quadrupole moment $\frac{7}{2}^-$ state (b)	Mean lifetime $\frac{3}{2}^- \rightarrow \frac{7}{2}^-$ (μsec)	Magnetic moment $\frac{7}{2}^-$ state (nm)	Mean lifetime $\frac{5}{2}^- \rightarrow \frac{7}{2}^-$ (nsec)
Experiment	$\pm(0.015 \pm 0.015)$	85 ± 10	$\pm(0.095 \pm 0.002)$	21.5 ± 1.35
Moszkowski estimate		495		0.31
Malik and Scholz	+0.092	71	-0.66	19
MBZ	-0.073	91	-0.38	6.0
New $f_{7/2}$	-0.068	86	-0.59	8.5

[a] R. G. Cornwell and J. D. McCullen, Phys. Rev. 148, 1157 (1966).

[b] F. B. Malik and W. Scholz, Phys. Rev. 150, 919 (1966); 153, 1071 (1967).

[c] J. D. McCullen, B. F. Bayman, and L. Zamick, Phys. Rev. 134, B515 (1964).

[d] M. Moinester, J. P. Schiffer, and W. P. Alford, Phys. Rev. 179, 984 (1969).

of the ground state. We have measured the mean lives of this doublet by use of pulsed-beam techniques at the tandem accelerator. The mean life of the 36.68-keV state is 4.5 μsec and that of the 40.15-keV level is 17.2 nsec. Figure 23 shows a sequence of pulse-height spectra. These results are consistent with an E2 and M1 transition, respectively. Although the experiments cannot conclusively pin down the spins of the states, they are consistent with the spins of $\frac{3}{2}^-$ and $\frac{5}{2}^-$ assigned by Jett et al. Mean lives were calculated by use of both the rotational model and the $f_{7/2}$ shell model. The predictions of the two models are quite similar for these lifetimes and are quite close to the experimental values. Table II lists the experimental and theoretical values obtained.

b. Studies of the (^{3}He,t) Reaction

Existing data suggest that the (^{3}He,t) reaction selectively populates proton-particle neutron-hole states based on the target ground state. The angular distributions in the reaction have also been observed to have a shape characteristic of the total angular-momentum transfer. The reaction can thus be a powerful tool for obtaining information about spins and dominant configurations of nuclear levels. While the mechanism is not yet fully understood, systematic studies of (^{3}He,t) reactions are providing significant information about nuclear levels and interactions.

(i) The ^{48}Ca(^{3}He,t)^{48}Sc and the ^{42}Ca(^{3}He,t)^{42}Sc Reactions

A. Richter, J. R. Comfort, and J. P. Schiffer

The structure of states other than those associated with the $(f_{7/2})^2$ configuration were studied in the odd-odd nucleus ^{48}Sc by measuring the ^{48}Ca(^{3}He,t)^{48}Sc reaction induced by the 23-MeV ^{3}He beam from the Argonne tandem. Altogether, the data taken with the Enge split-pole spectrograph showed 28 fairly strongly excited states

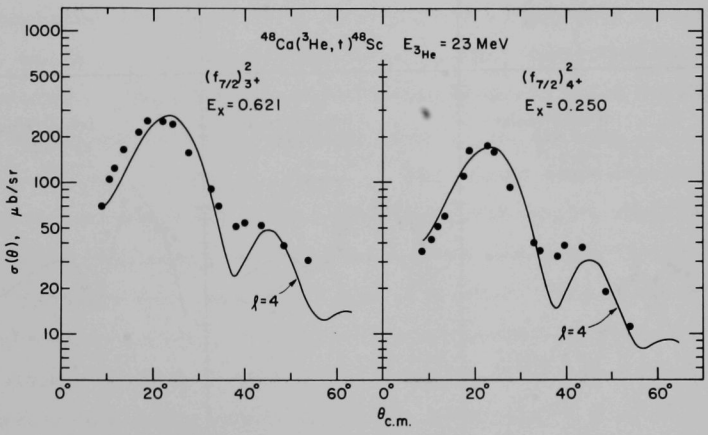

Fig. 24. Angular distribution for the 3^+ and 4^+ states belonging to the $(f_{7/2})^2$ configuration in ^{48}Sc together with microscopic DWBA calculations employing a pure central force. The transition into the odd-J (3^+) state, for which an angular momentum transfer $\ell = J \pm 1$ is possible, is described below by the higher ℓ value.

at excitation energies up to about 6.6 MeV. Eight of these belong to the $(\nu f_{7/2}^{-1})(\pi f_{7/2})$ configuration. Some angular distributions are shown in Fig. 24. The excitation of most of the other states may be expected to occur through a cross-shell (^{3}He,t) reaction in which an $s_{1/2}$ or $d_{3/2}$ neutron is replaced by an $f_{7/2}$ and odd-parity multiplets are excited. On the other hand, replacing an $f_{7/2}$ neutron with a $p_{3/2}$ or $f_{5/2}$ proton should lead to even-parity multiplets in the same region of excitation. The experimental angular distributions are at present being

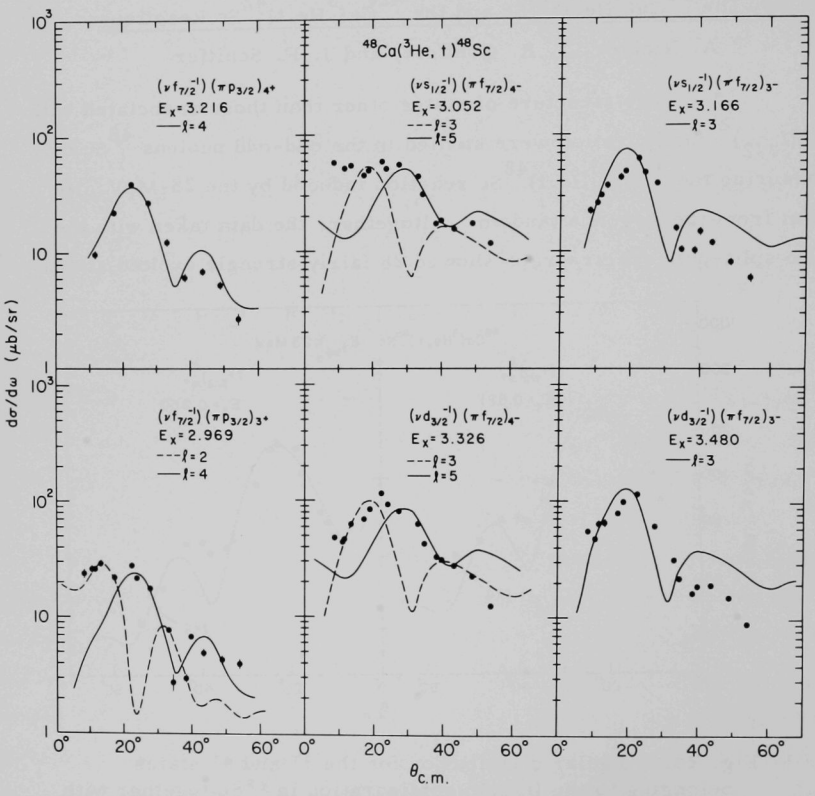

Fig. 25. Examples of angular distributions from the ^{48}Ca(^{3}He,t)^{48}Sc reaction possibly due to cross-shell transitions. Excitation energies and possible configurations as well as microscopic DWBA calculations are indicated in the figure.

analyzed in this spirit. Some of the preliminary results are shown in Fig. 25. Excitation energies and possible configurations are given with each angular distribution. Microscopic DWBA calculations for a pure central force fit the natural-parity states but the ones we assigned to be of non-natural parity seem to be a mixture of two ℓ values.

The $^{42}Ca(^{3}He,t)^{42}Sc$ reaction was studied also in order to compare the cross sections for feeding the $(f_{7/2})^{2}$ multiplet states in ^{42}Sc, which are related by a Pandya transformation to the corresponding states in ^{48}Sc.

(ii) The $^{88}Sr(^{3}He,t)^{88}Y$ Reaction

R. C. Bearse, J. R. Comfort, J. P. Schiffer, J. C. Stoltzfus, and M. M. Stautberg

This reaction has been studied with the 25-MeV ^{3}He beam of the Argonne tandem Van de Graaff. The tritons were detected in photographic emulsions in the focal plane of a split-pole spectrograph, which in turn were scanned on a computer-controlled automatic plate scanner. The proton-neutron configurations to which the final states belong were tentatively identified as $p_{1/2}g_{9/2}^{-1}$, $(g_{9/2})^{2}$, $(p_{1/2})^{2}$, $g_{9/2}p_{1/2}^{-1}$, and $p_{1/2}p_{3/2}^{-1}$. The ground-state doublet in ^{88}Y belongs to the first of the above listed configurations; its observation is one of the best examples in which so-called odd-parity "cross-shell" transitions have been seen in this type of reaction. The cross sections to these states are not at all inhibited in comparison with those to other states. A measurement of the $^{87}Sr(^{3}He,d)^{88}Y$ reaction was also undertaken. This would, of course, select states in which the neutron hole is $g_{9/2}$. We also studied the $^{89}Y(^{3}He,\alpha)^{88}Y$ reaction, which selects out the components of the wave function in which the proton is in a $p_{1/2}$ orbit. Typical spectra for these reactions leading to ^{88}Y are shown in Fig. 26. It is hoped that a detailed analysis of

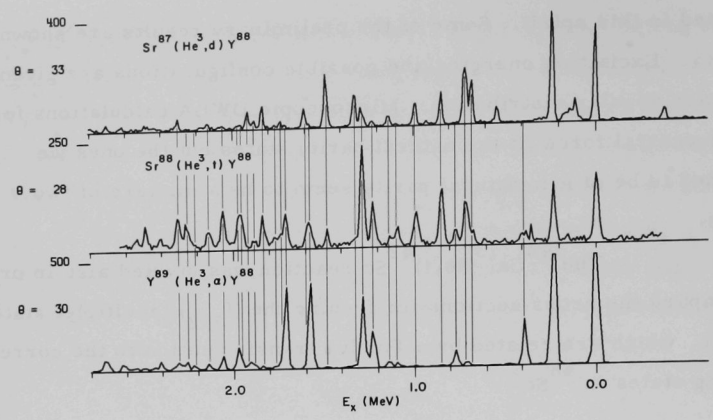

Fig. 26. Typical spectra from neutron-pickup, proton-stripping, and charge-exchange reactions leading to ^{88}Y. Levels are identified with vertical lines.

these reactions will lead us to better understanding of the ^{88}Y nucleus, which should have a rather special simplicity in view of the doubly magic nature of ^{88}Sr.

(iii) The ^{90}Zr(^{3}He,t)^{90}Nb Reaction

R. C. Bearse, J. R. Comfort, J. P. Schiffer, M. M. Stautberg, and J. C. Stoltzfus

This reaction has been studied with the 21-MeV ^{3}He beam from the Argonne tandem Van de Graaff and a position-sensitive semiconductor detector in the focal plane of a split-pole spectrograph. Nine states, apparently belonging to the $(g_{9/2})^2$ configuration, were identified. The multipole coefficients extracted from this spectrum seem to be almost identical to those extracted from the $(f_{7/2})^2$ ^{48}Sc spectrum, the only other completely known two-body spectrum in which the two orbits are identical. The quadrupole coefficients from both spectra are substantially larger than those extracted from all other known two-body spectra.

(iv) The $^{96}Zr(^{3}He,t)^{96}Nb$ Reaction

J. R. Comfort, J. V. Maher, Jr., G. C. Morrison, and J. P. Schiffer

The nucleus $^{96}_{40}Zr_{56}$ represents a relatively good closed shell of 56 neutrons with the $d_{5/2}$ subshell closure, while the proportions in which its 40 protons are split between the $(g_{9/2})^2_0$ and $(p_{1/2})^2_0$ configurations are somewhat different from those in ^{90}Zr. The Z = 40 subshell in ^{96}Zr is at least as good as the one in ^{90}Zr. The $(^3He,t)$ reaction on ^{96}Zr will select the low-lying states of ^{96}Nb, and these should belong predominantly to the

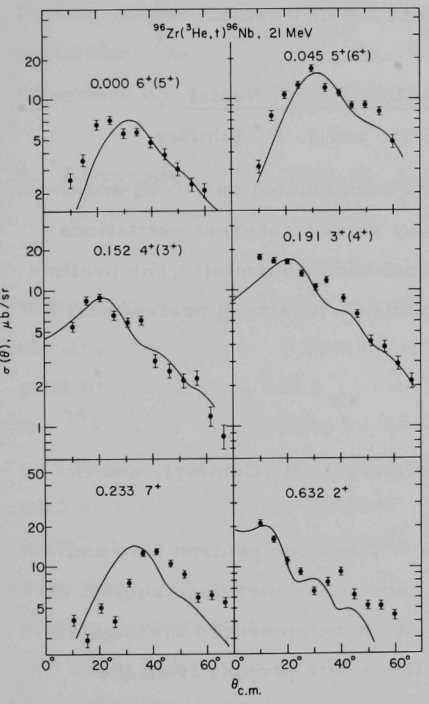

Fig. 27. Angular distributions from the $^{96}Zr(^3He,t)^{96}Nb$ reaction to states belonging to the $(\pi g_{9/2})(\nu d_{5/2})^{-1}$ configuration. The levels are identified by their excitation energies in MeV. Distorted-wave calculations and empirical rules relating to the $(^3He,t)$ reaction were used to assign spins. Alternative spin assignments are in parentheses.

TABLE III. Energies of $g_{9/2}d_{5/2}$ multiplets.

J^π	Excitation energies (keV) Nb^{92} Obs.	Pred.[a]	Obs.[b]
2^+	135	755	632
3^+	286	186	191
4^+	479	156	152
5^+	357	36	45
6^+	500	0	0
7^+	0	219	233
(2J + 1) weighted centroid	412 ± 20[c]	(-412)	-337 ± 20[d]

[a] Predicted from Nb^{92} by the Pandya transformation.

[b] Relative energies, accurate to ±5 keV.

[c] With respect to 2-particle energy from the ground-state energies of Nb^{91} [M. Moinester, J. P. Schiffer, and W. P. Alford, Phys. Rev. 179, 984 (1969)].

[d] With respect to the particle-hole energy predicted from the g.s. energies of Zr^{95} and Nb^{97}.

$(\nu d_{5/2})^{-1} \pi g_{9/2}$ configuration. Six such states were indeed identified in the experiment. The angular distributions are shown in Fig. 27. The spectrum of these states is related to the $d_{5/2} g_{9/2}$ spectrum in ^{92}Nb via the simple Pandya transformation. It is found (as seen in Table III) that this transformation is satisfied remarkably well, indeed much better than in any other part of the periodic table. The reasons for this surprisingly good agreement are not understood.

(v) The (^{3}He,t) Reaction on Non-Closed-Shell Nuclei

R. C. Bearse, J. R. Comfort, and J. P. Schiffer

The (^{3}He,t) reaction has been studied on a ^{64}Ni and a ^{120}Sn target in order to see whether any simple coherent excitations could be populated selectively in the final odd-odd nuclei. The preliminary results, taken at a few angles, indicate no strong preferential population of particular final states.

c. A Study of ^{50}V

J. W. Smith, L. Meyer-Schützmeister, J. R. Comfort, and G. Hardie*

The doubly-odd nucleus ^{50}V has one neutron hole and three proton particles outside a ^{48}Ca core and is therefore subject to reasonable shell-model calculations. We have measured the angular distributions of gamma rays in coincidence with protons from the (^{3}He,pγ)^{50}V reaction. We preferentially select levels populated by the neutron-proton pair being transferred with angular momentum $L_{np} = 0$ by positioning our particle detector at 0° with respect to the ^{3}He beam. Since the transferred neutron-proton pair may have either $S = 0$, $T = 1$ or $S = 1$, $T = 0$ and the target ground state has $J^\pi = 0^+$, $T = 2$, we expect to preferentially populate $J^\pi = 0^+$ or 1^+, $T = 2$ ($T_<$) levels and $J = 0^+$, $T = 3$ ($T_>$) levels. The $T_>$ (analog) levels are

*Western Michigan University, Kalamazoo, Michigan.

populated quite strongly and we see the gamma decay of the analogs of the two lowest 0^+ levels in ^{50}Ti. The decays of several $T_<$ levels are seen and branching ratios are being determined. Angular distributions of the charged-particle reaction $(^3\text{He},p)^{50}$V have limited the possible spin and parity values of several levels so that the gamma-decay data uniquely assign the spins and parities of a few of these levels. Further single-nucleon-transfer charged-particle reactions, in particular $(^3\text{He},d)^{50}$V and $(^3\text{He},\alpha)^{50}$V, are being investigated to determine the nucleon configuration of these levels.

d. J Dependence of ^{54}Fe(d,p)^{55}Fe and ^{50}Ti(d,p)^{51}Ti

J. L. Yntema, H. Ohnuma,* H. T. Fortune, and R. C. Bearse

The experimental data have been extended to 15 MeV with the Minnesota tandem and additional data have been taken with the Argonne tandem. It appears now that it is quite feasible to obtain good fits to the $p_{3/2}$ and $p_{1/2}$ experimental angular distributions for the ^{54}Fe(d,p)^{55}Fe reaction in the 8—12-MeV range with either surface or volume absorption in the deuteron potential. However, potentials such as the one used by Haeberli et al. do not fit the Fe data at 14—18 MeV. It is much easier to fit the ^{50}Ti(d,p)^{51}Ti angular distributions over the entire energy range. The extraction of absolute spectroscopic factors depends on the DWBA technique and on the potential types that are used, and at this point it is not evident that one can experimentally determine the appropriate procedure for the extraction of strength from distorted-wave calculations.

---

*University of Minnesota, Minneapolis, Minnesota.

e. Particle-Gamma-Correlation Measurements in fp-Shell Nuclei

Luise Meyer-Schützmeister, G. Hardie,* J. W. Smith, and J. R. Comfort

The many calculations which are available for the fp-shell nuclei make the experimental study of these nuclei attractive. We are investigating a number of these nuclei by particle-gamma-correlation measurements—in particular by using the reaction (^{3}He,pγ) in which the emitted protons are measured at 0° to the incoming ^{3}He beam. In earlier measurements at this angle, we have observed in the sd-shell nuclei that only a few states are populated strongly enough that their gamma decay can be studied. In fact, the gamma decay of the strongly populated higher excited states leads to only a few lower lying states. These states have two characteristics in common: (1) they belong to the small class of states that are strongly excited by the (^{3}He,p) reaction with a large proton yield at 0° and (2) they have the same parity as the gamma-emitting states. (Characteristic 2 was observed in all cases in which the parities of the states were known.) These observations indicate that the (^{3}He,p) reaction studied with the proton detector at 0° is very selective and that the strongly populated states have, to a large extent, relatively simple nucleon configurations so theoretical calculations should be applicable.

So far we have measured the ^{56}Fe(^{3}He,pγ)^{58}Co reaction with a gamma counter [a large Ge(Li) crystal] at 90° to the incoming beam and have analyzed the results in great detail. Very recently we measured this reaction with a gamma detector at different angles in order to determine the gamma branching ratios and, in some cases, the spins and parities of the gamma-emitting states. From these same measurements we can also extract the γ decays of a number of levels in ^{57}Co from the ^{56}Fe(^{3}He,dγ)^{57}Co reaction. We are making a detailed study of the angular distributions from ^{3}He-induced reactions leading to

---

*Western Michigan University, Kalamazoo, Michigan.

^{57}Co and ^{58}Co, namely the ^{56}Fe(^{3}He,p)^{58}Co, ^{59}Co(^{3}He,α)^{58}Co, and ^{56}Fe(^{3}He,d)^{57}Co reactions, in order to further investigate the gamma-emitting states. The results of these measurements will be compared with theoretical calculations.

f. Possible Spin Dependence in Proton Inelastic Scattering

J. C. Legg* and J. L. Yntema

An anomaly, apparently a final-state spin dependence, has been observed in proton inelastic scattering from ^{63}Cu, ^{65}Cu, and ^{67}Zn. The excited-core model of inelastic scattering cannot produce such an effect. Indeed, no current theory of inelastic scattering based on the distorted-wave Born approximation can even qualitatively predict such an effect. Subsequent experiments with deuterons have exhibited a similar result.

*Kansas State University, Manhattan, Kansas.

g. Isomeric States in ^{90}Nb

R. E. Holland and F. J. Lynch

We have begun an examination of isomers produced when a 12-MeV proton beam from the tandem impinges on a ^{90}Zr target. The system used in this investigation is suitable for activities with lifetimes from about 0.5 μsec to many seconds or minutes and thus extends the region of lifetimes which can be examined at the tandem from a fraction of a nanosecond to very long times.

Most of the activity (Fig. 28) induced in the ^{90}Zr target could be identified with previously known isomers in ^{90}Zr and ^{90}Nb. However, the radiation from the first excited state of ^{90}Nb (a γ ray of 122 keV) was observed to decay with a probability equal to the sum of two exponentials with $\tau = 98.4 \pm 8$ μsec and 24 sec. The 24-sec period is well known and arises from the decay from a higher

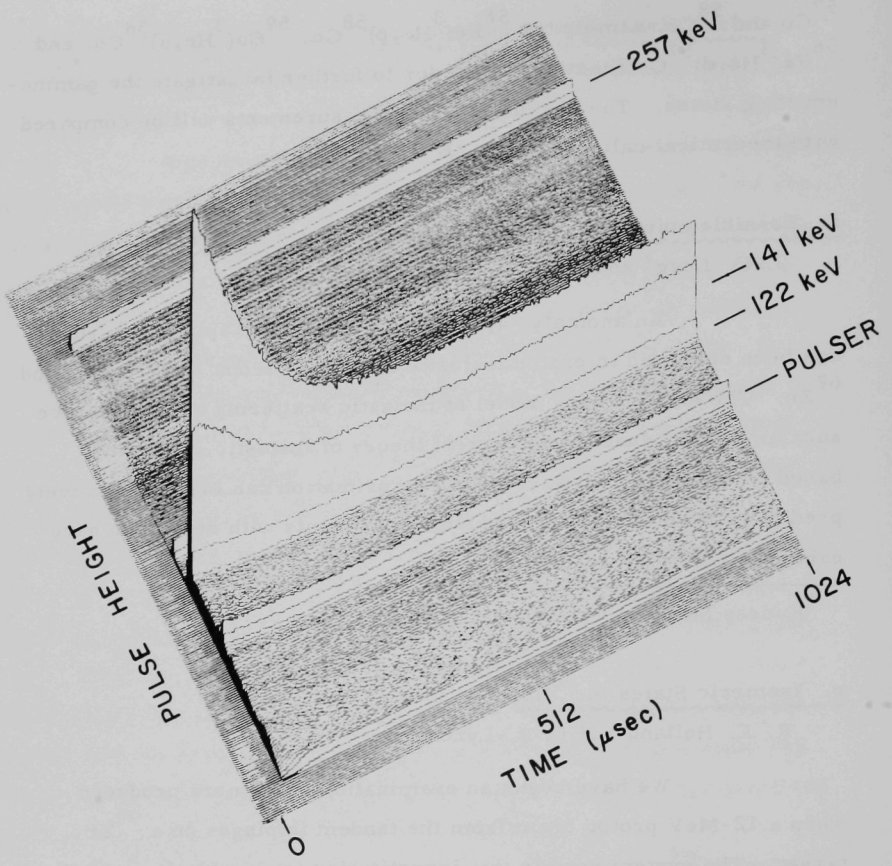

Fig. 28. An isometric plot of a 256×256-channel two-dimensional array. The number of counts from a Ge(Li) detector is plotted as a function of time (measured from the end of the beam pulse) and pulse height. The gamma ray of interest is that at 122 keV, which arises from the first excited state of ^{90}Nb. The 98.4-μsec period evident in this plot had not previously been seen. In this peak, the counts that occur at longer times arise from a well known 24-sec isomer which decays to this state. The other peaks arise from previously known isomers in ^{90}Nb and ^{90}Zr and from a pulser which injected pulses at random times.

level in ^{90}Nb to the first excited state. The 98-μsec period could arise from another level which feeds the first excited state, or it could represent the lifetime of the first excited state as directly excited in the

^{90}Zr(p,n)^{90}Nb reaction. Preliminary data indicate that the latter postulate is the correct one. If this is true, the transition (which goes from a state with spin 6^+ to one with spin 8^+) is an E2 transition which is inhibited by a factor of 100. One expects these states to be formed by coupling a $g_{9/2}$ proton and $g_{9/2}$ neutron hole. This has been confirmed by a study of the reaction ^{90}Zr(^{3}He,t)^{90}Nb described in Sec. I. D4b(iii). In the absence of a detailed computation, one estimates that such states should be connected with an E2 matrix element having nearly the single-particle value. The large inhibitions of this E2 transition would then indicate that the wave function contains large admixtures of configurations other than the $g_{9/2}$ one-particle, one-hole configuration. This is unexpected since the nucleus ^{90}Zr is thought to represent a closed shell. We plan to pursue the study of this isomer and other isomers in nuclei in this neighborhood.

h. Particle-Hole Multiplets and (d,α) Reactions in the A ≈ 90 Region

J. R. Comfort, J. V. Maher, G. C. Morrison, and H. T. Fortune

Angular distributions of the (d,α) reactions on ^{90}Zr, ^{92}Mo, and ^{98}Mo targets have been obtained with the Enge split-pole spectrograph and 17-MeV deuterons from the Argonne tandem. The spectrum of the reaction on ^{92}Mo is shown in Fig. 29. The targets were rolled foils of thickness 200—250 μg/cm^2. Particle-hole multiplets in ^{88}Y, ^{90}Nb, and ^{96}Nb observed in the (^{3}He,t) reaction are also excited in the (d,α) reaction. However, the fact that the (d,α) reaction is prohibited from populating even-spin states of j^2 configurations makes possible a test of the purity of configuration assignments. For example, the 970-keV state of ^{88}Y identified in the (^{3}He,t) reaction as the $J^\pi = 4^+$ member of the $(g_{9/2})^2$ multiplet, is unobserved in the (d,α) reaction. The analysis should be completed soon.

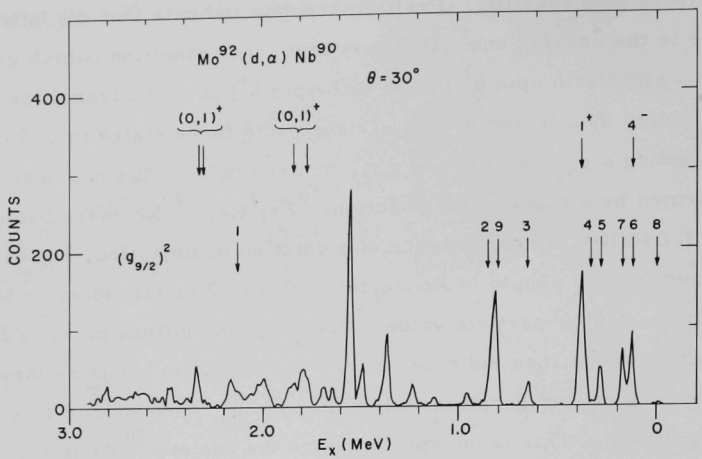

Fig. 29. Spectrum of the ^{92}Mo(d,α)^{90}Nb reaction observed at 30°. Positive-parity states of the $(g_{9/2})^2$ configuration are indicated by the lower group of levels, and other known states by the upper group. As expected, the 8^+ and 4^+ states are weakly populated. The 6^+ state is obscured by a strong 4^- state. The sizeable cross section of the 2^+ state indicates configuration mixing.

i. ^{86}Sr(^{3}He,d)^{87}Y Reaction at 20 MeV

J. R. Comfort, J. V. Maher, and G. C. Morrison

Angular distributions for the ^{86}Sr(^{3}He,d)^{87}Y reaction have been obtained with the Enge split-pole spectrograph and the 20-MeV ^{3}He beam from the Argonne tandem. ^{87}Y has not been extensively studied previously and is of particular interest because of the possible shell closure of the 38-proton configuration. States of strong excitation in ^{87}Y are observed at E_x = 0.00 (ℓ = 1), 0.38 (ℓ = 4), 0.79 (ℓ = 3), 0.98 (ℓ = 1), 1.15 (ℓ = 2), 2.91 (ℓ = 2), and 3.00 MeV (ℓ = 2). DWBA fits to the first five levels are shown in Fig. 30. A detailed comparison between stripping strengths and strengths found in the ^{88}Sr(^{3}He,d)^{89}Y is in progress.

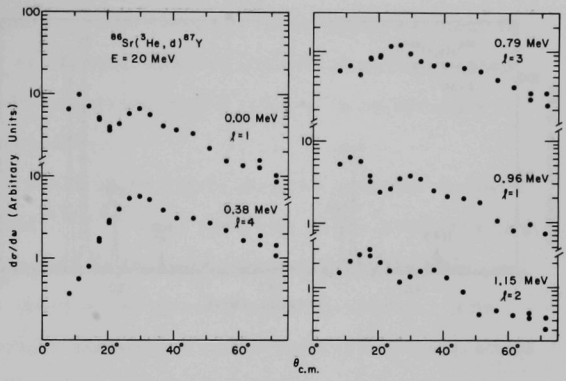

Fig. 30. DWBA fits to the first five levels of ^{87}Y formed in the ^{86}Sr(^{3}He,d) reaction.

5. NUCLEAR STRUCTURE AND REACTION MECHANISMS IN DEFORMED HEAVY NUCLEI

a. The (p,t) Reaction on Deformed Nuclei

J. R. Erskine, A. Friedman,* J. V. Maher, J. P. Schiffer, and R. H. Siemssen

Two-neutron transfer in deformed nuclei can be studied from several points of view. In the present experiment we have concentrated on searching for excited 0^+ states that are populated with a cross section that is appreciable compared to the ground-state cross section. Such states have been seen in earlier work in two sets of circumstances. The first is in the transition region between spherica and deformed nuclei, in which excited 0^+ states have been seen and interpreted as arising from the mixing between the two shapes—the best example being in the Sm isotopes. The second is in the middle of the rare-earth deformed region where excited 0^+ states were seen in the Yb isotopes, where their presence is explained by a minor gap in the spacing of Nilsson orbits.

---

*Chemistry Division.

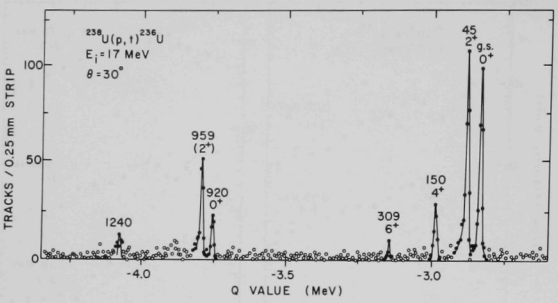

Fig. 31. Spectrum of tritons from the ^{238}U(p,t)^{236}U reaction. The target was 35 μg/cm² of ^{238}U evaporated onto a carbon foil. The peaks are labeled by the excitation energies (keV) and spins of the corresponding states in ^{236}U.

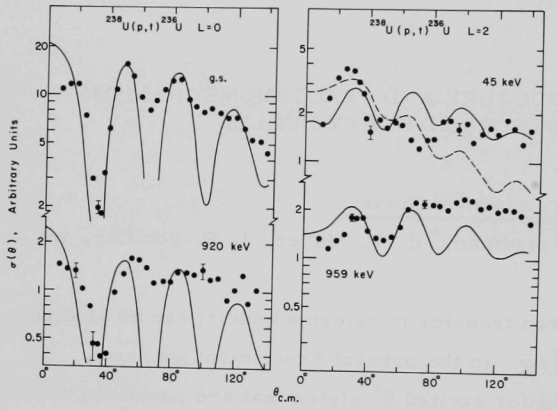

Fig. 32. Angular distributions for the ^{238}U(p,t)^{236}U reaction. The relative yields for the various experimental data sets are correctly shown. The DWBA curves were calculated with a spherical $3d_{5/2}$ form factor for the solid curves and $1j_{15/2}$ for the dashed curve. Relative error bars are shown on a few representative points.

We have searched in both types of nuclei. The nuclei ^{180,182,184}W and ^{196}Pt are on the upper boundary of the deformed region. We have studied the (p,t) reaction with 17-MeV protons from the ANL tandem Van de Graaff, detecting the tritons with a split-pole spectrograph. Their tracks in emulsions were counted by the automatic plate scanner. The results show no 0^+ states populated with more than a few percent of the ground-state cross section. Unlike the Sm isotopes, deformation changes only very slightly with neutron number but varies much more rapidly with proton number. This suggests that

the overlap between ground states of isotopes of the same element is rather good, even if they are mixed between spherical and deformed shapes; perhaps one should expect excited 0^+ states to be strongly populated in the $(^3He,n)$ reaction.

In the (p,t) reaction on six even-even actinide targets (^{230}Th, $^{234,236,238}U$, and $^{242,244}Pu$), the yield of the $\ell=0$ transition to the first 0^+ state at $E_x \approx 900$ keV in each case was found to be approximately 15% of the yield of the ground-state transition. The observation of such uniformly strong $\ell=0$ transitions is not understood in terms of present models. The spectrum of tritons from the $^{238}U(p,t)^{236}U$ reaction is shown in Fig. 31 and the associated angular distributions are displayed in Fig. 32.

b. Single-Nucleon Transfer Reactions on Deformed Rare-Earth Nuclei

J. R. Comfort, J. R. Erskine, J. V. Maher, and R. H. Siemssen

Most studies of transfer reactions on the deformed rare-earth nuclei have been limited to a few angles only and to low bombarding energies ($\leq$12 MeV). Level assignments have often been based on a comparison between the experimental "signatures" and the Nilsson model rather than on measurements of spins, and thus are model dependent. The present systematic study, in which we measure (d,p) angular distributions on a series of rare-earth nuclei, is aimed at determining these spectroscopic properties and includes a search for j-dependent effects and for a possible dependence of the angular distributions on the Nilsson orbit into which the transferred particle is captured. Indications of such effects had been found in a previous study of the $^{182}W(d,p)^{183}W$ reaction at 12 MeV in this laboratory. In the present investigation we have repeated these measurements at 16 MeV with the split-pole magnetic spectrograph and have found effects similar to those observed at 12 MeV. Measurements on neighboring nuclei are under way.

In our study of the spectroscopy of the rare-earth nuclei, we are particularly interested in the excited states above 1 MeV of which very little is known. Until very recently it had been thought that the spectra at these excitation energies would be hopelessly complex as a result of the high level densities in the deformed odd-A nuclei; but now there are some indications that single-nucleon transfer selectively populates only states belonging to simple configurations.

For the investigation of the higher excited states, studies with Coulomb stripping are also planned. Since these experiments are made at very low bombarding energies and at backward angles, they offer the advantages of better resolution and freedom from carbon and oxygen contaminants in the spectra up to about 3 MeV excitation.

(i) Energy Levels of ^{181}W Observed with the (d,t) and (p,t) Reactions

J. R. Erskine

The energies and single-particle excitations of ^{181}W were investigated with the split-pole magnetic spectrograph and the automatic plate scanner. This is a continuation of the earlier (d,p) studies on ^{183}W, ^{185}W, and ^{187}W.

Angular distributions of the ^{182}W(d,t)^{181}W reaction were recorded at 14 MeV. These data (resolution width = 10 keV FWHM) allowed ℓ values to be determined for most of the observed levels. Excitation energies and differential cross sections derived from the (d,t) data were sufficient to identify the hole states $\frac{9}{2}$+[624], $\frac{5}{2}$-[512], $\frac{1}{2}$-[521], and $\frac{7}{2}$-[514] at 0, 365, 386, and 408 keV, respectively. However, the particle state $\frac{1}{2}$-[510], expected on the basis of systematics to lie at an excitation of 200—400 keV, was not observed in the (d,t) data. Consequently, the ^{183}W(p,t)^{181}W reaction was studied at 17 MeV bombarding energy. A strong peak with an L=0 angular distribution was seen at 457 keV excitation, the presumed band head of the $\frac{1}{2}$-[510] state.

Further experiments are planned to investigate the single-particle properties, deformed wave functions, and vibrational excitations of nuclei in the rare earth region.

(ii) Study of Levels in ^{182}Ta with the ^{181}Ta(d,p)^{182}Ta Reaction

J. R. Erskine

New data have been taken with the ^{181}Ta(d,p)^{182}Ta reaction to try to understand the discrepancy between recent results

of ^{181}Ta(n, γ) studies and an old investigation of the ^{181}Ta(d, p)^{182}Ta reaction by the author. The split-pole magnetic spectrograph and the automatic plate scanner were used to obtain these data. In the original study made at 7 MeV bombarding energy, states at 99 and 115 keV were assigned $J^{\pi} = 4^-$ and 5^-, respectively. These assignments were made by comparing calculated differential cross sections with the measured cross sections. The angular distributions gave no information on the ℓ value. Recently, however, the ^{181}Ta(n, γ)^{182}Ta reaction has been studied at Argonne as well as at other laboratories. These studies indicated that both the 99- and 115-keV states were $J^{\pi} = 4^-$, in conflict with the earlier (d, p) assignments.

Since the reaction mechanism and the shape of the angular distributions for the ^{181}Ta(d, p)^{182}Ta reaction were similar to those for the ^{182}W(d, p)^{183}W reaction, previously studied in detail at 12 MeV, the new data were taken at this same energy. These data (particularly the portion taken at forward angles) show that the ground state and the excited states at 115 and 292 keV were excited predominantly by $\ell = 1$ transfers. All other states were predominantly $\ell = 3$. This ℓ-value information agrees with a new nuclear-structure calculation in which both the 99- and 115-keV state have $J^{\pi} = 4^-$. The previous 4^- and 5^- assignments were traced to an obscure error in sign in the old calculations.

^{182}Ta is the first odd-odd nucleus for which one has information on ℓ values as well as differential cross sections and precise energies so that a stringent test of the single-particle rotational model can be made. Further studies of odd-odd deformed nuclei, including ^{180}Ta, ^{166}Ho, and ^{164}Ho, are planned.

(iii) ^{3}He-Induced Reaction in Rare-Earth Nuclei

J. R. Erskine, A. M. Friedman,* and B. Zeidman

Analysis of preliminary data for the (^{3}He, α) reaction on rare-earth nuclei showed that high ℓ values are preferentially

*Chemistry Division.

excited, while other neutron-transfer reactions accentuate low ℓ values. The $\ell = 5$ [505] state which had previously been elusive was clearly identified as well as the high-spin components of several other Nilsson orbitals. Together with previous work in this region, the present data allow more precise determination of input parameters which are used in theoretical calculations of the properties of deformed nuclei.

c. Coulomb Excitation of ^{185}Re and ^{187}Re

H. H. Bolotin, D. A. McClure, and G. B. Beard

Some of the levels below ~1 MeV in the odd-mass nuclides ^{185}Re and ^{187}Re have been suggested as candidates for $(K_0 + 2)$ and $(K_0 - 2)$ γ-vibrational states, and the vibrational characteristics of levels in this mass region are of continuing theoretical interest. In an attempt to elucidate their nature more definitively, we have studied these states by Coulomb excitation both by α particles and by ^{16}O ions from the tandem. The de-excitation γ rays were viewed with a large-volume high-resolution Ge(Li) detector. The preliminary results from the partially completed analysis of the data disagree with the older Coulomb-excitation studies—which were conducted with poor-resolution NaI(Tl) scintillators—for all but the first two excited states of each nucleus. In addition, states not reported in these earlier studies have been observed to be populated in the present work. Further studies, including angular distributions of the de-excitation γ rays, will follow in an attempt to make definitive spin assignments. Complete analysis of the present data will result in B(E2) values of the observed excitations.

d. Search for Induced Alpha Emission

P. Kienle, A. Richter, and J. P. Schiffer

The possibility of inducing alpha emission from a nucleus by the presence of a heavy projectile has not been investigated

in any detail. We have sought such an effect by bombarding various targets in the A ≈ 160 region with oxygen beams with energies 20—30% below the Coulomb barrier and looking for characteristic residual activities with a Ge(Li) gamma spectrometer and a Si(Li) x-ray spectrometer. The lack of any evidence for such a process enables us to set an upper limit well below a microbarn on its cross section. Induced activities arising from a few ppm of light contaminants prevented us from setting the limit appreciably lower.

e. Coulomb Stripping Studies of Heavy Nuclei

J. R. Erskine

An investigation of energy levels in ^{210}Bi has been started to determine the origin of levels above 2.2 MeV excitation. Most levels in this good near-closed-shell nucleus observed in a previous (d,p) study by the author could be attributed to simple hole-particle excitations. However, the cluster of levels observed near 1.9—2.2 MeV excitation contained three more states than could be attributed to the $h_{9/2}d_{5/2}$ configuration. Recent information on the character of vibrational excitations in nuclei near ^{208}Pb can probably furnish an explanation of the extra levels. However, new data were needed for ℓ-value determinations.

Yield curves of the ^{209}Bi(d,p)^{210}Bi reaction at 7—10.5 MeV bombarding energies have been taken with the split-pole magnetic spectrograph at 120° and 140°. The slope of these yield curves should determine the ℓ value of the transferred neutron, as was shown by Hering in the case of the ^{207}Pb(d,p)^{208}Pb reaction. Analysis of these data is incomplete.

Further Coulomb stripping studies have been started with the ^{238}U(d,p)^{239}U and ^{238}U(d,t)^{237}U reactions in the hope of learning something of the deformed wave functions in these nuclei. This can be done directly since the Coulomb stripping reaction has the

advantage that no uncertainties exist in the extraction of spectroscopic factors. At the same time, the low bombarding energy usually means that data will have excellent energy resolution.

6. STUDIES WITH HEAVY-ION BEAMS

a. Heavy-Ion Scattering

The scattering of heavy ions has attracted much renewed interest recently as a result of the observation of pronounced gross structure in the $^{16}O + {}^{16}O$ excitation functions.[1] The investigations

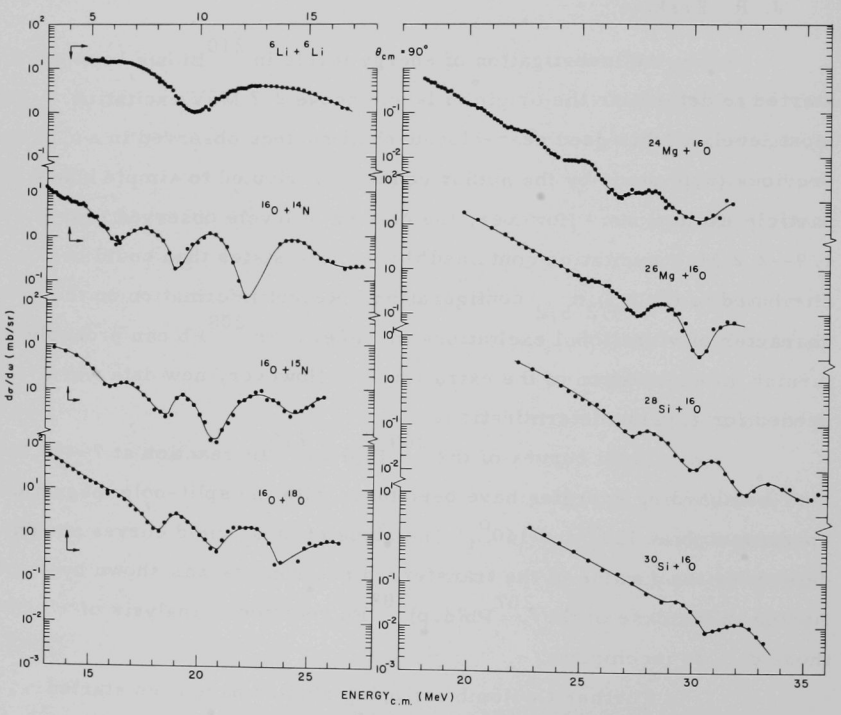

Fig. 33. Comparison of the 90° excitation functions for all systems studied. The curves have no theoretical significance.

[1] R. H. Siemssen, J. V. Maher, A. Weidinger, and D. A. Bromley, Phys. Rev. Letters 19, 369 (1967).

reported here are performed with the apparatus described in Sec. I. D1g; they are part of a continuing study aimed at obtaining a better understanding of the heavy-ion/nucleus interaction. In particular, we are interested in determining whether or not effects similar to those observed in the $^{16}O + ^{16}O$ scattering are present in the scattering of other systems of identical and nonidentical particles. The excitation functions for the systems studied are shown in Fig. 33.

Traditionally, heavy-ion scattering has been analyzed with two models which, in their extreme forms, are contradictory to each other. One is the strong-absorption model and its derivatives, the various diffraction models. The other is the potential-scattering model. In the strong-absorption model, the predominant process between two interacting heavy ions is absorption, and as a consequence we have diffraction if the surfaces of the colliding ions are well defined. In the extreme form of the potential model, the heavy ions maintain their identity even as they deeply interpenetrate. The optical model is capable of describing both extremes. One aim of this work is to seek evidence for or against these various models.

(i) $^{6}Li + ^{6}Li$ Elastic Scattering

G. C. Morrison, H. T. Fortune, and R. H. Siemssen

In the interpretation of the $^{16}O + ^{16}O$ scattering, possible parallels with the scattering of α particles from ^{4}He have been pointed out. The phenomenological potentials derived for this system are ℓ-dependent and cored. After $^{4}He + \alpha$, the lightest identical-particle system accessible to scattering studies is $^{6}Li + ^{6}Li$. An investigation of this system is therefore of particular interest. However, in contrast to the $\alpha + ^{4}He$ system in which no channels are open below ~15 MeV (c.m.), one will

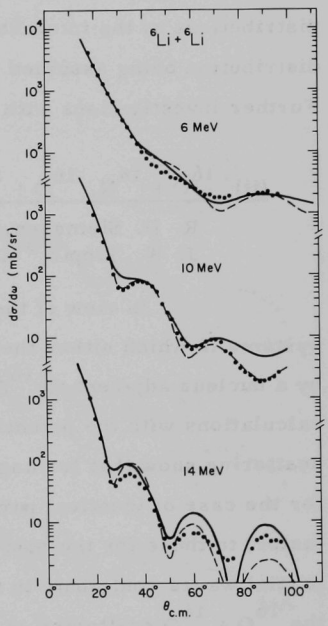

Fig. 34. $^{6}Li + ^{6}Li$ angular distributions measured at c.m. energies of 6, 10, and 14 MeV. The solid and dashed curves represent optical-model calculations with two different sets of parameters.

expect the $^{6}Li + {}^{6}Li$ scattering to be dominated by absorption due to breakup of ^{6}Li. This is indeed borne out by the optical-model analysis of our data.

Excitation functions have been measured at 60°, 70°, 80°, and 90° in 250-keV steps from 6 to 17 MeV (c.m.) and angular distributions (Fig. 34) were obtained at 6, 10, and 14 MeV. The excitation functions are rather featureless, though a broad gross-structure peak centered around 14 MeV is seen in the one taken at 90°. Optical-model calculations led to an imaginary potential with a shape which is very similar to that obtained from folding the two matter distributions of the interacting ^{6}Li ions into each other, the matter distribution being assumed to be the same as the charge distribution. Further investigations with such microscopic potentials are under way.

(ii) $^{16}O + {}^{14}N$, $^{16}O + {}^{15}N$, and $^{18}O + {}^{16}O$ Scattering

R. H. Siemssen, H. T. Fortune, R. Malmin, A. Richter, J. W. Tippie,* and P. P. Singh†

In view of the $^{16}O + {}^{16}O$ results, an investigation of systems in which either the ^{16}O target or the ^{16}O projectile is replaced by a nucleus adjacent to ^{16}O is of special interest. Optical-model calculations with the potential that best reproduces the $^{16}O + {}^{16}O$ scattering show that for angles $\leq 90^{\circ}$ the gross structures predicted for the case of identical particles are very similar (except for a scaling factor) to those for the nonidentical-particle case, although only even-ℓ partial waves contribute in the identical-particle scattering. Therefore the $^{16}O + {}^{16}O$ scattering can readily be compared with the scattering of ^{16}O from neighboring nuclei, and a study of these systems becomes of special interest.

---

*Applied Mathematics Division.

†Indiana University, Bloomington, Indiana.

Beams of ^{14}N, ^{15}N, and ^{16}O have been accelerated to measure the $^{16}O + ^{14}N$, $^{16}O + ^{15}N$, and $^{18}O + ^{16}O$ scattering. Excitation functions have been obtained for at least five angles for all systems studied, and angular distributions have been measured at several energies. Very pronounced gross structure is found in the excitation functions of all the systems. In contrast to results of the $^{16}O + ^{16}O$ scattering, however, the gross structure is more regular and in better agreement with the optical-model predictions. Calculations with the $^{16}O + ^{16}O$ potential give a good description of the $^{16}O + ^{18}O$ data, although for best agreement an energy-dependent real potential (increasing with energy) has to be introduced for all systems.

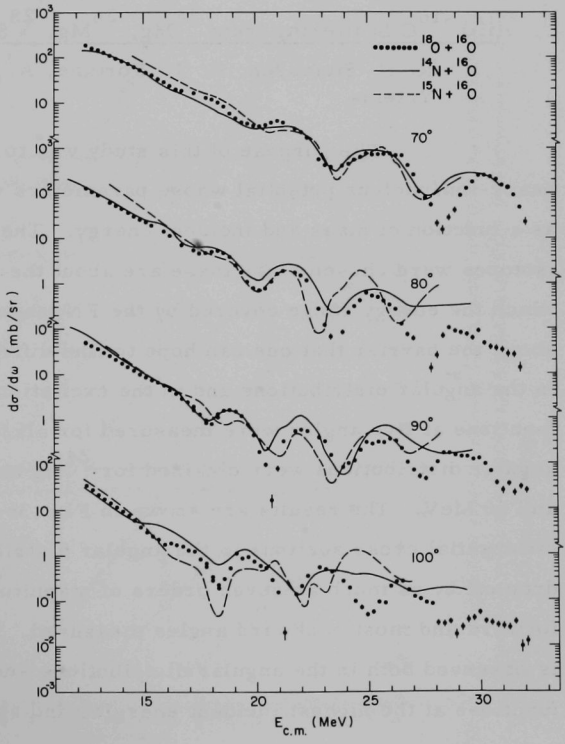

Fig. 35. Comparison of the excitation functions for $^{16}O + ^{14}N$, $^{16}O + ^{15}N$, and $^{16}O + ^{18}O$. The ^{14}N and ^{15}N data have been shifted in energy to compensate for differences in barrier height, and the data have been normalized to each other.

Most strikingly, there is a close similarity in the gross structures of the excitation functions from the different systems for angles $\lesssim 90^{\circ}$, as can be seen in Fig. 35. A common difficulty in heavy-ion scattering is that one often cannot exclude competing reaction modes such as compound elastic scattering and elastic (Q = 0) transfer processes, which coherently add to the potential-scattering amplitude. From the similarity of the $^{16}O + ^{18}O$ and the $^{16}O + ^{14}N$ excitation functions it can be concluded that the same (simple) mechanism is responsible for the gross structure, independent of the microscopic properties of projectile and target. Hence these data offer the possibility of determining the heavy-ion/nucleus interaction potentials (aside from the ever-present ambiguities) with greater confidence.

(iii) ^{16}O Scattering from ^{24}Mg, ^{26}Mg, ^{28}Si, and ^{30}Si

R. H. Siemssen, H. T. Fortune, A. Richter, and J. L. Yntema

The purpose of this study was to search for a consistent heavy-ion/nucleus potential whose parameters vary systematically as a function of mass and incident energy. The even-A Mg and Si isotopes were chosen since these are about the heaviest nuclei for which the energy range covered by the FN tandem is still sufficiently above the barrier that one can hope to find diffraction structure both in the angular distributions and in the excitation functions. Excitation functions at five angles were measured for all four isotopes, and angular distributions were obtained for ^{24}Mg and ^{26}Mg at 35, 40, 45, and 50 MeV. The results are shown in Fig. 36. At 50 MeV the differential cross sections in the angular distributions were found to drop off by as much as seven orders of magnitude between the most forward and most backward angles measured. Diffraction-like structure is observed both in the angular distributions and in the excitation functions at the highest incident energies and at the most backward

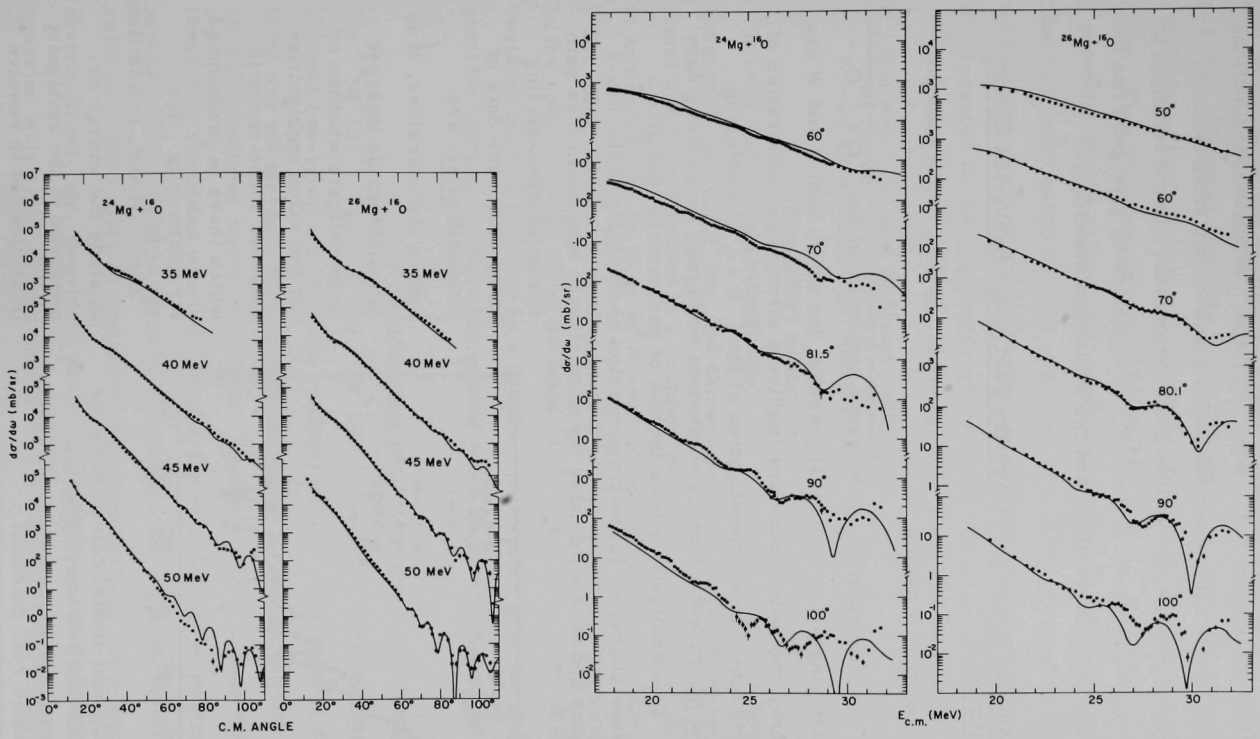

Fig. 36. Angular distributions (left) and excitation functions (right) for $^{24,26}Mg + ^{16}O$ scattering. The curves are optical-model calculations with parameters very similar to those used to fit the $^{14,15}N + ^{16}O$ scattering.

angles. Most strikingly, the ^{26}Mg, ^{28}Si, and ^{30}Si excitation functions are very similar to each other but differ significantly from those of ^{24}Mg. Optical-model calculations with parameters almost identical to those used in the analysis of the ^{14}N + ^{16}O scattering give good fits to the ^{26}Mg angular distributions and the excitation functions.

(iv) Ambiguities in the Imaginary Part of the Heavy-Ion Optical Potential

J. V. Maher, R. H. Siemssen, M. Sachs,* A. Weidinger,* and D. A. Bromley*

The analysis of the gross structure in the ^{16}O + ^{16}O elastic scattering led to an optical potential for which both V and W are very shallow, and which therefore implies a strong interpenetration of the colliding ions. In an investigation of the ^{10}B + ^{16}O scattering, Krubasik et al. recently found a continuous ambiguity in the imaginary potential. This ambiguity allows the use of parameters that give a black-nucleus character to the transmission coefficients of the low-ℓ partial waves and thus eliminates the anomalously long mean free path of the interpenetrating ions. Since the data of Krubasik et al. are rather structureless, it is of considerable interest to investigate whether or not the same ambiguities exist for those cases in which there is pronounced structure (e.g., for ^{16}O + ^{16}O) and, in addition, to study the energy dependence of the ambiguity in an attempt to resolve it.

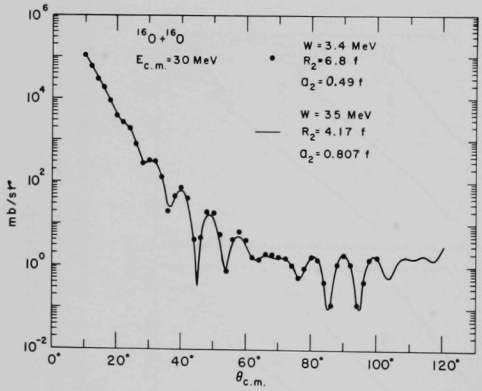

Fig. 37. Optical-model calculations for ^{16}O + ^{16}O with two very different imaginary form factors and well depths but the same real potential.

*Yale University, New Haven, Connecticut.

As seen in Fig. 37, optical-model calculations employing synthetic cross sections computed from the $^{16}O + {}^{16}O$ potential show that the same ambiguities in the imaginary potential exist even for this extreme case. Thus it is possible to describe the $^{16}O + {}^{16}O$ scattering with a potential that is effectively "black" to the low-ℓ partial waves. The "surface" partial waves are non-monotonic functions of energy; they appear to arise from potential-scattering effects not easily incorporated in the framework of the cutoff model.

b. Nucleon-Transfer Reactions with ^{6}Li

K. -O. Groeneveld, A. Richter, and B. Zeidman

In the initial experiments, targets of ^{14}N, ^{12}C, ^{16}O, and ^{11}B were bombarded with 32-MeV ^{6}Li ions from the FN tandem. Emergent ^{6}Li, ^{7}Li, ^{7}Be, and some heavier reaction products were simultaneously detected in a counter telescope. The (^{6}Li, ^{7}Li) reaction is analogous to a (p, d) or (d, t) neutron-pickup reaction, while the (^{6}Li, ^{7}Be) reaction is analogous to a (d, ^{3}He) proton-pickup experiment. In the spectra (Fig. 38) of detected ^{7}Li or ^{7}Be, each state of the residual nucleus appears as a doublet corresponding to the mass-7 particle leaving in either the ground state ($\frac{3}{2}^-$) or first excited state ($\frac{1}{2}^-$).

Angular distributions (Fig. 39) have been obtained for the $^{14}N(^{6}Li, ^{7,7*}Li)^{13}N$ and $^{14}N(^{6}Li, ^{7,7*}Be)^{3}C$ reactions leading to several low-lying states in the residual nuclei. The angular distributions are all strongly forward peaked and show the oscillatory behavior characteristic of direct reactions. Together with previous data, these new reactions provide a means for elucidating the reaction mechanism involved in transfer reactions with complex nuclei. The ratio of ground-state to excited-state cross section, the angular distributions, etc. provide a probe for examining the details of the reaction which may depend upon a spin-spin interaction or perhaps

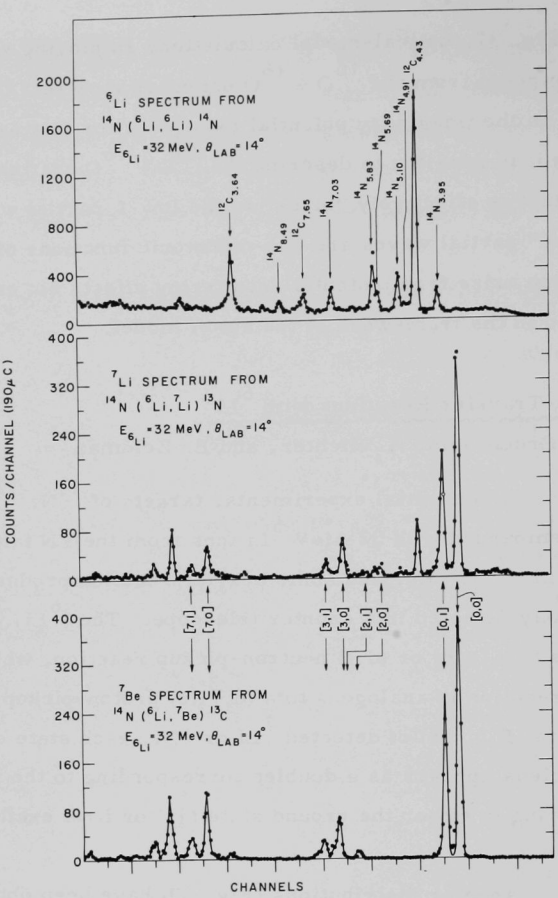

Fig. 38. Spectra from ^{6}Li-induced reactions on ^{14}N. Spectra for the reactions ^{14}N(^{6}Li,^{6}Li')^{14}N, ^{14}N(^{6}Li,^{7}Li)^{13}N, and ^{14}N(^{6}Li,^{7}Be)^{13}C were obtained simultaneously by use of a counter telescope. The notation used in labeling the spectra involving nucleon-transfer reactions of the form ^{14}N(^{6}Li, C)D is that the double index [i,j] linked with the peaks in the D spectrum indicates that D is left in its ith excited state and C in its jth excited state. As anticipated, only the negative-parity states of ^{13}C and ^{13}N are strongly excited.

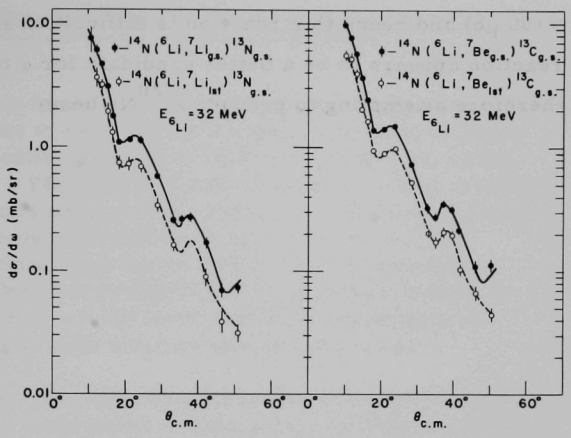

Fig. 39. Angular distribution for the (^{6}Li, ^{7}Li) and (^{6}Li, ^{7}Be) reactions on ^{14}N, which involve single-nucleon transfer leading to the mirror ground states of mass-13 nuclei. The curves through the data points are very similar for all transitions. The major deviation occurs at angles near 50°, where the excited-state transitions continue to fall while those for the ground-state transition indicate the beginning of another oscillation.

even mutual deformation of the two relatively large projectiles. In order to establish a base for detailed analysis, comprehensive study of a number of 1p-shell and 2s1d-shell nuclei is under way.

c. The ^{40}Ca(^{16}O, ^{12}C)^{44}Ti Reaction and States in ^{44}Ti

A. M. Friedman,* H. T. Fortune, G. C. Morrison, and R. H. Siemssen

The present experiment was undertaken to investigate the potential of the (^{16}O, ^{12}C) reaction for the study of α transfer. Previous investigations of this reaction had been limited to light nuclei only. Partial angular distributions for transitions to the ground state and four excited states in ^{44}Ti were measured at 45 and 48 MeV, with counter telescopes and with a broad-range magnetic spectrograph. The angular distributions at these energies are relatively smooth and structureless. As a result of the poor overlap of ^{12}C + α with the ground state of ^{16}O, cross sections are very low (peak cross section

*Chemistry Division.

≤ 100 μb) and hence this reaction is difficult to study; the (^{20}Ne, ^{16}O) reaction appears to be a better candidate for α transfer. We are therefore attempting to produce a ^{20}Ne beam.

E. RESEARCH AT THE CYCLOTRON

Research at the cyclotron has been primarily of two kinds—a pioneering series of experiments on single-nucleon transfer reactions and, more recently, studies of cluster transfers resulting in ions heavier than ^{4}He. The current work on single-nucleon transfer is concerned both with extracting nuclear-structure information [such as the systematics of proton-hole states by means of the (d,^{3}He) reaction] and also with obtaining a more complete understanding of reaction mechanisms. Detailed comparisons of reactions leading to mirror states and similar reactions involving different projectiles further our understanding of both mechanisms and structure.

The studies of cluster transfers are intended to amass a body of data from which systematic relations may be deduced about reactions in which (1) a given cluster is transferred, (2) the same final states are reached by different reactions, and (3) a combination is kept fixed. The theoretical techniques necessary for understanding these reactions are quite primitive and will be spurred by these experiments. Included in these studies is a unique test of isospin conservation through the application of the Barshay-Temmer theorem to the reaction ^{10}B(α,^{7}Be)^{7}Li.

The recent completion of the split-pole magnetic spectrograph at the cyclotron has greatly strengthened the research capabilities of the accelerator system.

1. REACTION MECHANISM AND STRUCTURE OF LIGHT NUCLEI

a. ^{3}He-Induced Reactions on ^{12}C

H. T. Fortune and B. Zeidman

The reactions ^{12}C(^{3}He,^{3}He')^{12}C, ^{12}C(^{3}He,α)^{11}C, ^{12}C(^{3}He,d)^{13}N, and ^{12}C(^{3}He,t)^{12}N were investigated by use of the 35.6-MeV ^{3}He beam of the 60-in. cyclotron. A sizeable fraction of the data was obtained with experimental configurations in which two or more reactions were studied simultaneously, thereby reducing relative errors. The ^{12}C(^{3}He,α)^{11}C reaction, together with ^{10}B(^{3}He,d) data from the tandem, resulted in a unique assignment of $J^\pi = \frac{3}{2}^-$ for the

8.1-MeV state in ^{11}C. The data from all the reactions studied are being analyzed in parallel in order to extract sets of optical-model parameters that yield consistent results for all reactions and whose relationships satisfy reasonable physical requirements. While each of the reactions may be fitted in a somewhat satisfactory manner when considered separately, it has not yet been possible to find parameter families that provide good detailed fits to all the data. Analysis is continuing in the expectation that the range of parameters has now been considerably narrowed.

b. ^{4}He-Induced Reactions in Light Nuclei

H. T. Fortune, R. H. Siemssen, and B. Zeidman

Proton- and deuteron-transfer reactions in 1p-shell nuclei have been studied by means of the (α,t) and (α,d) reactions at $E_\alpha = 46$ MeV. The results are being compared with $(^3He,d)$ and $(^3He,p)$ reactions on the same nuclei. In both cases, the data are consistent with a direct reaction, but the range of transferred momentum is substantially different for α-induced reactions because of the large binding energy of the alpha particle. Angular distributions have been measured for low-lying levels in all targets in both reactions. The (α,t) data are being fitted with a conventional DWBA program, while a two-nucleon code is being used for the (α,d) reactions. The two-nucleon transfer will be compared with the two-nucleon fractional-parentage-coefficient calculations of Kurath.

Evaluation of preliminary results from elastic and inelastic scattering of α particles by 1p-shell nuclei indicated that excessive time was required to obtain the high-quality data desired. Accordingly, this facet of the α-induced-reaction program has been terminated.

c. High-Lying Neutron-Hole States Populated in the Reaction $^{13}C(p,d)^{12}C$ at E_p = 63 MeV

L. J. Parish,* A. Brown,* K. A. Eberhard,* A. Richter, and W. von Witsch†

The neutron-hole strength in ^{12}C between 15 and 23 MeV excitation energy has been measured by studying the $^{13}C(p,d)^{12}C$ reaction with the ORIC cyclotron and its associated spectrograph at Oak Ridge National Laboratory. Spectra (Fig. 40) were taken at $\theta_{lab} = 6^{\circ}$, 12°, 18°, and 25°. States may be clearly identified at E_x = 15.11, 16.11, 17.79, 18.84, 21.5, and 22.5 MeV, and an accumulation of strength is found around E_x = 20 MeV. The results are in agreement with Cohen and Kurath's intermediate-coupling calculations. By comparison with other available experimental information, possible configurations for some of the high-lying states ($E_x \geq 15$ MeV) can be assigned.

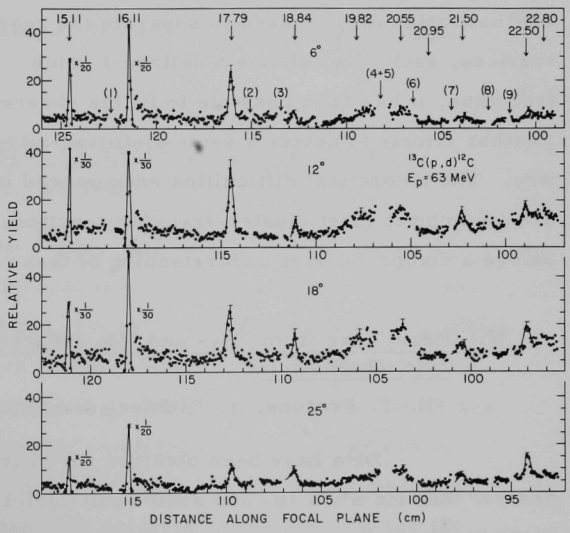

Fig. 40. Spectra of the reaction $^{13}C(p,d)^{12}C$ at E_p = 63 MeV, corresponding to excitation energies in ^{12}C between 15 and 23 MeV. The spectra are plotted one above another such that states with the same Q value lie on a straight line. The relative yield is given per unit charge and solid angle so that the strength of the different states may be compared directly.

---

*Florida State University, Tallahassee, Florida.

†Rice University, Houston, Texas.

d. Reactions Resulting in Ions Heavier Than He

(i) $^{12}C + {}^{3}He$

H. T. Fortune and B. Zeidman

Angular distributions of ions heavier than He have been measured at E(^{3}He) = 36 MeV in the 18-in. scattering chamber at the cyclotron. The angular distributions of ^{7,7*}Be and ^{6}Li show definite evidence for a direct-interaction mechanism. The angular distributions for ^{7}Be and ^{7*}Be from the reaction $^{12}C(^{3}He, {}^{8}Be)^{7,7*}Be$ are qualitatively similar, but differ in the sharpness of the oscillation pattern. This difference suggests a j-dependent effect. On the assumption that the spectroscopic factors for the two states are equal in a cluster expansion in (α + ^{3}He) states, the anticipated cross sections are in the experimentally observed ratio $\sigma(^{7}Be)/\sigma(^{7*}Be) = 2/1$. While it is not possible to define an ℓ value in a conventional DWBA calculation, a plane-wave approximation may be used to separate the reaction into two interaction vertices, each of which has a defined ℓ value. With the use of this technique, it has been possible to fit the observed angular distributions. Further efforts to devise a semi-distorted-wave analysis are under way. The theoretical difficulties encountered in analyzing this reaction are common to most cluster-transfer reactions and must be solved before a comprehensive understanding of these reactions is achieved.

(ii) Heavy Ions from ^{3}He- and ^{4}He-Induced Reactions on 1p- and 2s1d-Shell Nuclei

H. T. Fortune, A. Richter, and B. Zeidman

Data have been obtained for reactions yielding ions heavier than He when 1p- and 2s1d-shell nuclei are bombarded with 36-MeV ^{3}He and 46-MeV alpha particles from the 60-in. cyclotron. Angular distributions (Fig. 41) are strongly forward peaked and some show an oscillatory behavior. The reaction $^{10}B(\alpha, {}^{6}Li)^{8,8*}Be$ has

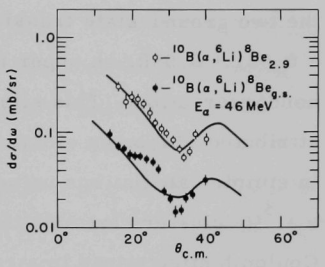

Fig. 41. Angular distributions for $^{10}B(\alpha, ^{6}Li)$ reactions leading to the ground state and the 2.9-MeV state of ^{8}Be, shown together with DWBA curves calculated for two-nucleon transfer with L = 2.

been fitted successfully with a two-nucleon-transfer modification of a DWBA code, but the relative spectroscopic factors for the two ^{8}Be states are not in good agreement with Kurath's calculations.

Analysis of data from both ^{3}He- and ^{4}He-induced reactions is proceeding in parallel, since one of the most intriguing aspects of cluster-transfer reactions is comparison of the cross sections for transfer of similar clusters and similar final states. The understanding of these complex reactions is still in a primitive state and a large body of data is required before consistent trends and patterns are evident.

(iii) Experimental Test of the Barshay-Temmer Theorem

H. T. Fortune, A. Richter, and B. Zeidman

The reactions $^{10}B(\alpha, ^{7}Be)^{7}Li$ and $^{11}B(^{3}He, ^{7}Be)^{7}Li$ were used in an experimental test of the Barshay-Temmer theorem, as reported last year. In brief, the theorem implies that if the initial system is prepared in a pure isospin state (i.e., if either target or projectile has T = 0) the angular distributions and cross sections are identical for all reactions in which both products are members of the same isospin multiplet, provided isospin is strictly conserved. The system $^{10}B + \alpha$, in which both nuclei have T = 0, satisfies the initial conditions and hence provides a test of isospin conservation. By calculating the ratio between the differential cross sections for

the two ground-state transitions, namely $[d\sigma(^{7}Li_{g.s.})/d\omega]/[d\sigma(^{7}Be_{g.s.})/d\omega]$ = 0.021 ± 0.030, an upper limit of ≤3% was deduced for the isospin nonconservation. This slight asymmetry could very reasonably be attributed to isospin violation resulting from electromagnetic effects. In simple calculations using Woods-Saxon wave functions for α + t and α + ^{3}He clusters forming the ground states of ^{7}Li and ^{7}Be, respectively, Coulomb effects lead to a ratio of wave functions $\psi(^{7}Li)/\psi(^{7}Be) \approx 1.01$ near the nuclear surface ($R + a \approx 2.7 \pm 0.6$ F). For a surface reaction, this ratio implies a cross-section ratio $\sigma(^{7}Li)/\sigma(^{7}Be) \approx 1.02$ in accordance with the experimental observation. These results have been published. Further experiments of this type are planned as a way of examining a T=1 isospin triplet for which strong charge-dependent effects could show up.

2. SINGLE-NUCLEON-TRANSFER REACTIONS ON N=14 NUCLEI

H. T. Fortune, J. V. Maher, G. C. Morrison, and B. Zeidman

The three stable N=14 nuclei, ^{26}Mg, ^{27}Al, and ^{28}Si, lie in the shape-transition region (prolate to oblate) of the 2s1d shell. Present understanding of this mass region is limited by experimental uncertainties and inconsistencies in the analysis of the existing data. For this reason the reactions (d,t), (d,^{3}He), (d,d'), and (d,p) have been measured simultaneously on targets of each of the N=14 nuclei, bombarded with the 23-MeV deuteron beam of the Chemistry Division cyclotron. One potential set has been found to yield excellent DWBA fits to all the strong transitions for each of the transfer reactions. Thus with consistent data acquisition and uniform analysis in the distorted-wave approximation, it is hoped that reliable single-particle strengths have been extracted for this mass region. Systematics of neutron and proton occupation numbers for these nuclei are under investigation. Several further topics arising from this work are of interest in themselves.

a. Mirror-State Spectroscopic Factors

Spectroscopic factors for transitions to the four strong states excited in the ^{28}Si(d, ^{3}He) reaction [the ℓ=2 transitions to the states at 0.00 MeV ($\frac{5}{2}^+$), 1.013 MeV ($\frac{3}{2}^+$), and 2.731 MeV ($\frac{5}{2}^+$), and the ℓ=0 transition to the $\frac{1}{2}^+$ at 0.842 MeV] and for their mirror transitions in the ^{28}Si(d,t) reaction have been compared both as a sensitive check on the accuracy of the DWBA and as a crude check on the assumption that these levels are good mirrors. With reasonable bound-state parameters, the binding-energy prescription indicates that the well depth for each ^{27}Si level is virtually identical to that found for its mirror in ^{27}Al. The extracted spectroscopic factors agree within 5% for the three $\ell = 2$ pairs; the values for the two $\ell = 0$ transitions differ by a factor of two. This problem is attributed to the well-known difficulties of distorted-wave fitting on the second maximum of an angular distribution. The angular distribution will be extended farther forward with the new split-pole spectrometer in an attempt to measure the forward peaks of the $\ell = 0$ angular distributions.

b. ^{26}Mg(d, ^{3}He)^{25}Na

Although ^{25}Na lies in the shape-transition region of the 2s1d shell, it has not previously been studied via direct reactions. The ^{26}Mg(d, ^{3}He)^{25}Na reaction yielded strong transitions to the $\frac{5}{2}^+$ ground state and to the state at 1.07 MeV. Weak transitions were seen to the states at 0.09 and 2.20 MeV. The DWBA analysis described above assigns the spin-parity of the 1.07-MeV state to be $\frac{1}{2}^+$. Spectroscopic factors could only be assigned to two states, the ground state ($C^2S_{1d\ 5/2} = 3.6$) and the 1.07-MeV state ($C^2S_{2s\ 1/2} = 0.4$).

c. ^{27}Al(d,p)^{28}Al

Although much theoretical interest has centered on ^{28}Si and the projected shape crossover at A ≈ 28, ^{28}Al has been

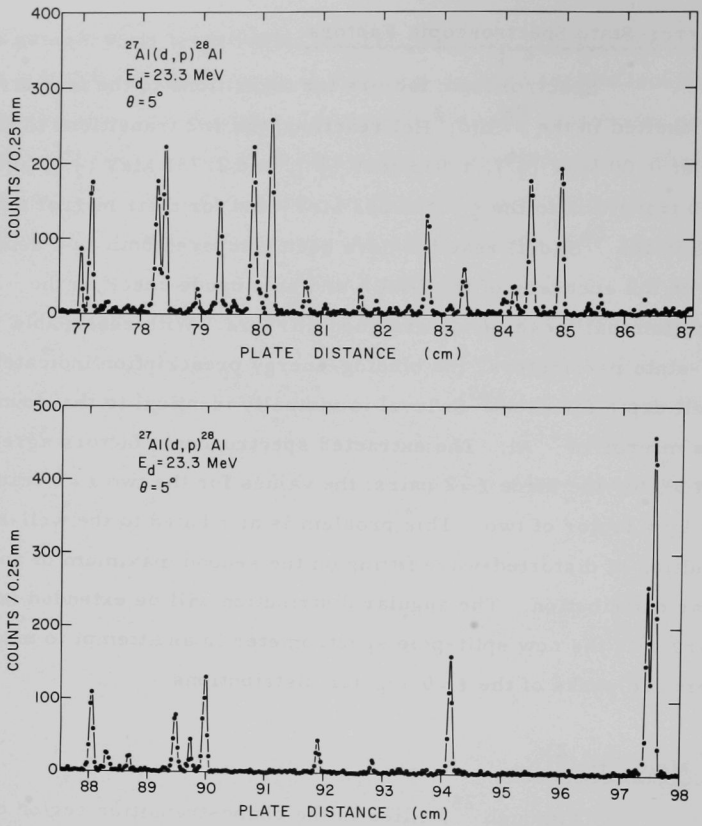

Fig. 42. Spectrum of the ^{27}Al(d, p)^{28}Al reaction at 5°(lab). This spectrum was obtained at the 60-in. cyclotron with the use of the new split-pole spectrograph. The resolution width is about 18 keV, which is sufficient to resolve the ground-state doublet whose separation is 30 keV. These forward-angle data were necessary to clarify some ambiguities in the extraction of spectroscopic factors.

almost entirely neglected. However, its energy spectrum (Fig. 42) is surprisingly simple for an odd-odd nucleus (6 known states in the first 2 MeV). Previous ^{27}Al(d, p) measurements were made with deuteron energies below 7 MeV and were analyzed with the plane-wave

Born approximation. Several revisions in angular-momentum-transfer assignments have been made on the basis of the present work and spectroscopic factors have been extracted. A strong $\ell=3$ transition is seen to a state at $E_x \approx 4.03$ MeV.

3. REACTIONS IN 1f2p-SHELL NUCLEI

a. (d,t) and (d, ^{3}He) Reactions on the Ca Isotopes

J. L. Yntema

The analysis of the nucleon-pickup reactions on the Ca isotopes was completed and additional work on the ^{46}Ca nucleon-pickup

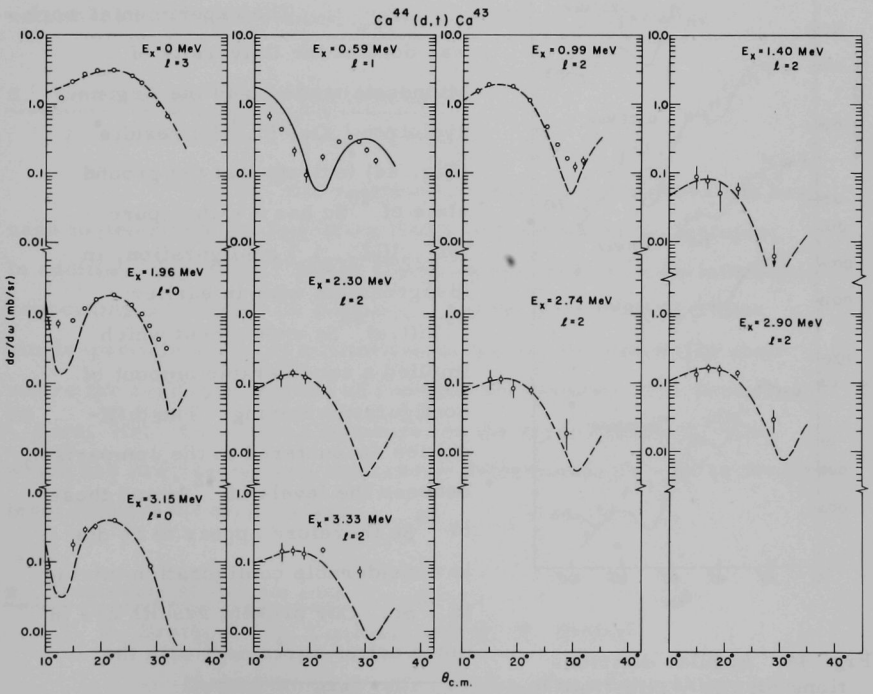

Fig. 43. Experimental angular distributions of transitions observed in the ^{44}Ca(d,t)^{43}Ca reaction, together with the distorted-wave curves.

reaction was performed. Angular distributions for the $^{44}Ca(d,t)^{43}Ca$ reaction are shown in Fig. 43.

In all even-even nuclei, evidence for $2p_{3/2}$ admixture in the ground-state wave function was found. A comparison of the (d,t) and (d,p) reactions leading to the same final nuclei indicate that considerable core excitation is present in the ground-state wave functions.

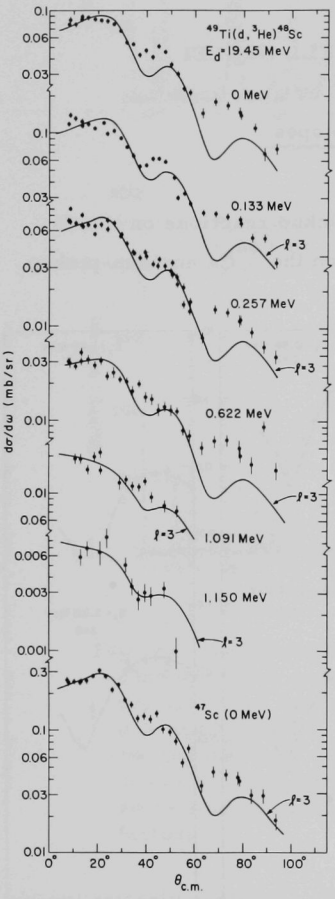

Fig. 44. Angular distributions for the $^{49}Ti(d,^3He)^{48}Sc$ reaction with $f_{7/2}$ pickup at E_d = 19.45 MeV. The curves are DW calculations.

b. Nuclear Structure of ^{48}Sc from the $^{49}Ti(d,^3He)^{48}Sc$ Reaction

H. Ohnuma* and J. L. Yntema

The experimental work was done at the University of Minnesota tandem and the Argonne cyclotron. Our (d, ^{3}He) results (Fig. 44) indicate that the ground state of ^{48}Sc has a rather pure $(\pi f_{7/2})(\nu f_{7/2})^{-1}$ configuration, in disagreement with an earlier $^{49}Ti(t,\alpha)^{48}Sc$ experiment which implied a considerable amount of configuration mixing. The difficulties encountered in the comparison between the levels of ^{42}Sc and those of ^{48}Sc therefore appear to be due to considerable configuration mixing in ^{42}Sc. Our present results are in much better agreement with the

*University of Minnesota, Minneapolis, Minnesota.

predicted position of the center of gravity of the $d_{3/2}$ and $s_{1/2}$ hole states (as calculated by Bansal and Franch) than are the previous results.

c. Proton Levels in 1f2p-Shell Nuclei

T. H. Braid, J. A. Nolen, Jr.,* and B. Zeidman

The data previously obtained from (d, ^{3}He) reactions on 1f2p-shell nuclei have been analyzed. The reactions on targets of ^{50}Cr and ^{52}Cr were re-examined in order to verify the existence of a previously unobserved level in ^{49}V which has a Q value very near that resulting from the ^{52}Cr(d, ^{3}He)^{51}V ground-state reaction. Systematics of level positions for the various orbitals have been established. Papers reporting this work are in preparation.

d. Levels in the Odd-A Cu Isotopes

J. A. Nolen, Jr.,* and B. Zeidman

The (d, ^{3}He) reaction on even-A zinc isotopes has been used to determine the low-lying levels of the heavier Cu isotopes. In addition, data from (^{3}He,d) reactions on nickel provide information concerning the lighter Cu isotopes. The fragmentation of proton single-particle states is maximized in the middle of the 1f2p shell where the available degrees of freedom are largest. The reaction ^{70}Zn(d, ^{3}He)^{69}Cu yields a measure for the mass excess of ^{69}Cu, which had previously been incorrectly determined, as well as the first level scheme for this nucleus.

e. Scattering of Helium Ions

T. H. Braid, T. W. Conlon,† and B. W. Ridley†

During the past year, values of the deformation parameter β for a number of the levels of ^{58}Ni and ^{40}Ca were extracted

*University of Maryland, College Park, Maryland.

†Nuclear Physics Division, Atomic Energy Research Establishment,

from the data on the inelastic scattering of ^{3}He by these nuclei. In this application of the DWBA theory, the parameters used for the nuclear potential were the ones previously determined from the elastic-scattering measurements. Since our measurements were made at a number of energies in the range 28—84 MeV, the data provide a good test of the reliability of such calculations. We extracted the value of β for the 3.73-MeV state in ^{40}Ca and for the 1.45-MeV and the 4.45-MeV state in ^{58}Ni and found that the resulting value of β_{ℓ} increases linearly with energy, being on the average 25% greater at the upper end of the energy range than at the lower. This indicates limitations in the method of extracting values of β, which we hope to remove by coupled-channels calculations which are being undertaken.

4. ISOMERIC STATES PRODUCED IN (^{12}C,xn) REACTIONS IN THE REGION $Z > 50$, $N < 82$

T. W. Conlon* and A. J. Elwyn

We have studied the gamma-ray spectra associated with new short-lived activities produced in the ^{12}C-ion bombardment of separated isotopes of Sn, Cd, and Sb nuclei at the Harwell Variable Energy Cyclotron. Both the energy of the gamma ray and its time of arrival after bombardment by the pulsed 88-MeV ^{12}C beam were measured simultaneously by use of a 4096-channel two-dimensional analyzer. Several isomers with half-lives between 60 nsec and 0.5 sec have been observed. These activities have been assigned to the odd-mass nuclei ^{121}Xe, ^{123}Xe, ^{125}Ba, ^{129}La, and ^{131}La. The basis upon which the observed isomeric activity was assigned exclusively to odd-mass nuclei was the lack of any observed gamma-ray transitions associated with the known low-lying energy levels of some of the

*Nuclear Physics Division, Atomic Energy Research Establishment, Harwell, Berks., England.

even-even nuclei that could be produced in ^{12}C-induced reactions [mainly (^{12}C,4n) and (^{12}C,5n) reactions] at a beam energy of 88 MeV. Further experimental studies are necessary to determine the level structure in the final nuclei as well as the properties of the isomeric transitions.

5. INSTRUMENTATION AT THE CYCLOTRON

a. Split-Pole Magnetic Spectrograph

B. Zeidman

During the past year, installation of the split-pole spectrograph has been completed and the magnet has been calibrated. Magnetic field stability has proved excellent and resolution checks with naturally radioactive sources show that field quality exceeds specifications. Considerable effort has been expended in determining optimum operating parameters, both for the spectrograph and for the beam analysis and transport system. Inasmuch as the cyclotron itself produces a low-quality beam, it is necessary to reduce the energy spread in the beam by magnetic analysis, which also reduces the available beam intensity. Together with the awkward beam-transport system required to bring the beam on target, the parameters of the analyzing system result in a large number of combinations of operating parameters, from which optimum sets must be chosen to yield maximum current and resolution.

In order to facilitate such studies, position-sensitive solid-state counters have been used in the focal plane of the spectrograph. With the best of the counters and extremely thin targets to minimize the effects of target thickness, resolution widths of 14—18 keV are obtained for 46-MeV ^{4}He and 36-MeV ^{3}He elastically scattered from gold at forward angles. A clearly less-than-optimum arrangement also yielded a width of about 18 keV with 23-MeV deuterons. In data

taken with photographic emulsions, spectra from the $^{27}Al(d,p)^{28}Al$ reaction (Fig. 42) indicated a resolution width less than 18 keV.

In principle, better beam resolution may be obtained by narrowing the slits of the beam analyzer, but such a procedure reduces the available beam rapidly. In addition, target thickness provides another limit to observed resolution. For targets ~100 $\mu g/cm^2$ thick, the nominally useful thickness, resolution widths of ~25 keV have been obtained. Only a few data runs have been made to date, but the system is now sufficiently optimized to allow regular use with helium ions. With deuterons, useful data have already been taken, but additional work is needed in order to determine the ultimate operational capabilities of the system.

In the near future, attempts to operate in a slitless mode will begin. For small angle, low-background measurements, this mode is greatly to be preferred to conventional operation. Considerable care and study are needed to provide a stable beam spot without collimators.

b. The 60-in. Scattering Chamber at the Cyclotron

J. L. Yntema

The basic design work necessary for conversion of the 60-in. chamber to a computer-controlled device for angular-correlation measurements has been completed. No further improvements can be undertaken until funds become available.

F. OTHER NUCLEAR EXPERIMENTS

Several experimental nuclear investigations in the Physics Division are not closely associated with any of the major sources of neutrons or charged particles. These independent studies are collected for convenience in this section.

a. Pattern Recognition for Nuclear Events

C. Harrison,* D. Jacobsohn,* and G. R. Ringo

The mechanization of the procedure for identifying interesting events is a problem of increasing importance in nuclear and particle physics. It is particularly critical in the case of emulsions where it is desirable to scan large volumes of material with microscopes showing volumes of 10^{-8} cc or less in a view. Our approach to this problem uses a two-layer random-connection network similar in its general character to the Perceptron of F. Rosenblatt, but differs from it in that many completely different sets of connections are tried, and those most useful in the learning phase are kept.

Recent work has tested programs that weight the learning patterns to produce a more uniform response over the learning set. The results would be called encouraging rather than remarkable, but numerous improvements in the strategy have been devised and are fairly easy to test with the present program. We plan to test a number of these in the coming year.

*Applied Mathematics Division.

b. Microscopic Location of ^{17}O, ^{18}O, and ^{15}N

G. R. Ringo and V. E. Krohn

A technique by which the tracer isotopes ^{17}O, ^{18}O, and ^{15}N could be located (possibly simultaneously) within a resolution diameter of 1 micron or better would have obvious value in biological research. We believe this could best be done by scanning a specimen

with a focused beam of ions (e.g., Ne^+) to convert the tracer isotopes to ions which would be identified in a mass spectrometer with high resolution (a resolution of, say, 5000). The high-resolution mass spectrometer is available, but an ion beam with less than 1 μ diameter and more than 1 pA current remains to be produced.

A duoplasmatron ion source and an ion-lens system have been obtained. The particle optics for collection of the secondary ions have been designed and the instrument is now under construction. This instrument should be assembled and tested in the coming year.

c. Detectors and Circuits for Fast Electronic Timing

F. J. Lynch

(i) Time Resolution of Scintillation Detectors

In the past we have measured the efficiency of various scintillators and their light intensity as a function of time and the conversion efficiency and transit-time spread of photomultipliers. From these measured characteristics, time resolutions have been calculated and found to agree well with experimental values. Similar calculations have enabled us to project the improvements in resolution that may be expected from forseeable improvements in scintillators and photomultipliers. Since they indicate that the largest improvements in time resolution can be anticipated from faster multipliers, new photomultipliers employing high-gain dynodes in reflection and in transmission will be tested when they become available.

(ii) Time Resolution with Ge(Li) Detectors

Although the time resolution of semiconductor detectors is inferior to that of scintillation detectors, their superior energy resolution encourages their use in many experiments. The time resolutions of several detectors have been measured with a new

low-noise fast amplifier, a pulse-shaping amplifier, and a zero-crossing discriminator. Although the time resolutions obtained are better than any reported previously, further improvements can be effected by using thinner Ge(Li) detectors, and a preamplifier with a cold input stage.

d. Simple Technique for Precise Determinations of Counting Losses in Nuclear Pulse-Processing Systems

H. H. Bolotin, M. G. Strauss,* and D. A. McClure

In experimental studies of absolute cross sections, radioactive decay, determinations of relative radiation intensities recorded under differing experimental conditions, etc., the recorded nuclear spectrum must be corrected for losses due to pileup rejection and deadtime resulting from pulse-amplitude gating, ADC, memory, etc. present in the pulse-processing and recording system.

Recent advances in the development of multichannel pulse-height analyzers have materially reduced the deadtime associated with the digitizing and storage of input signals. In addition, of late there has been widespread recognition and implementation of the need to impose paralysis of relatively long duration in the pulse-handling circuitry of systems associated with solid-state radiation detectors—e.g., Ge(Li), Si(Li), and surface-barrier Si detectors—in order to preserve the excellent energy-resolution characteristics of these devices under conditions of high counting rates. This paralysis had led to sizeable increases in the overall counting losses in those portions of the counting system that precede the multichannel analyzer. Thus, it often is not sufficient to treat the deadtime in the multichannel analyzer as the sole or dominant cause of experimental counting losses. Indeed, at high counting rates the losses due to pileup rejection increase, thus decreasing the rate for pulses addressed to the analyzer and thereby reducing the analyzer deadtime. It is, therefore, clear

*Electronics Division.

that the deadtime registered by the analyzer fails to reflect a potentially sizeable fraction of the counting losses incurred.

A new technique has been developed to determine precisely the fraction of all counting losses suffered in systems for counting and pulse-height analysis. Of particular significance is the applicability of this method to time-dependent counting rates. The method is based on a technique in which the rate of radiation incident upon the detector is sampled continually. Upon the detection of a preset number of counts, a pulser signal is injected into the preamplifier. At the end of the experiment, the total number of injected pulses is compared with the number of these pulses that are recorded in the multichannel analyzer or scaler. Since the pulser peak suffers the same fractional losses as the spectral components of the detected nuclear events, such a comparison provides an accurate representation of the counting losses due to all loss-producing effects. These include losses incurred in ADCs, computers, pileup rejectors, etc. Losses suffered due to pileup may not be negligible compared with those due to the ADC and memory of fast multichannel analyzers.

This technique has been successfully applied to cases in which counting rates were subjected to severe and unreproducible fluctuations encountered in charged-particle-induced reactions and in studies of radioactive decay. This method has been demonstrated to yield corrections for counting losses to a precision of a few tenths of a percent. Of prime importance, it requires no a priori or a posteriori knowledge of either the time dependence of the counting rate or the mechanisms by which counting losses are incurred.

II. MEDIUM-ENERGY PHYSICS

Although the program in Medium-Energy Physics is small, it is divided into two distinct parts. One part is a study of accelerators for the production of particles in the medium-energy range. The other part is concerned with preparations for use of the Los Alamos Medium-Energy Physics Facility (LAMPF).

It is planned that our participation in activities associated with LAMPF should increase substantially during the next few years. This will include continued involvement in various aspects of the development of the facility itself and also the preparation of experiments to be carried out at LAMPF. Two projects related to this area of research are summarized in Secs. II a and b.

In June 1969 we submitted a proposal for the construction of a Midwest Tandem-Cyclotron (MTC) accelerator system to be used for the acceleration of both light and heavy ions. This proposal (issued as ANL-7582 and summarized in the Physics Division Annual Review last year) was prepared as a joint project of the Physics and Chemistry Divisions working in collaboration with a group from the AUA universities. Recently we have re-examined this proposal and have concluded that it is still technically sound and has great potential for research in nuclear science. Therefore, we are resubmitting the proposal.

Several technical problems connected with the design and use of an accelerator for medium-energy physics have led to investigations that are of interest in their own right, independent of their relationship to the MTC proposal. Sections II b and c report work of this kind.

a. Activation Cross Sections for the Reactions $^{19}F(\pi^-,\pi^-n)^{18}F$ and $^{31}P(\pi^-,\pi^-n)^{30}P$ at the (3,3) Resonance

H. S. Plendl,* K. A. Eberhard,* D. Burch,* M. Kirby,* C. J. Umbarger,* A. Richter, and W. P. Trower†

In order to gain insight into the very scantily investigated single-nucleon knockout reaction $(\pi,\pi N)$ at the (3,3) resonance, total

*Florida State University, Tallahassee, Florida.

†Virginia Polytechnic Institute, Blacksburg, Virginia.

activation cross sections for the neutron knockout reactions $(\pi^-, \pi^- n)$ on ^{19}F and ^{31}P have been measured from 160 to 240 MeV by detecting the annihilation quanta from the residual β^+ activity with two NaI(Tl) counters in coincidence. Beams of 10^4 and 10^5 pions/sec over the 20-cm^2 target area were obtained from an internal Be target in the 600-MeV proton beam from the synchrocyclotron of the Space Radiation Effects Laboratory, Newport News, Virginia. Degraders were used to vary the pion beam energy. The absolute beam intensity at each energy was determined by use of the $^{12}C(\pi^-, \pi^- n)^{11}C$ reaction for which the cross section is well known. The cross section has the resonance shape expected from the free-nucleon interaction, except that the Fermi motion inside the nucleus broadens it and shifts the maximum to lower energies. The results are now being compared with previously determined cross sections for $(\pi^-, \pi^- n)$ reactions and with dispersion-theory calculations.

b. Multi-Wire Proportional Counters

T. H. Braid, J. Himes, J. Becker, and G. G. Campbell

Within the last year or two it has been recognized that large arrays of small proportional counters might well be better than spark chambers or other detection devices for mapping the trajectories of energetic charged particles. Therefore, we have constructed and studied multi-wire proportional-counter arrays in which only every second wire in a counting plane operates as an anode, the others being held at cathode potential, and have investigated their response to α particles. The arrays perform very satisfactorily, and give a good proportional response. In contrast to the behavior of the normal Charpak arrangement (in which all wires in a counting plane are at the anode voltage), the voltage necessary to produce sufficient charge multiplication in the gas becomes less as the distance between adjacent anode and cathode wires is made smaller. A simple

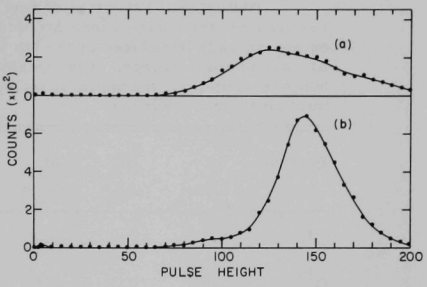

Fig. 45. Response of multi-wire proportional counters to α particles passing through the sensitive volume: (a) with a single plane of alternating anode and cathode wires, spaced 1 mm apart, and (b) with additional parallel cathode planes placed 1.3 cm from the counting plane. The amplifier gain in (a) was roughly 25 times that in (b).

plane consisting of such adjacent anode and cathode wires (placed in a large volume of gas) can be used alone to provide a very thin counter for particles of high specific ionization in special applications (Fig. 45a), or additional parallel planes at the cathode voltage can be used to define a larger sensitive volume (Fig. 45b). Several counting planes can be operated close together in the same counting volume to provide more sophisticated position selection than is possible with a single array.

c. Design of Buncher for Ions with $1 < A < 333$ for the Midwest Tandem Cyclotron

F. J. Lynch and J. E. Monahan

Bunching by velocity modulation of the ion beam before injection into the tandem accelerator has been used for many years at ANL and elsewhere for low-mass ions. The proposed Midwest Tandem Cyclotron (described in ANL-7582) requires efficient bunching for a wide range of particle masses ($1 < A < 333$). Calculations were made for an ungridded 2-gap buncher with sine-wave, triangular-wave, and ideal wave forms. These show that sine-wave bunching, which is employed in bunchers now in use, is not suitable for the heavier particles, but that the triangular or ideal wave form will give good results. The minimum pulse duration also depends on the energy spread in the source and stripper and on space charge. Estimates

TABLE IV. Estimates of rms time spreads. The total time spread Δt results from the contributions Δt_b due to the buncher, Δt_{is} and Δt_{st} due to the energy spreads introduced by the ion source and stripper, respectively, and Δt_c due to space charge. The remaining columns list the period T of the buncher excitation, the bunching factor F, and the beam-energy spread ΔE_m introduced by the buncher.

Particle	T (nsec)	Δt_b (nsec)	Δt_{is} (nsec)	Δt_{st} (nsec)	Δt_c (nsec)	Δt (nsec)	F	ΔE_m (keV)
H^1	100	0.2	0.03	0.01	<0.05	0.3	~ 41	20.9
O^{16}	100	0.3	0.1	0.01	<0.1	0.35	35	5.22
I^{127}	200	0.4	0.3	0.01	0.1	0.5	49	3.75
$U^{238}F_5$	400	0.5	0.5	0.2	0.2	1.0	49	4.54

of the size of these effects are shown in Table IV. A preliminary design of a practical bunching system has been prepared.

d. Calculations of Shielding for Very Energetic Neutrons

T. H. Braid, R. F. Rapids, R. H. Siemssen, and J. W. Tippie*

We have made calculations of the shielding necessary to give adequate protection of personnel from the fast neutrons produced in a target by very energetic light ions from a large cyclotron—in particular, by protons of energies up to 400 MeV. In such calculations it is common to approximate the neutron spectrum by that produced by the protons of a single energy and to calculate the number of neutrons transmitted but not their distribution in energy. We have made a more realistic estimate by using a neutron spectrum which corresponds more closely to that produced by protons in a thick target, and have calculated the total dose-equivalent transmitted through the shield.

We calculate the total cascade neutron spectrum produced by protons as they slow down in a thick target, by taking account of the probability of a neutron-producing reaction at the successive

*Applied Mathematics Division.

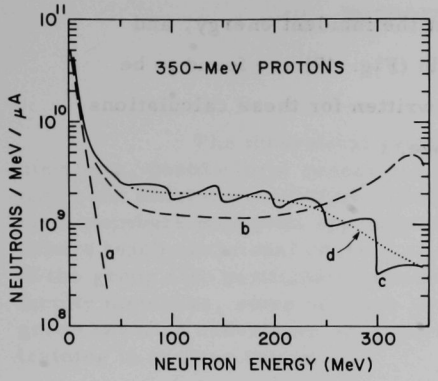

Fig. 46. Spectra of neutrons produced by 350-MeV protons. (a) Evaporation and (b) cascade spectra produced in inelastic collisions of 350-MeV protons on Cu. (c) Approximation to the total neutron spectrum produced by 350-MeV protons slowing down in a Cu target; it consists of a weighted sum of spectra of types (a) and (b) calculated for proton energies at 50-MeV intervals. The breaks in the curve correspond to these intervals. (d) Smooth curve drawn through (c). Curves (a) and (b) are normalized to the same number of inelastic collisions as (c).

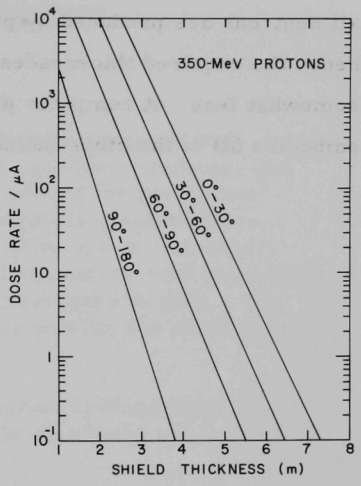

Fig. 47. Dose rate from neutrons penetrating a concrete shield wall when a Cu target is bombarded by 350-MeV protons. The unit on the dose-rate scale is the standard tolerance level (2.5 mrem/hr).

energies of the proton and applying Bertini's calculations for the cascade neutron spectra at these energies. The total spectrum is converted to dose equivalent by using the calculations of either Alsmiller or O'Brien for penetration of monoenergetic neutrons in concrete, interpolating as necessary between the neutron energies given by these authors, and then summing over all energies in the incident spectrum. The spectra calculated in this way (Fig. 46) show fewer high-energy neutrons than do cruder approximations in which it is assumed that

all neutrons are produced by protons at the incident energy, and hence the required thicknesses of shield (Fig. 47) are found to be somewhat less. A computer program written for these calculations embodies all of the steps indicated above.

III. THEORETICAL PHYSICS

The theoretical group consists of permanent staff members, postdoctoral research associates, graduate students, and long- and short-term visiting scientists. Three of the permanent staff members hold joint appointments at neighboring universities. Others teach occasional courses at various universities. Members of the group also participate in research collaborations with university faculty members, some of whom serve as consultants to ANL. The group has also undertaken an important responsibility for postdoctoral training in nuclear theory.

Although the largest concentration of theoretical effort is in nuclear physics, theoretical research is also being carried out

Fig. 48. A user examining input being composed on a RESCUE terminal in the new Physics Division computer center. Card images can be manipulated from this type of terminal.

in superconductivity, statistical mechanics, hypernuclear structure, elementary-particle physics, applied mathematics, and the mathematical structure of quantum mechanics. There is also a systematic development of software facilities for the numerical computations needed in nuclear-structure calculations. This facility has by now become an important theoretical resource. Parts of it have successfully been transferred to other laboratories for the use of other groups, and that process is continuing.

The theoretical group maintains an active partnership in the experimental program of the Physics Division—through research collaborations, informal cooperative effort and mutual criticism, and also through joint seminars whose principal purpose is to facilitate the flow of ideas between theorists and experimentalists.

The major programs of theoretical research are computer-based studies of nuclear structure via the spherical or deformed nuclear shell models, and studies of the nuclear many-body

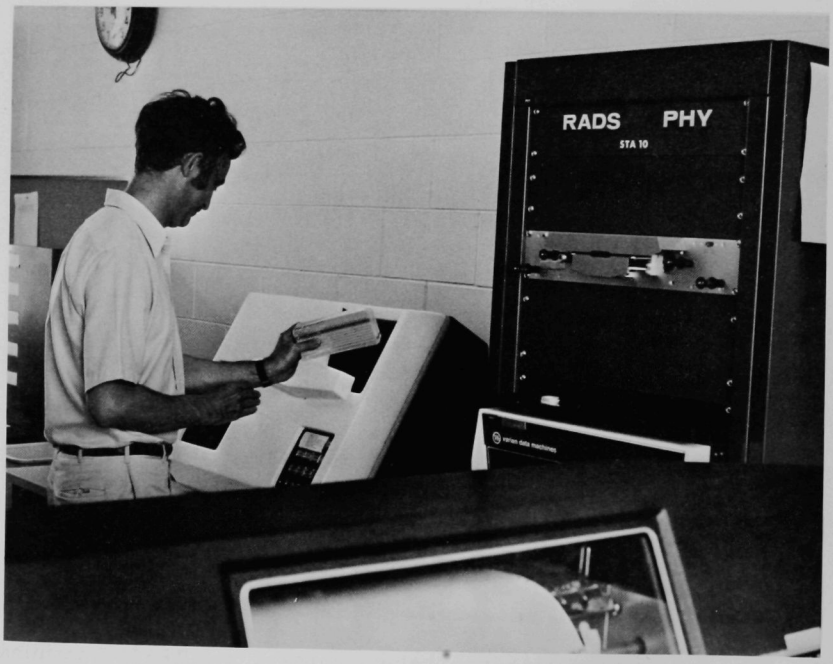

Fig. 49. The new Physics Division RADS station. This station communicates with the IBM-360 system.

problem. Features common to both problems, such as the nucleon-nucleon interaction and some of the computational techniques, are developed in active discussion sessions. The aims and achievements of these and other research efforts are described briefly below.

a. The New Physics Division Computer Center

S. Cohen and C. M. Vincent

An imaginative new computer center has been set up in the Physics Division. It consists of a suite of rooms devoted to the expeditious use of the Argonne IBM-360 computer system. A primary consideration in designing this area has been to provide the quiet, pleasant atmosphere essential to effective computer work.

Fig. 50. A view of the central discussion area in the new computer center.

There are several RESCUE stations in individual rooms. Sitting at a RESCUE terminal (Fig. 48), a physicist can compose, edit, and submit jobs for the 360 computer. So powerful is this interactive system that it is soon expected to be the most popular means of job input.

Output can be directed to the Physics Division RADS station (Fig. 49). This station, which is also located in the center, provides means for conventional card and paper-tape input to the 360. Printed output from this station is filed in individual users' bins. A keypunch and card-storage files are conveniently nearby.

Additional work space and a library of computer information are available in a central area. Part of this area is shown in Fig. 50.

b. The DELPHI System

It is in the nature of every theoretical investigation that new or modified techniques must constantly be developed to augment existing methods. DELPHI is an advanced system for the development of algorithms and their synthesis into programs for carrying out physics computations. This system is now available for computers of the IBM-360 series and is actively being used in several studies in the Physics Division.

Built into the structure of DELPHI are many features that greatly ease the task of constructing new computational programs. One major facility (developed in collaboration with Keith Rich of the National Accelerator Laboratory) provides a simple way of storing, cataloging, and modifying such programs. A second major part of the system comprises the various SPEAKEASY processors which provide the means for carrying out transient types of calculations in a quick and natural way. Major programs written within DELPHI draw on the large and growing set of linkable subprograms. Each new program in turn adds new facilities for other parts of the system. It is the flexible use of available facilities that provides the growth potential of this approach.

(i) The SPEAKEASY Programming Language

S. Cohen and C. M. Vincent

(α) Standard SPEAKEASY. The power and scope of SPEAKEASY continues to be extended. This user-oriented language is already in use at several other institutions and has been accepted for distribution by the IBM Contributed Program Library.

Several new features were added over the past year, among the more important being: (1) automatic contour plotting, (2) means for solving coupled linear differential equations, (3) new smoothing and interpolation features, and (4) means of including user-written FORTRAN subroutines. Future plans include the addition of facilities for multiparameter fitting and for the automatic execution-time inclusion of subroutines of the DELPHI system into the processor.

(β) Console SPEAKEASY. The interactive console version of SPEAKEASY has become a tool for the analysis of data by several members of the Physics Division. This version combines this compact, easily understood language with the real-time interactive capabilities of the IBM-2250 console.

(γ) Generic SPEAKEASY. An extended version of SPEAKEASY, designed to provide cataloged stored data is now operational. It enables users to easily address and operate on data produced in earlier computer calculations and to add new data to this stored library. The original data library can be created by SPEAKEASY, by any of the major DELPHI system programs, or (making use of a special subroutine package) by any other computer program.

This version of SPEAKEASY makes available to scientific users the full power of the DELPHI system. Such users are able to formulate a new problem in the concise directive language of SPEAKEASY. They are able to use any of the data generated previously by any of the programs of the DELPHI system. In the future we will be able to make use of any of the extensive sets of operators defined in the DELPHI system.

(ii) The Shell-Model System

(α) The 3600 Version (S. Cohen and D. Kurath). The CDC-3600 version of the nuclear shell-model programs is still operational and have been used for several studies during the past year. Calculations relating to two-nucleon-transfer experiments were carried out for the p-shell nuclei.

(β) The 360 Version (S. Cohen, D. Kurath, J. Soper,* and A. Stamp†). The adaptation of the shell-model system is now under way. Several of the major computational programs of the older 3600 version are now available for use on the IBM-360 system.

The newer versions of these programs have been constructed as part of the larger DELPHI system with the intent of making all the facilities of the Shell Model programs available to the SPEAKEASY processors. The adapted version of the basis program has provided the means of specifying determinantal wave functions and operations such as J+, J-. The program for extraction of coefficients of fractional parentage adds this operation to SPEAKEASY.

*AERE, Harwell, England.

†Physics Department, Oxford University, Oxford, England.

c. Nuclear Structure and Spectroscopy

(i) The Shell Model in a Spheroidal Basis

M. H. Macfarlane and A. Shukla

Shell-model calculations are usually carried out in large finite vector spaces spanned by determinants whose constituent single-particle states are eigenstates of spherical average potentials. Linear combinations of huge numbers of basis states are then necessary to describe observed nuclear levels. It is clear that in many nuclei much of this undesirable complexity stems from the need to describe spheroidal deformations—a pronounced tendency of nearly all nuclei—in a spherical basis. It seems clear therefore that much smaller

dimensions should result if shell-model calculations are carried out with spheroidal single-particle basis states.

Programs have been written to carry out such calculations for identical-nucleon (all-neutron or all-proton) configurations. Extension to cover systems with both protons and neutrons outside closed shells is now in progress. The technique being followed is to compute and store on tape or disk all information pertinent to the neutron and proton parts of the system and to synthesize the complete calculation from its identical-nucleon components. As a first application, shell-model calculations of N=Z nuclei in the ds shell (^{20}Ne, ^{24}Mg, ^{28}Si) are planned.

(ii) Shell-Model Matrix Elements from a Realistic Potential

R. D. Lawson

The level schemes of nuclei with two particles outside an inert core can be obtained by finding the eigenvalues of the coupled integro-differential equations

$$\{H_0(1) + H_0(2) + V(r_1 - r_2, \sigma_1, \sigma_2) - E\}\,\psi = \sum_j \phi_j(1,2) \int \phi_j^*(1,2)\, V\psi(1,2)\, d1\, d2,$$

where $H_0(i)$ is the single-particle shell-model Hamiltonian, V is the residual two-body force, and ϕ_j represents the jth two-particle state which must be excluded because of the Pauli principle. The eigenfunctions of the problem contain all correlations due to excitation of the valence nucleons and hence can be used to calculate other nuclear properties. Programs to solve these equations are now operational on the IBM-360 computer.

The level scheme, transition rates, and static properties of ^{6}Li have been studied with the aid of these programs. The results all strongly indicate that the properties predicted when V is taken to

be the Hamada-Johnston potential would be greatly improved if the tensor force were weakened.

The theory, which has been shown to be equivalent to the Bloch-Horowitz theory with all possible valence states included in the "model space," will be applied to other nuclei which can be reasonably described as two valence nucleons outside an inert core. For more than two particles outside a closed shell, the interaction energies and wave functions emerging from this calculation can be combined with the Argonne shell-model programs to compute more complicated level schemes.

A paper covering this research has been accepted for publication in Nuclear Physics.

(iii) Gamma Decay of Isobaric Analog States

D. Kurath

Gamma decays of several high-lying $J=0^+$, $T=2$ states have been observed in light self-conjugate nuclei. It is a curious fact that these decays cascade to the $J=0^+$, $T=0$ ground state through the same $J=1^+$, $T=1$ states which are strongly excited via inelastic electron scattering. The ground states for the nuclei A = 12, 20, and 24 are well represented by the many-particle Nilsson model, and one might hope that such a description also applies to the isobaric analog excited states.

Sum-rule calculations with this deformed-field model indicate that most of the M1 strength from the ground state should lie in the region of the lower $J=1^+$, $T=1$ states, in agreement with the electron-scattering data. The same treatment for the $J=0^+$, $T=2$ analog state gives moderate M1 matrix elements to the lower $J=1^+$, $T=1$ states, but much larger matrix elements connecting to states nearby in energy to the $J=0^+$, $T=2$ state. Nevertheless the E^3 energy dependence of the transition probability produces a favoring of branching

to the lower $J=1^+$, $T=1$ states in agreement with observation. The fact that these happen to be the states favored in inelastic electron excitation of the ground state is thus somewhat coincidental.

A more detailed application of the Nilsson deformed-field model would be required to calculate the relative strengths of individual transitions for comparison with experiment.

d. Nuclear Reactions

(i) Stripping to Unbound States

C. M. Vincent and H. T. Fortune

An article describing our theory of stripping to unbound states has been submitted to the Physical Review. The theory implies that the reaction measures the width Γ of the final state rather than the spectroscopic factor S. Since the external part of the on-resonance form factor is uniquely determined by the general requirements of scattering theory, it is not subject to the uncertainties that plague the bound case. Accordingly, if the width of a resonance can be measured both by elastic scattering and by the transfer reaction, there is an interesting opportunity to investigate the validity of the distorted-wave analysis of the reaction. Our distorted-wave analysis of the $^{16}O(d,p)$ reaction to the 5.08-MeV $d_{3/2}$ resonance of ^{17}O gives a width of 67 keV. For comparison, total-cross-section data for $^{16}O + n$ lead to $\Gamma = 90 \pm 5$ keV. To explain this discrepancy, better optical potentials are being sought and a new measurement of the (d,p) reaction is being made at the University of Pennsylvania.

In the $^{12}C(^3He,d)^{13}N$ reaction to the resonant $\frac{1}{2}^+$ first excited state, the cross section is smaller—by more than a factor of two—than the cross section for the mirror reaction $^{12}C(t,d)^{13}C$ to the bound mirror state (as seen in Fig. 51). Both experiments were performed at a bombarding energy of 16.0 MeV. These experimental

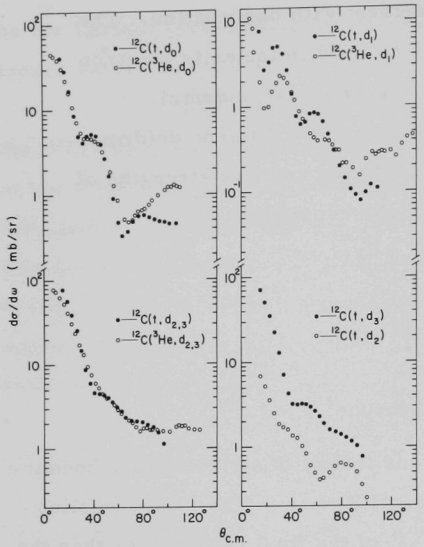

Fig. 51. Angular distributions for (t, d) and (^{3}He, d) reactions to mirror states in ^{13}C and ^{13}N. The ^{3}He and t bombarding energies were both 16.0 MeV. In (^{3}He, d) only the ground state is bound, while in (t, d) all states shown are bound. Evidently the unbound nature of the ($\ell = 0$) $\frac{1}{2}^+$ first excited state causes a drastic reduction in cross section. Since the second and third excited states in ^{13}C are resolved (lower right), it can be seen that the strength is mostly to the $\frac{5}{2}^+$ state. The (^{3}He, d) data are from H. T. Fortune, T. J. Gray, W. Trost, and N. R. Fletcher, Phys. Rev. 179, 1033 (1969). The (t, d) data are from D. D. Armstrong, J. G. Beery, P. W. Keaton, Jr., and L. R. Veeser, Los Alamos Scientific Laboratory Report No. LA-4177 (1969).

results are explained by the DWBA calculations—assuming identical spectroscopic factors for the two mirror states.

A similar effect could perhaps account for the fact that a certain $\frac{1}{2}^+$ state seen strongly as a resonance in ^{90}Zr + p elastic scattering is not observed in the ^{90}Zr(^{3}He, d) reaction.[1] Other possible explanations may lie in the fine structure of the analog states or in the interference of the resonant amplitude with direct three-body breakup.

Routine distorted-wave analysis of single-particle transfer reactions continues. The computer program for such analyses is being made available outside Argonne.

---

[1] P. J. Cooney, N. Cue, R. L. McGrath, and H. Rudolph, Bull. Am. Phys. Soc. 15, 625 (1970).

(ii) Continuum Shell Model

William J. Romo

In recent years there have been numerous attempts to extend the nuclear shell model to the continuum. Although such attempts usually employ rather simple phenomenological residual interactions, they still lead to rather complicated and time-consuming calculations. Thus, an even greater effort has been made to develop approximation schemes for continuum shell-model calculations. Part of the present effort along these lines consisted in the development of an approximation scheme based on a finite-rank approximation to the Green's function of the model system. In more recent work, the use of finite-rank approximations to the residual interaction have been studied as a basis for obtaining approximate solutions of the continuum shell-model equations. The accuracy of a number of existing calculational schemes that use separable interaction approximations have been investigated. The possibility of using a combination of both a finite-rank approximation of the Green's function and the residual interaction has also been explored. The continuum shell-model formalism is currently being applied to calculate the dipole photoreaction cross section of ^{12}C.

(iii) High-Energy Inelastic Scattering from a ^{6}Li Target

William J. Romo

Lawson and Soper recently developed a method of calculating correlated wave functions that describe the motion of two nucleons outside an inert core and interacting through a realistic two-nucleon potential. Lawson applied the theory to ^{6}Li, using a Hamada-Johnston potential for the residual two-body potential. Reasonable agreement with experiments were found in the calculated level schemes and E2 and M1 transition rates. The present study used the correlated ^{6}Li wave functions in calculating the differential cross sections for high-energy inelastic scattering of protons, electrons,

and neutrons from ^{6}Li, which was left in the 2.18- or 3.56-MeV level. The impulse approximation was employed in the calculations, and these were repeated with uncorrelated ^{6}Li wave functions. It was hoped that the computed differential cross sections or polarizations would provide a sensitive test of the short-range correlations, particularly at large angles; but no significant differences were observed.

(iv) Observation of Nonlocal Effects in Nuclear Scattering

J. E. Monahan and R. M. Thaler*

The question of how nonlocal effects might be observed in elastic scattering was considered under the assumption that the interaction could be represented by a Hamiltonian. The energy-dependent behavior of the real part of the forward-scattering amplitude is shown to be related to a dynamical quantity R with dimensions of length, which provides a measure of nonlocality. Possible off-energy-shell effects will be discussed in terms of this distance R.

*Case Western Reserve University, Cleveland, Ohio.

e. Statistical Properties of Nuclei

(i) Analysis of the Distribution of the Spacings Between Nuclear Energy Levels[1]

James E. Monahan and Norbert Rosenzweig

An empirical spacing distribution is always based on a finite, and usually small, number of observed levels. Thus, even if the spacing of levels were described exactly by Wigner's random-matrix model, the observed distribution would necessarily fluctuate about the theoretical mean—the Wigner distribution. A statistic $\Lambda(n)$ has been defined to enable one to judge whether the magnitude of the

[1] James E. Monahan and Norbert Rosenzweig, Phys. Rev. C5, 1714-1723 (May 1970).

observed fluctuations about the Wigner distribution is compatible with the random-matrix model. It is found that the correlations between the spacings implied by the model tend to reduce the expected fluctuations significantly. The statistical properties of $\Lambda(n)$ were studied by means of a Monte Carlo calculation with matrices of order 100 sampled from the Gaussian orthogonal ensemble. An illustrative analysis of the very long series of neutron resonances observed in ^{239}U by Garg et al. reveals no obvious discrepancy between theory and experiment up to neutron kinetic energies of about 2 keV. The statistic $\Lambda(n)$ permits a significant test of Wigner's model also for relatively short series of 10—15 neutron resonances. It is therefore planned to subject the extensive experimental material (obtained during the past decade or so) to a suitable analysis.

(ii) Theory of Nuclear Level Density for Periodic Independent-Particle Energy-Level Schemes[1]

Peter B. Kahn* and Norbert Rosenzweig

Accurate and perspicuous formulas were derived for the density of states of a degenerate system of any number of types of Fermions moving in arbitrary periodic single-particle energy-level schemes. The results are of the standard exponential form with the modification that the excitation energy is to be replaced by an "effective energy." The effective energy contains an additive correction which depends explicitly on the structure and ground-state occupation of the periodic level sequences. The spin-dependent level-density formula for two kinds of particles should be useful in a rough correlation of observed nuclear level densities with shell-model level sequences. The present work generalizes, unifies, and simplifies earlier treatments of related problems.

---

[1] Peter B. Kahn and Norbert Rosenzweig, Phys. Rev. 187, 1193 (1969).

* State University of New York, Stony Brook, New York.

(iii) Mean Level Width and Its Ratio to Mean Level Spacing in Highly Excited Compound Nuclei

K. A. Eberhard* and A. Richter

A statistical model with various approximations has been used to calculate the mean level widths as a function of energy and angular momentum of compound nuclei excited in the continuum region. The results are compared with all experimentally determined coherence widths available between mass numbers A = 16 and A = 116. Although only average parameter values were used throughout the calculations, the agreement achieved with experiment in general is good (as seen in Fig. 52). Furthermore, for these nuclei we have also calculated the ratio of the mean level width to the mean level spacing, which is useful in Hauser-Feshbach calculations. The results are compared with experiment in Fig. 53. It can be shown that for calculating average

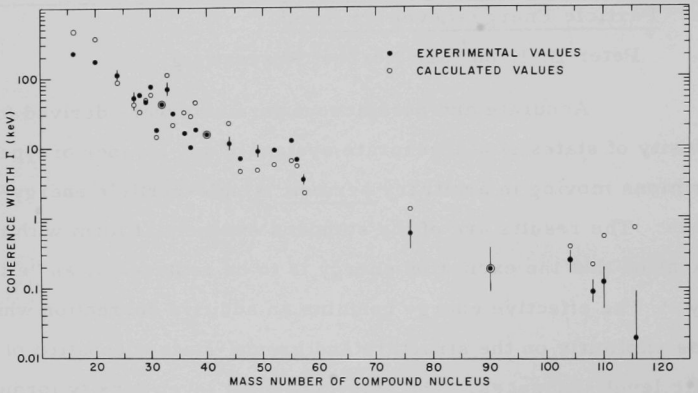

Fig. 52. Experimental and calculated values of the coherence width Γ as a function of the mass number of the compound nucleus. All experimental data available between A = 16 and A = 116 are included in the figure, and the comparison is made for an excitation energy of about 20 MeV in the compound nucleus.

*Florida State University, Tallahassee, Florida.

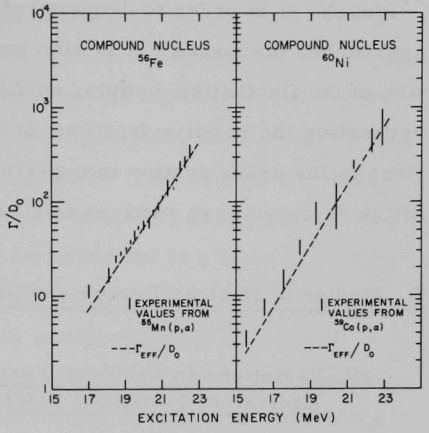

Fig. 53. The experimental ratio of the mean level width to the mean level spacing as determined by Huizenga et al. [Phys. Rev. 182, 1149 (1969)] for the compound nuclei ^{56}Fe and ^{60}Ni, plotted as a function of excitation energy, together with the calculations of the present model.

cross sections, the knowledge of the capture cross sections of all open compound-nucleus decay channels is not absolutely required.

(iv) The Number of Degrees of Freedom in Fluctuation Analysis

H. L. Harney* and A. Richter†

The number of degrees of freedom N_{eff} is a fundamental quantity in analyses of cross-section fluctuations since its knowledge allows one to estimate the relative values of the direct and compound-nucleus cross sections. We have investigated the "basic cross section" method for the calculations of N_{eff} and the modifications of it due to Gibbs. We show that the lack of statistical independence of the basic cross sections raises serious difficulties when one solves for N_{eff} within the Gibbs model. There are no difficulties, however, if N_{eff} is calculated not on the basis of basic cross sections but rather in the basis of statistically-independent collision matrix elements. We calculated N_{eff} for recently published experiments on ^{27}Al(α,p)^{30}Si and

*Max-Planck-Institut für Kernphysik, Heidelberg, Germany.

†Postdoctoral Appointee on leave from Max-Planck-Institut für Kernphysik, Heidelberg, Germany.

$^{31}P(d,\alpha)^{29}Si$ in order to demonstrate the differences between the approaches discussed. It is also emphasized that a realistic calculation of the fluctuation damping coefficient, which is important for estimating the relative fractions of direct and compound-nucleus contributions to the cross section in experiments, does not require the knowledge of the capture cross sections of all open compound-nucleus decay channels.

f. Studies of Nuclear Forces and Nuclear Matter

(i) Variations in Deuteron Form Factors with Phase-Shift-Equivalent Two-Body Potentials

F. Coester and F. C. Hsuan*

Computer programs have been developed to compute deuteron wave functions and the electromagnetic form factors as a function of the momentum transfer. The purpose is to investigate the sensitivity of the deuteron form factors to strong short-range distortions of the wave functions. For a meaningful comparison of the results with data on high-energy electron-deuteron scattering, it will be necessary to investigate the contributions of exchange currents.

*M.S. candidate, University of Iowa.

(ii) Nuclear-Matter Programs

F. Coester, S. Cohen, and C. M. Vincent

Work has continued on a system of programs for nuclear-matter calculations. The basic programs compute the binding energy of nuclear matter as a function of energy, using the Brueckner method with a self-consistent spectrum for the hole states. The interaction may be defined by a potential in coordinate space or momentum space, or by a reference-spectrum reaction matrix. A general routine for computing the momentum-space representations of one-boson-exchange potentials has been developed and checked. This routine will shortly

be used to calculate the binding energy of nuclear matter for the Ueda-Green meson-theoretic potential. The modularity of this routine allows easy variation of the number and parameters of the mesons exchanged, and permits replacement of the Yukawa shape by any desired function. The programs are interfaced to SPEAKEASY. This has the advantage that all data produced by the program can be stored at any time during execution, so that the calculation can be restarted in a later job. This capability is expected to save a great deal of computer time, and facilitate easy manipulation of the data produced by the calculation. The next major development of these programs will be to develop the capacity to compute the contribution of 3-body clusters to the binding energy.

(iii) Four-Hole-Line Diagrams in Nuclear Matter

B. D. Day

A paper describing the enumeration and evaluation of the four-hole-line diagrams, which constitute the third term in the Brueckner expansion for the ground-state energy of a many-body system, has been published. A numerical result of 0.5—1.5 MeV of additional binding energy was obtained for nuclear matter. This confirms quantitatively the convergence of the energy expansion for this system. The methods used for nuclear matter are directly applicable to liquid ^{3}He and liquid ^{4}He, for which four-hole-line terms are more important than for nuclear matter.

g. Studies of Hypernuclei and the Interactions of Λ Particles

(i) Λ in Nuclear Matter; Effective Interactions

The Λ-particle binding in nuclear matter (the Λ well depth) is an interesting many-body problem which is of great interest for hypernuclear physics. Not only can one confront the phenomenological Λ-binding energy in nuclear matter (obtained from hypernuclear

binding energies) with theoretical predictions in order to learn about the Λ-nuclear interactions, but this system also furnishes a useful theoretical laboratory for many questions of importance for hypernuclei generally. Examples are the effects of a repulsive core and of the p-state interaction, and the effect and possible suppression of a ΛN tensor force as well as of the coupling of the ΛN to the ΣN channel. Considerable progress has been made in these studies and several papers have been prepared as follows.

(a) Reaction-Matrix Calculation of the Λ-Particle Binding in Nuclear Matter (D. M. Rote* and A. R. Bodmer). The two principal procedures for obtaining the phenomenological Λ well depth D from the experimental separation energies B_Λ were critically discussed. A value $D \approx 30 \pm 2$ MeV, with an upper limit $D \lesssim 35$ MeV, is consistent with the results obtained from both procedures. A reaction-matrix calculation of D is made for central ΛN potentials with the use of recent nuclear many-body techniques. This calculation is exact in the g-matrix approximation, which gives the term proportional to the density ρ in an expansion of powers of ρ. To calculate the g matrix, the reference-spectrum method is used in the Kallio-Day form. The difference between the single-particle energies of the bound and excited states of the Λ involves an energy gap which is identified with the well depth. This then leads to a self-consistency condition for the determination of D. The angle-average approximation for the exclusion-principle operator, appropriate to a Λ in nuclear matter, is examined and found to be excellent. For hard-core potentials, a perturbation expansion in the strength of the attractive tail is in general inadequate (contrary to previous claims of other authors) and, especially for potentials of short range, it is necessary to obtain the g matrix exactly for the complete potentials.

---

*University of Illinois at Chicago Circle, Chicago, Illinois.

For given low-energy ΛN s-wave scattering parameters, the well depth is sensitive predominantly to two properties of the potential, namely the short-range repulsion and the p-state interaction. Thus, firstly, the s-state contribution D_s to the well depth decreases strongly as the hard-core radius increases. Here, the significant quantity is most probably the correlation volume (or "wound integral") associated with the hard core, and one expects D_s to decrease with this volume in a manner which is roughly independent of the details of the (short-range) repulsion. Secondly, the p-state contribution can be quite large and equal to about 20 MeV for a p-state interaction equal to the s-state one. (Thus a state-independent potential without any hard core would give a very large well depth $D \approx 75$ MeV.) For potentials that fit the binding energies of the A = 3 and 4 hypernuclei as well as the Λp scattering data and which have rather large hard cores, one can get close to the phenomenological value of D by assuming zero p-state interaction. The well depth is found to depend fairly linearly on ρ over a large range, and the Λ effective mass can be as small as $0.65\ M_\Lambda$.

A systematic study of a range of hard-core as well as soft-repulsive-core potentials is presently in progress. It is hoped that these results will establish a correlation between the Λ well depth and the correlation volume and, in particular, will provide a rather universal set of results which will allow one to read off the predicted well depth for any of a large class of ΛN potentials.

(β) The Effect of Tensor Forces and of ΛN-ΣN Coupling on the Well Depth. The following investigations are part of a study of the way in which the Λ well depth is affected by more complicated components of the ΛN force. Of particular interest is whether there are components which can be appreciably suppressed in nuclear matter—and thus perhaps also in finite hypernuclei—and thus enable one to relax the rather extreme assumptions (large hard core, very weak p-state interaction) which we have found are needed if purely central forces

are to account for the phenomenological well depth. So far we have studied the effects of ΛN tensor forces and of the coupling of the ΛN to the ΣN channel. A report on the former has been submitted for publication. The continuing work on the latter is reported in the second item of this subsection.

ΛN Tensor Forces for Scattering and for the Λ-Particle Binding in Nuclear Matter (A. R. Bodmer, D. M. Rote,* and A. Mazza*). The effect of tensor forces on nuclear binding energies is a problem of long standing. Of particular interest is the relation between the effect of a tensor force for scattering and for binding energies—in particular, the question of the so-called suppression of a tensor force in nuclei. In the present research we study these questions for a Λ particle in nuclear matter. Thus we consider the role of ΛN tensor forces for the binding energy of a Λ particle in nuclear matter (i.e., for the Λ well depth D), using both perturbation theory and Brueckner-Bethe reaction-matrix methods. Apart from the specific interest of the Λ well-depth problem, we have tried—in the context of this problem—to obtain a better understanding of the role of tensor forces. We believe our approach has some novel features and is also of wider interest.

One-boson exchange (OBE) models [Sec. III. g(ii)] indicate that the ΛN tensor force is expected to be of short range and moderate strength. For short-range tensor forces, the dominant momentum components are very large and the effects of such forces are only slightly modified by the nuclear medium. On the other hand, if the ΛN tensor forces were of rather long range they would be quite strongly suppressed in nuclear matter. These features are very clearly exhibited by consideration of the effective nonlocal central potentials that represent the (s-state) effect of tensor forces for nuclear matter and for scattering. The ratio of the (nuclear-matter) expectation values of these two effective potentials is a good measure of the suppression.

*University of Illinois at Chicago Circle, Chicago, Illinois.

The expectation value of the effective potential for nuclear matter is just the second-order perturbation-theory energy. Reaction-matrix calculations show that higher-order effects may become quite important for shorter ranges. Such calculations have, in particular, been made for various mixtures of central and tensor forces chosen to give a constant scattering length. Yukawa shapes corresponding to the kaon and one and two pion masses were used as well as "realistic" OBE potentials with a hard core and a tensor component due to kaon exchange (and also approximately due to η exchange). For a particular mixture the suppression is measured by the reduction in the well depth relative to the depth for a purely central potential which has both the same scattering length and the same effective range as the mixture. For the short-range tensor forces, there is rather little suppression even for very strong tensor forces which account for all the triplet scattering. We conclude that if central and short-range tensor forces are chosen to compensate each other for low-energy scattering, they will also compensate each other quite closely for nuclear matter. In particular, for the OBE potentials with strengths consistent with the phenomenological values of the $\Lambda N\overline{K}$ coupling constants, the reduction in the well depth is at most about 3 MeV. The conclusions about the ΛN interaction obtained from a comparison of the calculated and phenomenological well depths are, therefore, effectively unchanged by the presence of a ΛN tensor force. Some further calculations concerning the effect of tensor forces in higher partial waves are in progress.

Effect of ΛN-ΣN Coupling on ΛN Scattering and on the Well Depth (A. R. Bodmer and D. M. Rote*). The effect of the coupling of the ΛN to the ΣN channel on the well depth is the object of a continuing study. This coupling is quite possibly very important, probably largely through the strong and long-range one-pion-exchange coupling potential, which has predominantly a tensor character. The qualitative considerations concerning the effect of the nuclear medium on these couplings

*University of Illinois at Chicago Circle, Chicago, Illinois.

are quite similar to those for tensor forces except that now one has an additional gap of 77 MeV due to the $\Sigma\Lambda$ mass difference. Reaction-matrix calculations indicate that one could readily obtain an appreciable suppression of the ΛN-ΣN coupling in nuclear matter, corresponding to a reduction in the well depth by as much as 10—15 MeV.

If one accepts suppression of this order of magnitude, then one can tolerate a smaller hard-core radius and a weakened but still appreciable p-state interaction. Some of this work was reported at the International Conference on Hypernuclear Physics, Argonne, May 1969, and more complete results are presently being written up for publication.

Similar calculations are being extended to other types of meson-exchange coupling potentials and to higher partial waves.

Of great and fundamental interest are three-body ΛNN interactions and the clarification of the relation between these and suppression of the ΣN channel in hypernuclei if this channel is explicitly included in the two-body interaction.

Also very much needed are extensions of our studies of the effect of the ΛN-ΣN coupling to finite hypernuclei in order to obtain an understanding of the role of the ΣN channel—in particular the extent of its suppression—in finite hypernuclei. An interesting and potentially fruitful approach to this and a number of other problems is the use of effective central potentials to represent the effect of tensor forces (also for ordinary nuclei) and of the coupling of the ΛN to the ΣN channel.

(ii) Theoretical Models of the ΛN and $\Lambda\Lambda$ Interactions

A. R. Bodmer and D. M. Rote*

The interaction between a Λ particle and a nucleon (and also between two Λ particles) have been and are being studied.

*University of Illinois at Chicago Circle, Chicago, Illinois.

This work, not so far published, uses meson-exchange (one-boson-exchange) models which also include coupling of the ΛN to the ΣN channel. In spite of all the attendant uncertainties, such models can provide a valuable guide to the form of interactions to use in studies of hypernuclear structure. Thus, they can provide indications of the ranges and the importance of the possible components of the interaction, such as tensor and spin-orbit forces. In fact, even rather qualitative information about the components of the interaction may have very valuable implications for studies of hypernuclear structure (as in our studies of the effects of tensor forces and of coupling to the ΣN channel on the Λ binding in nuclear matter, as discussed in Sec. III. g(i). Conversely, the results of phenomenological hypernuclear analyses of binding energies and scattering data may give some fundamental information about coupling constants, hard-core radii, etc. To date, the emphasis has been on the low-energy and (in particular) on the s-state ΛN (and $\Lambda\Lambda$) interactions. These studies are being extended to higher partial waves (in particular, to the p-wave interaction which is important for nuclear-structure studies) and to higher energies. Eventually, we also intend to study momentum-dependent terms in the one-boson-exchange potentials.

(iii) Variational Studies of Bound Three-Body Systems

A. R. Bodmer and A. Mazza*

This work is continuing, although rather little progress has been made in obtaining definite results during the past year. Some attention is being given to the variational calculation of the binding energy of the hypertriton if tensor forces are included in the ΛN interaction. This is a complement of our study [second item in Sec. III. g(i)(β)] of the effect of ΛN tensor forces on the Λ-particle binding in nuclear matter.

*University of Illinois at Chicago Circle, Chicago, Illinois.

h. Quantum Mechanics and Quantum Liquids

(i) Quantum Theory of Sojourn Time

H. Ekstein and A. J. F. Siegert*

Is there a "time operator" in quantum mechanics? The question is of great conceptual importance and has attracted much attention. We have formulated a quantum-mechanical operator which appears to have none of the paradoxical features of those discussed in the past. A simple model is being studied both mathematically and with respect to physical realization.

While our aim is mostly clarification of principles, it may be that our results will shed some new light on some ill-understood features of decay theory.

*Northwestern University, Evanston, Illinois.

(ii) Magnetic Charge in Quantum Mechanics

H. J. Lipkin,* W. I. Weisberger,* and Murray Peshkin†

Dirac found in 1931 that, under some assumptions, electric and magnetic charges must be quantized in units (e and g, respectively) that obey

$$eg/c = n\hbar/2, \qquad (1)$$

where n is an integer. Dirac's quantization law (1) has usually been accepted in spite of questions that may be raised about his assumptions, principally because of qualitative arguments indicating that the quantity eg/c represents the angular momentum of an electromagnetic field. The result is an important one, because it implies that the minimum nonvanishing magnetic charge should be a strong one ($g \approx 70\ e$). Many experiments which search for magnetic charges assume that

*Weizmann Institute of Science, Rehovot, Israel.

†Work done partly while on assignment to the Weizmann Institute.

great strength, and would not detect a magnetic charge whose strength is comparable to e.

An accurate derivation has now been given in order to find reasonable assumptions under which the quantization law (1) is directly related to the quantization law for angular momentum. It has also been demonstrated that odd-integral values of n are possible in at least one quantum-mechanical model, contrary to some recent speculations.

(iii) Angular Distribution of Photoelectrons

Murray Peshkin*

Angular distributions of photoelectrons have often been calculated on the basis of particular dynamical models. It turns out that electric-dipole absorption by randomly-oriented atoms or molecules always leads to the same one-parameter angular distribution, and that changing the polarization state of the incident light varies that angular distribution in a predictable way, independently of the dynamics of the photoejection process. This result has been recognized as a manifestation of symmetry under rotation and space inversion, but the consequences of those symmetries for photoelectron angular distributions have not previously been pursued in a systematic way.

Such a systematic treatment has now been carried out, primarily for the benefit of people who design instruments or plan experiments to measure photoelectron angular distributions. The angular distributions of the electrons, for general multipole mixtures of the absorbed photons, have been determined for various polarization states of the absorbed light. The parameters that depend upon the specific dynamical properties of the target atoms or molecules have been identified. It has been found, for instance, that polarization never introduces new dynamical information in one-electron

*Work done partly while on assignment to the Weizmann Institute.

measurements but can introduce new information when two-electron angular correlations are considered. A complete report has been accepted for publication.[1]

[1] Murray Peshkin, Advan. Chem. Phys. 18, 1-14 (1970).

(iv) Brueckner Theory of Liquid ^{4}He

B. D. Day and B. H. Brandow*

The Brueckner-type theory of the many-boson system recently developed by Brandow is being used in calculations for liquid ^{4}He at zero temperature. The theory allows calculation of the ground-state binding energy, the excitation spectrum, and other properties of interest. Accumulated experience with the two-, three-, and four-body terms of nuclear matter is being extensively used. The Brueckner approach is completely different from the conventional methods of treating liquid ^{4}He; so it is hoped that the new theory will not only be quantitatively successful, but will also provide new physical insight into the properties of liquid ^{4}He.

* Battelle Research Center, 4000 NE 41st Street, Seattle, Washington.

IV. EXPERIMENTAL ATOMIC PHYSICS

Five entirely different kinds of physics are included in Experimental Atomic Physics. These are studies of the Mössbauer effect, the interaction of charged particles with surfaces and thin films, photoionization of gases, rf plasmas, and atomic beams. These investigations are continuing along generally the same lines as in the past, but several developments during the past year are likely to have an important influence on the future of the program.

Major technical developments are expected to strengthen these programs. Especially significant for the photoionization experiments are the continuing preparations for the use of the MURA electron storage ring as a source of synchrotron radiation and a concerted effort to develop refined analyzers for low-energy electrons. Similarly, in the atomic-beam program, the development of a specialized machine for measurements on radioactive materials is laying the foundation for future experiments.

Two recent experiments are likely to be of special importance for the future. One of these is the development and use of techniques that allow a Mössbauer absorption spectrum for ^{67}Zn to be measured routinely and with good quality. In view of the extremely narrow line width in the ^{67}Zn spectrum, this capability will probably open the door to important fundamental experiments such as a much better measurement of the gravitational red shift. The second achievement is the demonstration that nuclear projectiles can be polarized by channeling in metallic monocrystals. Work is now under way to determine how this new technique can be used most advantageously in the construction of a useful source of polarized ions.

A significant aspect of the work in atomic physics is that a fairly large fraction of it has a direct bearing on new applied programs being carried out or planned by the Laboratory. In particular, our investigations of plasma physics and of the interactions of nuclear radiations with metal surfaces are central in a current study of the ways in which the unique talents and facilities at Argonne can best contribute to the Controlled Thermonuclear Research program of the AEC. One very natural contribution would be to provide the experimental data needed for a better understanding of the problems arising from the interaction of intense nuclear radiation with the vacuum wall of a plasma reactor.

1. MÖSSBAUER MEASUREMENTS

In the last few years, the Mössbauer effect has become a powerful tool for the study of many phenomena in solid-state, chemical, and low-energy nuclear physics. The experiments are aimed in two directions: (a) to yield accurate measurements of previously unobtainable nuclear properties (e.g., the quadrupole moments and magnetic moments of excited nuclear states) and (b) to make accurate determinations of the environment in which a nucleus is immersed (e.g., to determine the charge transfer from an iodine atom as it forms a chemical bond with chlorine). Recent Argonne experiments have been concerned with such diverse nuclear species as ^{40}K, ^{57}Fe, ^{67}Zn, ^{119}Sn, ^{121}Sb, ^{129}I, ^{133}Cs, ^{133}Ba, ^{191}Ir, ^{152}Sm, ^{237}Np, ^{238}U, and ^{243}Am, and others are being considered.

Two expecially interesting developments in the past year have been the extension of the Mössbauer technique to the study of anomalous magnetic moments (^{193}Ir) and to successful measurements on ^{67}Zn, which is the Mössbauer nucleus with the longest life and hence the narrowest line width. The latter increases the available resolution by a factor of 600 and thereby opens the way to such experiments as an improved measurement of the gravitational red shift.

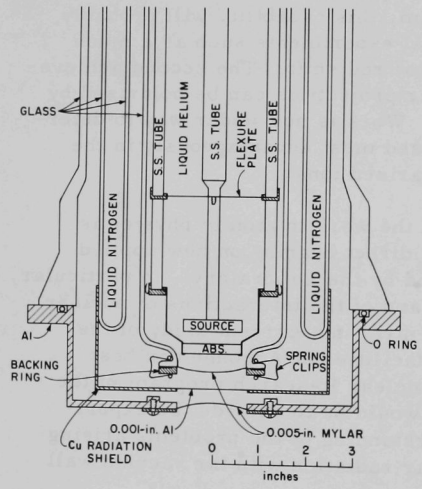

Fig. 54. Tail section of the cryostat.

a. Helium Cryostat for Mössbauer Experiments

S. L. Ruby and B. J. Zabransky

The frequent demands for large solid angle, low temperatures, and high transmission in Mössbauer experiments increase the cost and complexity of helium cryostats. A glass cryostat (Fig. 54) has been constructed that meets these requirements with the simultaneous advantages of low cost and easy construction.

A commercial cryostat was modified to accept a 0.005-in.-thick Mylar window bonded to the bottom of the helium container and to the outer vacuum shroud. It gives a transmission $I/I_0 = 0.89$ at 14 keV, its holding time is nearly 4 days on a 3-liter filling, and no window failures have occurred during 19 months of service. The cryostat is now available commercially.

b. Hartree-Fock Self-Consistent-Field Calculations for Iridium

L. W. Panek and G. J. Perlow

Nonrelativistic Hartree-Fock self-consistent-field (HFSCF) calculations have been carried out for a set of 55 outer-electron configurations (core) $5d^N 6s^M 6p^K$ in iridium (Z = 77) by use of the CDC-3600 computer and the program of Froese and Wilson. Of central interest are the calculation of the electron density at the nucleus, $\rho(0)$, as a function of N, M, and K and a fit by an analytical expression containing lowest-order shielding effects. The results are plotted in Fig. 55. The calculations are a basis for a quantitative study of the isomer shifts in the Mössbauer spectra of iridium compounds. In addition to $\rho(0)$, we tabulated the values of the one-electron energy parameters, the mean values of various functions of r, the screening parameters, and the initial slope parameter $a_{n\ell}$. The results were published in topical report ANL-7631.

c. The Mössbauer Effect of the 93-keV Transition in ^{67}Zn

H. de Waard and G. J. Perlow

The first excited state in ^{67}Zn at 93 keV has a half-life of 9.4 μsec and a width $\Gamma = 4.8 \times 10^{-11}$ eV. This is only 1% as wide as the well known 14.4-keV line of ^{57}Fe. When compared on the basis of the ratio of linewidth to gamma-ray energy, a more important criterion for most purposes, it fares even better; the ratio $\Gamma/E = 5.2 \times 10^{-16}$ for ^{67}Zn is 0.16% of that for ^{57}Fe. This is a

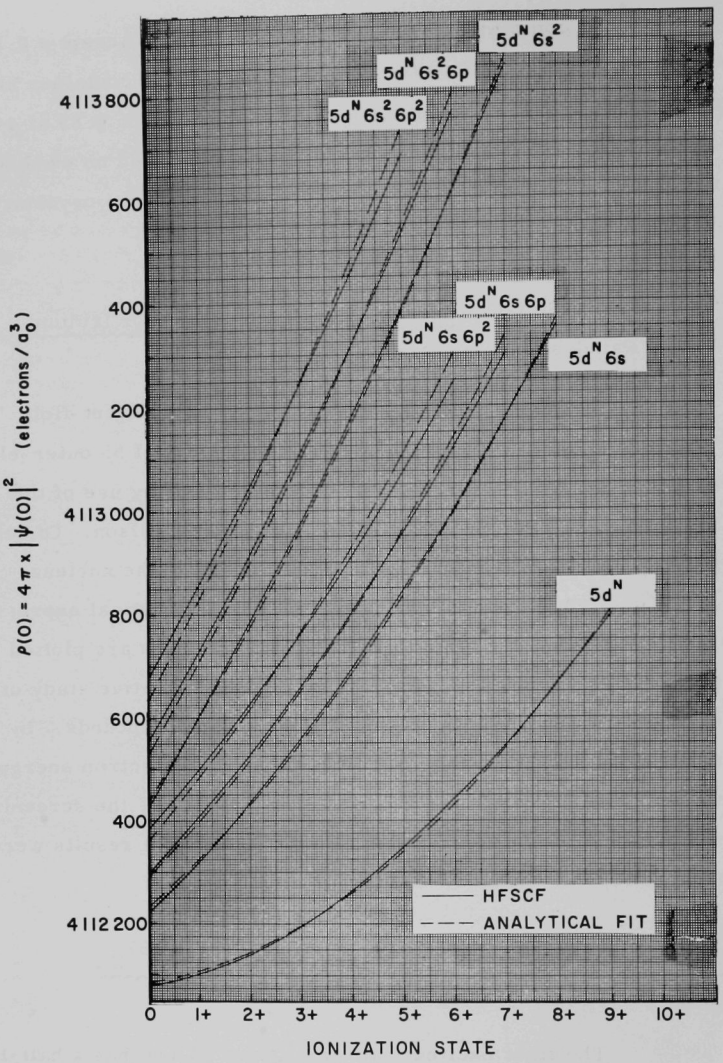

Fig. 55. Electron densities at the iridium nucleus, calculated with the Froese-Wilson program, for a variety of electron configurations: (core)$5d^N 6s^M 6p^K$. The analytical fit is of the form

$$\delta\rho = A[M + \gamma_{di}(10 - N)^2 - \gamma_{ds} NM - \gamma_{ss} M(M - 1) - \gamma_{ps} KM],$$

with the values $A = 562$, $\gamma_{di} = 0.0129$, $\gamma_{ds} = 0.097$, $\gamma_{ss} = \gamma_{ps} = 0.060$.

very narrow line indeed. The gravitational red shift becomes equal to Γ for a vertical distance of only 4.8 meters at the earth's surface. Because very sophisticated experiments on this and similar phenomena might thus be performed in the laboratory, experimenters have sought for a decade to obtain good-quality Mössbauer spectra of the transition. The resonance was in fact observed at Los Alamos in 1960 by Craig and collaborators, who used magnetic scanning. In the following year, a Russian group used a piezo-electric crystal as a velocity spectrometer and were able to observe a spectrum in the traditional manner by Doppler scanning. The absence of further published work since 1962 testifies to the difficulties of obtaining spectra of even quite modest quality.

We have constructed a piezo-electric spectrometer consisting of a stack of quartz crystals suspended by strings in an acoustic shield immersed in liquid helium. With this spectrometer, good-quality spectra (Fig. 56) have been obtained with an absorber of enriched ^{67}ZnO used with sources of ^{67}Ga contained in a host lattice of ^{66}ZnO. In preparing the source, the sintered oxide was bombarded with deuterons from the cyclotron and then carefully annealed. The resulting well-resolved quadrupole-split spectrum corresponded to a quadrupole coupling of 2.5 MHz. The coupling was observed to diminish by

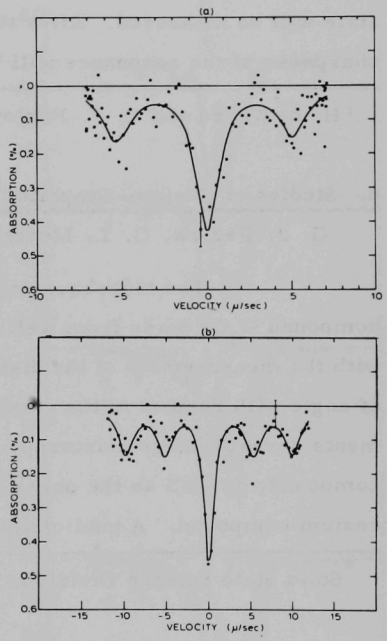

Fig. 56. $Zn^{67}O$ Mössbauer spectra for two velocity ranges: (a) from -7 to +7 μ/sec, (b) from -12 to +12 μ/sec. Source: 70-h Ga^{67} activity produced in $Zn^{66}O$ by (d,n) reaction. Absorber: 2.11-g/cm² $Zn^{67}O$ enriched to 89.6%.

8% when the source was compressed with about 40 kbar. Linewidths of 0.8—2.7 microns/sec were measured with various combinations of source and absorber and intensities ranging to about 0.5%. The narrowest line corresponds to about 2.5 times the minimum observable width 2Γ, and is only 0.4% as wide as the ^{57}Fe line. A report on this first experiment has been published.[1]

The next steps are expected to be a search for improved source-and-absorber combinations and modifications of the spectrometer to obtain greater versatility. The magnetic moment of the excited state will be measured. After this, experiments utilizing the extreme sharpness of the resonance will be attempted.

[1] H. de Waard and G. J. Perlow, Phys. Rev. Letters 24, 566 (1970).

d. Studies of Cesium-Graphite Compounds

G. J. Perlow, G. L. Montet,* and L. E. Campbell

The Mössbauer experiments on the cesium-graphite compound C_8Cs made from well-oriented graphite have been completed with the measurement of the distribution of γ-ray emission as a function of angle with respect to the c axis of the crystallites. These experiments reveal a large anisotropy of the recoilless fraction for this compound, as well as the only clear case of quadrupole splitting in a cesium compound. A publication is being prepared.

*Solid State Science Division.

e. Iodine in Starch

S. L. Ruby

The use of nuclear-gamma-resonance techniques for iodine in organic compounds is barely beginning; this work is the first attack on a somewhat biological problem. During the last decade, the long-known iodine-starch complex has been attributed to long chains of

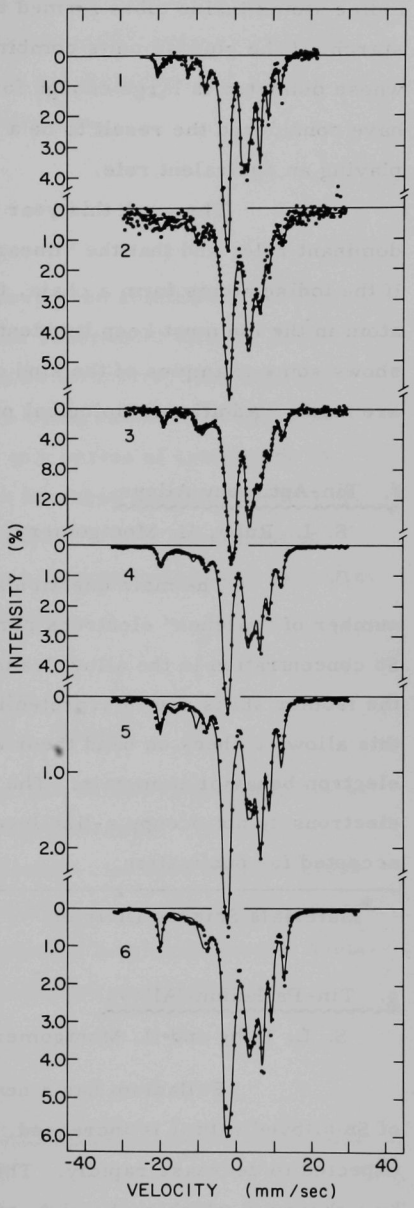

Fig. 57. Mössbauer spectra of (1) CsI_3, (2) CsI_3 in frozen aqueous solution, and iodine complexed with the starch-like compounds (3) amylose, (4) benzamid, (5) α-cyclodextrin, and (6) β-cyclodextrin. To make adequate fits to these spectra, at least three distinct microenvironments for the iodine atoms are required. The overall similarity of the spectra indicates that the I_3^- ion dominates in all these samples.

iodine atoms inside tubes formed by the amylose constituent of the starch. (The glucose units combine to form a rather linear α-helix whose diameter is large enough for the iodine atoms.) Several authors have considered the result to be a "linear metal," with all the iodines playing an equivalent role.

The work this year indicates that the I_3^- ion plays a dominant role, and that the "linear metal" model is not appropriate. If the iodine atoms form a chain, the links must be I_3^- ions and each atom in the ion must keep its identity for at least 20 nsec. Figure 57 shows some examples of the kind of evidence on which these deductions are made. Additional biological problems are being sought.

f. Tin-Antimony Alloys

S. L. Ruby, H. Montgomery,* and C. W. Kimball*

The main question asked was whether an increasing number of "valence" electrons per atom (achieved by increasing the Sb concentration in the alloy) leads to increased isomer shifts. Since the isomer shifts are interpreted in terms of s and p electron densities, this allows a check on band theories that attempt to understand the electron behavior in metals. The results show clearly that the additional electrons do not occupy s-like levels. A report on this work has been accepted for publication.

*Materials Science Division.

g. Tin-Palladium Alloys

S. L. Ruby and H. Montgomery*

Palladium has a nearly full d band; and as the amount of Sn alloyed with it is increased, the number of holes in this band is expected to decrease rapidly. This charge-transfer picture is opposed by a theory in which each solute atom is pictured as being screened

*Materials Science Division.

by the conduction electrons (Friedel's theory). Our main result is that the simple charge-transfer band-filling model seems to fit our data rather well, but Friedel's theory is not disproved. A report on this work has been accepted for publication.

h. Organo-Antimony Compounds

S. L. Ruby and J. G. Stevens

Organo-tin compounds have been studied intensively by use of the Mössbauer (nuclear gamma resonance) effect. Such measurements (which yield information on structure, bonding, and mechanisms of transformation) are now being extended to antimony. Comparison between the isomer shifts in a series of compounds in which the ions are isoelectronic, which has been useful in studies of inorganic compounds of Sn and Sb, continues to be a good guide in these organic compounds. Most of these measurements will hereafter be made at the University of North Carolina.

i. Lattice Dynamics of Tin Tetramethyl

S. L. Ruby, B. J. Zabransky, and I. Pelah*

The Debye-Waller factor can be determined by nuclear gamma resonance as well as by x-ray spectroscopy. This factor corresponds to the rms amplitude of thermal vibration of the nucleus under study. At low temperatures, $Sn(CH_3)_4$ is a typical molecular solid; but the present study has demonstrated large anharmonic deviations from typical solid behavior as the temperature is raised.

*Solid State Science Division.

j. The Recoil-Free Fraction for ^{182}W in a Sodium Tungsten Bronze

L. E. Conroy and G. J. Perlow

The recoil-free fraction f_a of the 100.1-keV line of ^{182}W was measured with the Mössbauer effect in an absorber of a

tungsten bronze $Na_{0.8}WO_3$ at 4.2°K by the variation of line width with thickness. The result is $f_a = 0.18 \pm 0.01$, corresponding to $\theta_M = 298$°K and rms zero-point motional amplitude R = 0.044 Å. The amplitude is almost as small as that in tungsten itself and considerably smaller than the amplitudes in beryllium or diamond.

k. Mössbauer Investigation of Iron Minerals in Meteorites

E. Segel

The recoilless resonance absorption of 14-keV gamma rays from ^{57}Fe was used to identify the iron minerals present in meteorites and to determine the amount of iron present in each mineral. The absorption spectra are used to test theories of the origin of meteorites and the genetic relationships that might link the various meteorite groups.

A recent study of the unequilibrated ordinary chondrites (published in Meteorite Research) was used to test the suggestion of Dodd, Van Schmus, and Koffman that the equilibrated ordinary chondrites evolved from unequilibrated chondrites by a diffusion mechanism that enhanced the silicate iron content at the expense of other iron minerals such as magnetite. The Mössbauer absorption spectra showed that this model was clearly incorrect, since the large quantities of iron required to enhance the silicate iron content did not appear in the magnetite absorption intensity of the unequilibrated ordinary chondrites.

Another study of the oxidation products present in meteorites was performed at the request of the curator at the U. S. National Museum in order to resolve some ambiguities that arose in an x-ray diffraction investigation. Because of the uncertainty that the substitution of Ni for Fe introduces into the x-ray parameters, the x-ray analysis of a particular meteorite could not distinguish between Fe_3O_4 and γ-Fe_2O_3. The Mössbauer investigation showed large quantities of γ-Fe_2O_3 but only a small amount of Fe_3O_4. The similarity between

some meteoritic and lunar materials has produced great interest in the recoilless fractions we have measured for meteoritic minerals.

Work on this project is being continued.

ℓ. Hyperfine Anomaly in ^{193}Ir by the Mössbauer Effect, and Its Application to Determination of the Orbital Part of Hyperfine Fields[1]

G. J. Perlow, W. Henning, D. Olson, and G. L. Goodman*

A 7% hyperfine anomaly is found in Mössbauer measurements of the 73-keV transition in ^{193}Ir. A 2% difference is found between the anomalies in antiferromagnetic IrF_6 (Fig. 58) and Ir-Fe alloy. The difference is ascribed to orbital contributions which differ for the two iridium environments. By using known details of IrF_6 we find the orbital field in the Ir-Fe to be $H_1 = +335 \pm 200$ kOe. A variety of magnetic effects can be studied by the technique of measuring the variation of this anomaly.

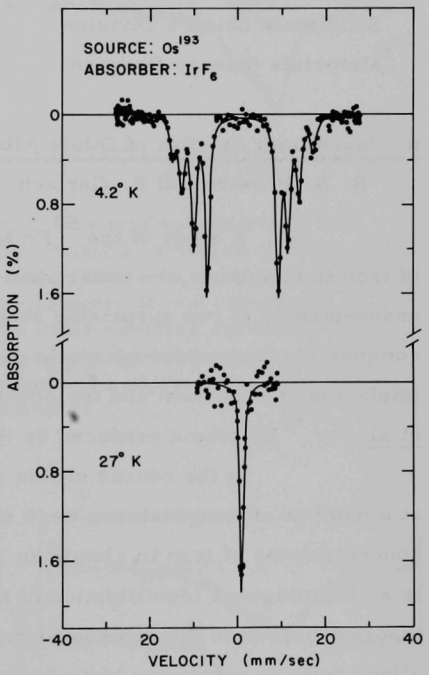

Fig. 58. Velocity spectrum of IrF_6 below and above the magnetic transition temperature.

---

*Chemistry Division.

[1] G. J. Perlow, W. Henning, D. Olson, and G. L. Goodman, Phys. Rev. Letters 23, 680 (1969).

m. Uranium

S. L. Ruby, G. M. Kalvius,* and M. Kuznietz†

We have attempted to apply the nuclear-gamma-resonance technique to the study of some interesting problems in the ferromagnetism and antiferromagnetism in the cubic lattices of the compounds US and UP and of alloys between them, but its resolution was found to be inadequate for useful measurements. A very large nuclear magnetic field (4×10^6 G) has been found in the case of US.

*Solid State Science Division.

†Materials Science Division.

n. Mössbauer Spectra of Dilute Alloys of Iron in Aluminum

R. S. Preston and R. Gerlach

A study of the ^{57}Fe Mössbauer spectrum of dilute alloys of iron in aluminum was undertaken in the hope that it would lead to an understanding of two surprising results, namely the unexpectedly complex spectrum Sprouse et al. observed for ^{57}Fe nuclei recoil-implanted in aluminum and the equally unexpected results of Bara et al. for ^{57}Fe atoms produced by the decay of ^{57}Co within aluminum.

In the course of this work, Mössbauer measurements at a number of temperatures were made on samples containing various concentrations of iron in aluminum (Fig. 59). The results have led to an unambiguous identification of the two components of the spectrum that correspond to the two equilibrium phases which coexist in these alloys down to extremely low concentrations. The effective Debye temperatures for iron in these two phases have also been estimated.

The recoil-implantation spectrum was compared with the absorption spectrum for a dilute alloy that had been rapidly quenched from the molten state. These spectra are shown in Fig. 60. It was concluded that there is melting and quick refreezing along the path of

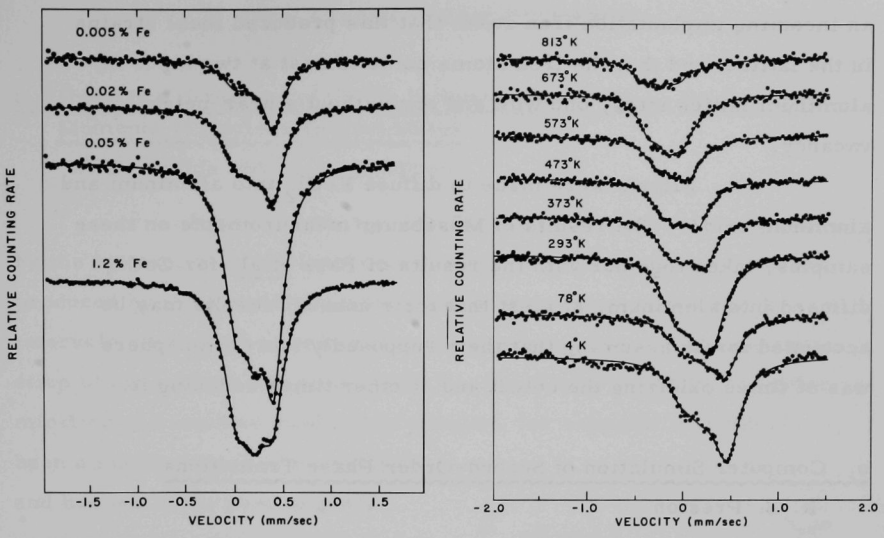

Fig. 59. Mössbauer spectra (left) for various concentrations of iron in aluminum and (right) for the 0.02% sample at a series of different temperatures. Each spectrum consists of two components corresponding to the two alloy phases. The intensity of one component increases with iron concentration; the other remains constant. The solid lines are theoretical fits to the previously determined shapes of the two components. The only parameters adjusted for the fits were the intensities of the two components.

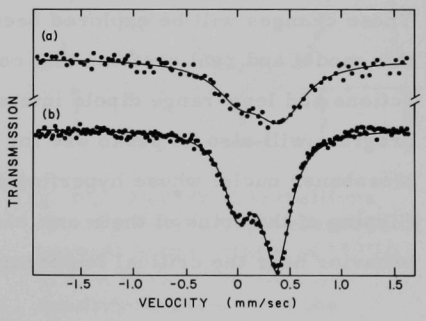

Fig. 60. Comparison of the effects of radiation damage with the effects of quenched-in vacancies: (a) recoil-implantation spectrum for ^{57}Fe in aluminum, in which the broadening represents radiation damage produced in the lattice by the implanted iron atom; (b) spectrum of a dilute alloy of iron in aluminum containing many quenched-in vacancies. The similarity of the two spectra suggests that the radiation damage in the vicinity of the recoil-implanted atoms also consists largely of vacancies.

an incoming implantation iron atom; that this produced local strains in the lattice; and that the iron atoms come to rest at two kinds of aluminum lattice sites, one with and one without a near-neighbor vacancy.

Efforts were made to diffuse $FeCl_2$ into aluminum and aluminum oxide. The results of Mössbauer measurements on these samples, taken together with the results of Bara et al. for $CoCl_2$ diffused into aluminum, suggest that their unusual results may be accounted for by assuming that their supposedly inert atmosphere was at times oxidizing the cobalt and at other times reducing it.

o. Computer Simulation of Second-Order Phase Transitions

R. S. Preston

The computer program for simulating the time development of spin configurations in an Ising lattice has been modified for use on the 360-75 computer, and to include time realistically in the cinematographic display of the behavior of the spins, as well as in the calculation of time averages of thermodynamic quantities. It has been found possible to modify the exchange interaction so that it is a mixture of nearest-neighbor and infinite-range (molecular field) interactions. This produces dramatic changes in the behavior near the critical point. These changes will be explored because of the analogy that exists between this model and real systems that combine short-range exchange interactions and long-range dipole interactions among the spins. The program will also be put to use for calculating relaxation spectra for Mössbauer nuclei whose hyperfine fields are being modulated by the flipping of the spins of their own electrons, with special emphasis on the behavior near the critical temperature.

2. ATOMIC-BEAM RESEARCH

a. Hyperfine Structure of Stable Isotopes, and Electric-Quadrupole Moments of Nuclear Ground States

W. J. Childs and L. S. Goodman

Hyperfine energy differences in free atoms are caused by the interaction of nuclear moments with the electromagnetic fields produced by the atomic electrons, and measurement of the energy intervals yields both atomic and nuclear information. Accurate separation of the nuclear and atomic effects, which is a necessity for determination of a nuclear quadrupole moment, for example, has always been a major source of uncertainty, and has led in the past to gross errors in evaluation of nuclear moments. Our experiments, using the atomic-beam magnetic-resonance technique, are intended to reduce the uncertainty in the atomic part and thereby to give more accurate values for nuclear moments for comparison with the results of nuclear theory. The procedure is (1) to measure the hfs for a particular isotope in a number of different atomic states (preferably including states of two different electron configurations), and (2) to make a detailed comparison between the results and atomic theory. The (atomic) analysis should take account of any

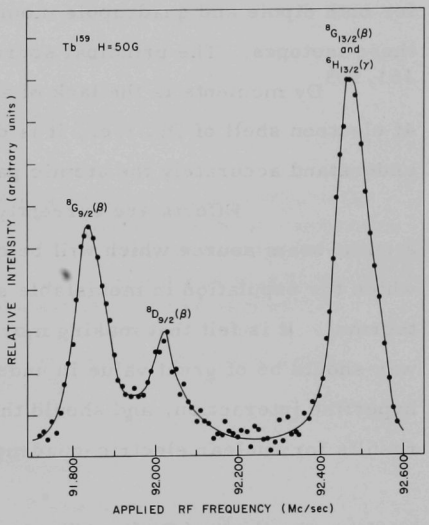

Fig. 61. Hyperfine transitions ($F, M_F \leftrightarrow F', M_F'$) observed in several atomic states of ^{159}Tb at H = 50 G. The electric-quadrupole moment of the nucleus is deduced from consideration of many such observations.

departure of each state from the L-S limit, the effects of configuration interaction and relativity, and both magnetic-dipole and electric-quadrupole shielding effects caused by inner-shell distortions.

Measurement of the hfs in 17 atomic states in two electron configurations of ^{159}Tb has been completed, and a detailed analysis of the type described leads to the value Q = +1.34 b for the electric-quadrupole moment of the ^{159}Tb nuclear ground state, with an overall uncertainty of only 8%. A great deal of atomic information was also accumulated. Figure 61 shows three of the hyperfine transitions observed in ^{159}Tb at H = 50 G. Quantitative understanding of the resonance frequencies for hundreds of such transitions is required for the analysis. Similar, though less detailed, studies in ^{161}Dy and ^{163}Dy lead to values for both dipole and quadrupole moments in the nuclear ground states of these isotopes. The principal source of the uncertainties quoted for the ^{161,163}Dy moments is the lack of a dependable value for $\langle r^{-3} \rangle$ in the 4f electron shell of Dy, i.e., it is due to our present inability to understand accurately the atomic part of the hyperfine energy.

Efforts are currently going into development of an atomic-beam source which will be capable of producing a beam in which the population in metastable states is greatly enhanced over thermal. It is felt that making more states available for study in this way should be of great value in understanding the atomic part of the hyperfine interaction, and should thereby lead to more dependable results for nuclear electric-quadrupole moments.

b. Investigations of Radioactive Isotopes

H. Diamond,* L. S. Goodman, J. A. Dalman, and H. E. Stanton

Through determinations of the hyperfine interactions, atomic-beam measurements of the actinide elements can yield information on nuclear spins and magnetic moments as well as on the electronic

*Chemistry Division.

structure of these elements. Apparatus for this purpose was constructed in the Hot Laboratory (M Wing of the Chemistry Building) and was tested with radioactive materials. Two mass-spectrometer detectors are now under construction. One will be used to measure several Fr isotopes, the other will be used for beam alignment and for research on several long-lived radioisotopes (e.g., ^{235}U, ^{233}U, and ^{229}Th). The gyromagnetic ratio for the atomic ground state and the first excited state of fermium is now being investigated by use of ^{254}Fm. We are also attempting to demonstrate that a transition which the literature assigns to ^{141}Ce ($g_J = 0.76515$) is actually due to ^{143}Pr.

Measurements on ^{223}Fr, ^{253}Es, ^{250}Bk, ^{235}U, ^{243}Pu, and several metastable atomic states in ^{141}Ce and ^{143}Ce are planned in the next year or two.

3. RADIO-FREQUENCY PLASMAS

The central purpose of this research is to advance the understanding of the basic properties and mechanisms of low-pressure plasmas produced by rf fields, with special emphasis on aspects relevant to controlled thermonuclear research. The two lines of experimental and theoretical investigation being pursued are studies of plasmas produced (a) in the approximately uniform rf electric field between parallel-plate electrodes and (b) in the nonuniform standing-wave electromagnetic fields in resonant cavities.

a. Plasmas in Uniform RF Electric Fields

A. J. Hatch, M. Hasan,* and W. P. Allis†

Work has continued on the slab-model theory of the impedance of bounded resonant rf discharges (including rf plasmoids) in the two-decade pressure range just below the collision-frequency transition pressure. This theory has been used to calculate values of

*Consultant, Northern Illinois University.

†Consultant, Massachusetts Institute of Technology.

internal plasma parameters such as density and electric field from values of the gross external impedance measured earlier. These calculated values have been found to correlate well with the few existing measured values of the corresponding parameters, which are much more difficult to measure than impedance. More importantly, they are the basis for the first comprehensive description of the plasma mechanisms in this two-decade pressure range.

Development of the four-probe method of measuring impedance, combined with computer reduction of data, has continued. This system has the two main advantages of flexibility in permitting measurements of nonlinear plasma impedance under any condition of tuning or detuning of the exciting circuit, and of accuracy about 1—2 orders of magnitude better than that obtainable with more conventional data-reduction methods involving direct graphical use of the Smith chart. We intend to use this system to study the changes in plasma mechanisms as manifested by impedance changes measured when a circuit initially tuned with no plasma becomes detuned as a plasma forms and then is retuned with plasma present. The importance of understanding these changes arises in part from the fact (already established in our earlier work[1]) that rf power coupled into the plasma can be increased by as much as an order of magnitude merely by retuning the exciting circuit with plasma present.

[1] A. J. Hatch and L. E. Heuckroth, J. Appl. Phys. 41, 1701 (1970).

b. Plasmas in Nonuniform Cavity Fields

A. J. Hatch and J. L. Shohet*

Two computer programs have been written for the simulation of rf confinement of low-density plasmas ($n < n_c$, where n_c is the cutoff density above which the field does not penetrate the plasma). One program is for the two-dimensional behavior of a single particle

*Consultant, University of Wisconsin.

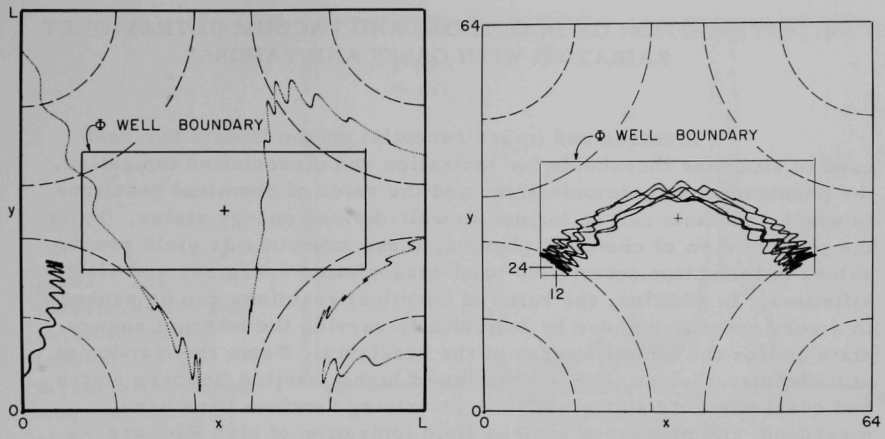

Fig. 62. Electron trajectories in the x-y midplane of a cubical resonant cavity as computed with the plasma-simulation program. The inner rectangle is the boundary of the theoretical Φ potential well for confinement of individual charged particles or low-density plasmas ($n < n_c$) in the quadrupole electric mode. Electric field lines are approximately as indicated by the dashed curves. All electrons are released with zero initial velocity at positions of maximum amplitude of field-driven oscillatory motion. Nonconfinement (left): five electrons released one at a time at various positions outside the Φ well. Confinement (right): one electron released inside the Φ well.

in a resonant-cavity field. This has been used to determine quiet-start conditions in an rf field and to verify the potential-well concept of rf confinement in a quadrupole electric mode as shown in Fig. 62. The other program is for the two-dimensional behavior of a low-density two-component plasma (e. g., electrons and ions) in a resonant-cavity field and is currently being used with an array of 900 superparticles initially in a 30 by 30 lattice. (A superparticle is a large number of particles all acting in unison.) This program will be used to study the effects of self-developed quasistatic space-charge fields of rf confinement of a cold plasma.

4. INTERACTION OF ELECTRONS AND VACUUM ULTRAVIOLET RADIATION WITH GASES AND VAPORS

Electron and (more recently) photon impact has been used to study the thresholds for ionization and dissociative ionization, the phenomenon of autoionization, and the rates of chemical reactions in which reactants can be formed in well-defined energy states. From the point of view of chemical physics, these experiments yield precise values of ionization potentials, band-dissociation energies, and electron affinities. In addition, the rates of chemical reactions can be probed in a very specific manner by individually varying the internal energy state and/or the kinetic energy of the reactants. From the standpoint of molecular physics, the interaction of highly excited Rydberg states and quasi-discrete states with the underlying continua have been measured; and processes such as field ionization of high Rydberg states and passage of protons through potential barriers—both tunneling phenomena—have been explored. In summary, the aim is to define and characterize the various energy states of ions and molecules and to understand the rates of reaction of these species in well-defined states. In contrast to the chemical approach to the thermodynamics and kinetics of reactions (in which one looks at the statistical behavior of matter in bulk), the present investigations look at phenomena in individual molecules and ions.

Preliminary studies on the angular distribution of photoelectrons have yielded information on the symmetry of the orbitals from which electrons are ejected. Extensive investigations of this type are planned for the synchrotron storage ring, which provides an intense source of continuum radiation in the far ultraviolet.

A recent Argonne determination of the electron affinities of important atmospheric gases is expected to be of great significance in elucidating the negative-ion reactions which control the transmission and reflection of radio-frequency waves in the D and E layers of the ionosphere.

a. Photoionization Mass Spectroscopy of Gases

J. Berkowitz, W. A. Chupka, P. Guyon, J. Holloway,* and R. Spohr

The thresholds for various ionization processes in F_2 and HF have been measured, using a vacuum ultraviolet monochromator to select photon energies from a helium-continuum light source. The

*Chemistry Division.

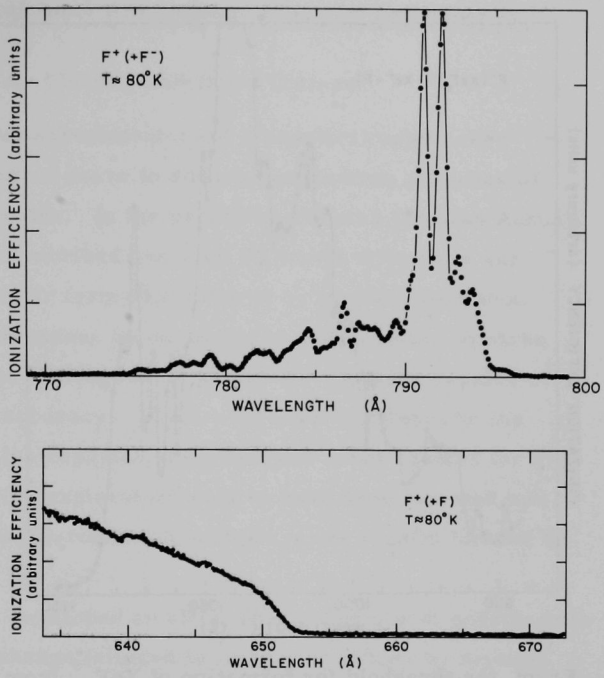

Fig. 63. The thresholds for ion-pair formation (above) and for dissociative ionization (below) in F_2 at 80°K.

thresholds for ion-pair formation and dissociative ionization in F_2 (Fig. 63) are consistent with a dissociation energy $D_0(F_2) = 1.59 \pm 0.01$ eV. For HF, the corresponding thresholds yield $D_0(HF) = 5.85 \pm 0.01$ eV, consistent with the results of Johns and Barrow.[1] Studies with DF have corroborated the results with HF. Both the F_2 and HF results are in significant disagreement with the conclusions reached in recently published photoionization experiments, although in each case the thermochemical combination of $D_0(F_2)$ and $D_0(HF)$ yields $\Delta H_f(HF)$ = 65 kcal/mole. In studies with XeF_2 (Fig. 64), a weak ion-pair process was observed, corresponding to the formation of $Xe^+ + F^- + F$. Its threshold yields the value $\Delta H_f(XeF_2) = -28.0 \pm 0.5$ kcal/mole. The value of ΔH_f for XeF_2^+ was readily obtained in the same experiment.

[1] J. W. C. Johns and R. F. Barrow, Nature 179, 374 (1957).

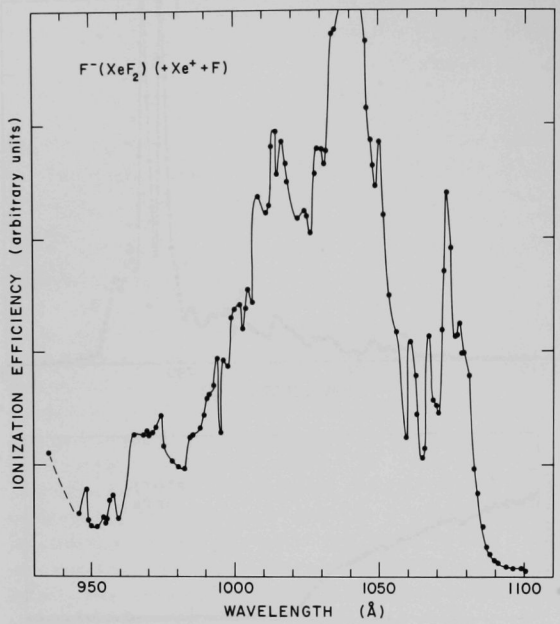

Fig. 64. The ion-pair process in XeF_2. The threshold for this process yields the heat of formation $\Delta H_f(XeF_2)$ and hence the energy of the Xe—F bond.

From the threshold for formation of XeF_2^+ from XeF_4, the value $\Delta H_{f_0}(XeF_4) = -57.9 \pm 1.5$ kcal/mole was then obtained. In a similar bootstrap fashion, the threshold for formation of XeF_4^+ from XeF_6 was used to deduce $\Delta H^0_{f_0}(XeF_6) = -79 \pm 3$ kcal/mole.

In a preliminary study of some gases of atmospheric interest, the ionization potential of ozone (O_3) was found to be 12.58 eV, and the appearance potential of NO_2^+ from HNO_3 to be 12.11 eV. The ionization potential of HNO_3 was determined to be 11.92 eV in the same set of experiments. Other properties of these atmospheric gases are described in Sec. IV. 4b.

Isotope effects in the ionization and dissociative ionization of formaldehyde (CH_2CO) are currently being explored.

b. Electron Affinities of Some Atmospheric Gases by Endothermic Charge Exchange

J. Berkowitz, W. A. Chupka, and David Gutman

Numerous experimental and theoretical approaches have been utilized in recent years to deduce the electron affinities of atoms and simple molecules. In the preceding Physics Division Annual Review (ANL-7620) we described one such technique utilized in our laboratory, that of ion-pair formation induced by photon absorption. The desired ion-pair processes do not occur in enough cases to make this a general approach, although it is potentially a method capable of yielding values of high accuracy. It has been used to determine the electron affinity of CN (as reported last year) and could be used for SH and OH, but our extensive exploratory studies have demonstrated that the negative ions of most diatomic molecules are not readily formed by this process.

We have developed an alternative technique of endothermic negative-ion charge exchange (alluded to last year) which can be used to obtain fairly accurate values for the electron affinities of simple molecules. In this technique, an atomic negative ion of known electron affinity is produced by ion-pair formation, and is then accelerated by a staircase voltage into a second chamber containing the molecule of interest. If endothermic charge transfer occurs, the negative ion of interest is mass analyzed and its intensity as a function of projectile energy is monitored by a multichannel analyzer. For the present study, the most convenient projectile ion was I^-, because of its relatively high production rate, its relatively low electron affinity (compared to other halogens), its well established electron affinity, and its favorable expansion of the energy scale in converting from laboratory to c.m.; and in addition, its ion-pair process occurs in a wavelength region that is free from other ionization processes that might yield background electrons.

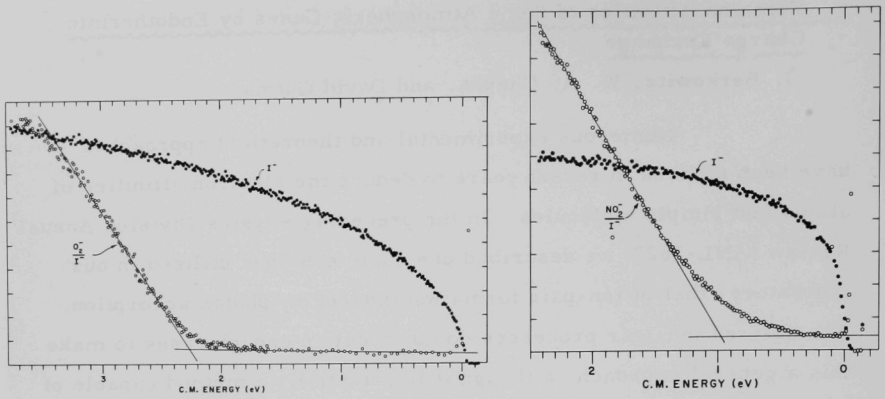

Fig. 65. The threshold behavior of the reactions $I^- + O_2 \rightarrow O_2^- + I$ (left) and $I^- + NO_2 \rightarrow NO_2^- + I$ (right). These plots show the intensity of the projectile ion I^- and the intensity ratios (O_2^-/I^-) and (NO_2^-/I^-) as a function of the energy available in the collision.

This technique was employed to study a number of atmospheric gases, whose electron affinities (as measured by a variety of methods) were still in great dispute. From studies of I^- impacting on O_2, O_3, NO, NO_2, and HNO_3, the following lower limits on the electron affinities (in eV) were obtained:

O_2	O_3	NO	NO_2	NO_3
0.73 ± 0.1	2.14 ± 0.1	0.23 ± 0.1	2.01 ± 0.2	2.68 ± 0.2

Figure 65 compares the threshold behavior of the reactions (a) $I^- + O_2 \rightarrow O_2 + I$ and (b) $I^- + NO_2 \rightarrow NO_2^- + I$. The tailing in reaction (b) clearly spans a larger energy range and is very likely attributable to variations in reaction cross section near threshold rather than to thermal contributions to tailing (as observed in the O_2 and other cases studied). The value measured for SO_2 was near zero, and CO and CO_2 yielded no detectable negative ions. These results are of importance in the unraveling of reactions in the upper atmosphere.

c. Determination of Electron Affinities of Halogen Molecules by Endoergic Charge Transfer

J. Berkowitz, W. A. Chupka, and D. Gutman

Ion-pair formation by photon absorption at threshold wavelengths has been used to prepare I^-, Br^-, Cl^-, and F^- ions with approximately room-temperature thermal energies. These ions have been accelerated and their reactions with halogen molecules studied at laboratory kinetic energies from 0.0 to 4.0 eV by use of the photoionization mass spectrometer. Thresholds were determined from endoergic reactions of the type $X^- + Y_2 \rightarrow X + Y_2^-$, where X may be the same as Y. As an example, the cross section for the reaction $I^- + I_2 \rightarrow I_2^- + I$ as a function of collision energy is shown in Fig. 66. At least two reactions were used for the determination of each electron affinity. The agreement was good in all cases. The preliminary values obtained for the electron affinities are:

F_2	Cl_2	Br_2	I_2
3.14 eV	2.55 eV	2.65 eV	2.71 eV

Interhalogen molecular ions such as IBr^- were also observed and some energies of formation were determined from reaction thresholds. The values of the electron affinities of the diatomic halogens are of importance to the understanding of color centers and other properties of halide crystals. They also enter prominently in the interpretation of experiments on the scattering of

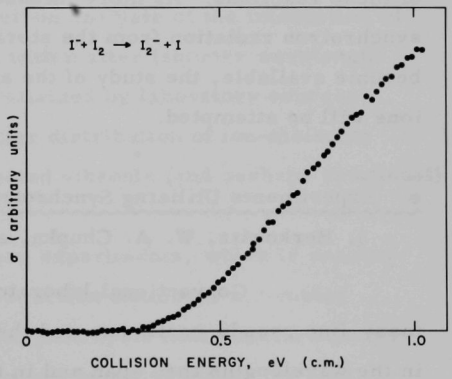

Fig. 66. Cross section σ as a function of collision energy near the threshold for the reaction $I^- + I_2 \rightarrow I_2^- + I$.

chemically reactive beams. Further experiments of this type will be carried out to determine the electron affinities of other molecules and to determine energies of formation of certain positive ions. The latter are not readily measured by other techniques.

d. Reactions of Ions in Prepared States

J. Berkowitz, W. A. Chupka, and D. Gutman

In earlier work (reported last year), pure preparations of H_2^+ ions in vibrational states from v = 0 to v = 5 were made by photoionization, and the cross sections for reaction with He and H_2 were measured as a function of both vibrational and kinetic energy. An apparatus with an ionization and collision chamber now being constructed will enable us to carry out these studies over a range of temperatures (at least from 78 to 300°K) in order to better control the rotational energy as well as the thermal translational energy of the reactants. In addition, the kinetic energy distribution of the product ions, which are scattered along the direction of motion of the center of mass, will be measured in order to help understand the mechanism of these reactions. As more intense sources of photons (such as synchrotron radiation from the storage ring in Stoughton, Wisconsin) become available, the study of the angular distributions of product ions will be attempted.

e. Experiments Utilizing Synchrotron Radiation

J. Berkowitz, W. A. Chupka, and R. N. Spohr

Conventional laboratory light sources (usually the hydrogen many-line pseudo-continuum and the helium continuum) are limited in the wavelengths they span and in their photon fluxes. Radiation from an electron synchrotron, which provides a continuum that becomes more intense in the extreme ultraviolet before its high-energy cutoff (ca. 50 Å for a 200-MeV synchrotron) has loomed as an attractive

source for a number of years, and has been used advantageously for ultraviolet absorption measurements. In the past, the radiation from conventional synchrotrons has not been intense enough to make studies of photoionization and photoelectron spectroscopy attractive. Recently, a synchrotron storage-ring complex has been put into operation at Stoughton, Wisconsin, and promises to increase the photon flux by at least two orders of magnitude. This now appears to make possible a number of experiments, including:

(1) Higher resolution studies of such fundamental processes as the autoionization of individual states of H_2, providing specific rates of autoionization to compare with theory.

(2) The photoelectron energy distribution produced by individual autoionizing states.

(3) The angular distribution of photoelectrons as a function of incident wavelength, with particular emphasis on autoionizing states.

(4) The photoionization efficiencies of molecular vapors which can be produced only in beams, because of either their instability or their nonvolatility.

(5) The photoelectron energy analysis of vapors produced in beams.

(6) The photoionization and photoelectron analysis of the interaction of extreme ultraviolet radiation with matter (shorter wavelength radiation than can be readily attained by laboratory sources).

(7) The detailed energetics and angular distribution of ion-molecule reactions resulting from selected vibronic (and perhaps rotational) states of ions.

The equipment for these experiments, which is nearing completion, includes an all-purpose reaction chamber, a 3-meter vacuum ultraviolet monochromator, a quadrupole mass spectrometer, and several designs of electron analyzers (intended either for high sensitivity or applicability to angular-distribution measurements), as well as attendant electronics. Preliminary measurements of the

synchrotron radiation indicate that a significant fraction of the above experiments should be within the capability of the equipment.

f. Kinetic Energy Distributions of Fragmentation Products

H. E. Stanton

The investigation of the kinetic energy liberated in the fragmentation of polyatomic molecules under electron impact was undertaken to check on existing theories of fragmentation, the mass distributions of the radicals and ions formed, and possibly their states of excitation after formation. Measurements have been made on the mass spectrometer MA-17. Values of these energies, as determined experimentally, have been subject to a large instrumental smearing which makes their interpretation difficult. Analytic methods have been devised to eliminate all of the known instrumental effects and determine the true laboratory kinetic-energy distribution of ions formed under electron impact in the mass spectrometer. Continued treatment of data by this process is expected to result in refinements in the theories of fragmentation.

5. INTERACTION BETWEEN PARTICLE BEAMS AND SOLIDS

When energetic charged particles penetrate through a monocrystalline solid, their trajectories can under certain conditions be influenced by the regular arrangement of the lattice atoms. In particular, they may be guided through the spaces between low-index lattice planes (planar channeling) or along the even more open channels in the low-index directions (axial channeling). In such cases, the impact parameters of successive collisions can become correlated (channeled) and their distribution is not random as in the case of motion through amorphous solids. In the experiments described below, it was of interest to study how the crystallographic orientation of the monocrystalline target with respect to the direction of the incident ion beam affects the yields from different secondary-emission phenomena (e.g., sputtering or secondary-electron emission) or primary processes (e.g., charge-changing collisions or the characteristic energy loss of an ion).

a. Atomic and Solid-State Effects Associated with the Penetration of Energetic Ions Through Solids

The group of experiments reported below is an attempt to understand the processes that take place when energetic ions (p, d, ^{3}He, α from the 2-MeV Van de Graaff) penetrate thin metal foils (Cu, Ni, Ag, Au, Mo, or W). Both monocrystalline and polycrystalline foils were used; in some cases they were magnetized. The energies of the incident ions were varied over the range from approximately 0.15 to 2.00 MeV.

In each of the experiments described below, the incident beam was highly collimated (angular spread $<0.01^\circ$) and its direction deviated less than 0.1° from one of the low-index directions of the monocrystal (e.g., the [100] direction) and was perpendicular (within 0.1°) to the surface of the polycrystalline targets. The energy spectrum of the beam emerging from a monocrystalline foil consisted of two well-separated peaks, the mean energy $\overline{E}_n$ of the lower one corresponding to the normal energy loss observed with polycrystalline targets while the mean energy $\overline{E}_{ch}$ of the high-energy peak reflects the reduced loss rate for channeled ions.

(i) Polarization of Particles by Channeling

M. Kaminsky

The angle between the directions of the intrinsic spins of a pair of interacting nuclear particles is one of the factors determining the force between them. Therefore studies of spin-dependent effects are essential in elucidating the nature of the nuclear force, and much effort has been expended in developing polarized sources. A new process for producing beams of polarized deuterons has recently been developed.[1]

In the new technique of producing a beam of polarized deuterons, the incident deuterons are directed parallel (within 0.1°) to the axial channeling directions of a monocrystalline nickel foil magnetized to saturation. If their energies are in an appropriate range, the deuterons capture polarized electrons from the nickel crystal

---

[1] M. Kaminsky, Phys. Rev. Letters 23, 819 (1969).

TABLE V. Values for the tensor polarization P_{zz} or P_{yy} as determined for the measured ratios $R_{\mu\nu} = r_{pol}/r_{unpol}$, where r_{pol} is the ratio of the counting rates at the two angles ϕ_μ and ϕ_ν for the polarized deuterons, and r_{unpol} is the corresponding ratio for the unpolarized deuterons.

Polarization direction	Detector angles ϕ_ν ϕ_μ	$R_{\mu\nu}$	Tensor polarization
∥ to ±z axis	ϕ_1 ϕ_2	+1.260 ± 0.010	P_{zz} = -0.32 ± 0.01
	ϕ_1 ϕ_3	+1.258 ± 0.010	P_{zz} = -0.32 ± 0.01
∥ to ±y axis	ϕ_1 ϕ_3	+0.787 ± 0.011	P_{yy} = -0.32 ± 0.01
	ϕ_2 ϕ_3	+0.852 ± 0.010	P_{yy} = -0.32 ± 0.01

(e.g., electrons in 3d states). The resulting deuterium atoms with their polarized electrons emerge from the crystal and subsequently pass through a weak magnetic field which maintains the direction of the electron polarization for a time long enough that the "hyperfine interaction" between the nucleus and the electron on an atom can bring the spin of the nucleus into alignment with that of the electron.

Experiments have demonstrated that this method produces good tensor polarizations P_{zz} (or P_{yy}) as can be seen in Table V. These values of P_{zz} (or P_{yy}) are higher than those attained in more standard techniques (such as the atomic-beam method). Furthermore, intensities of $\sim$500 nA/cm^2 of channeled deuterium atoms with polarized nuclei were obtained. It offers a simple and relatively inexpensive source of polarized ions for particle accelerators. A U.S. patent has been applied for.

The next step will be an attempt to increase the polarized-beam intensities by cooling the target foils, by somewhat relaxing the present requirements of strong collimation (half angle of divergence less than 0.01°) without a significant decrease in beam polarization, and by using films whose thicknesses are optimal for the deuteron

velocity ranges used. Another process deserving study is the conversion of the polarized neutral deuterium atoms into negative ions by passing the polarized D^0 beam through a thin monocrystalline "adder" foil. Further plans include an extension of these experiments to other particles (e.g., tritons, ^3He, etc.) and to monocrystalline targets of other ferromagnetic and paramagnetic materials (e.g., Gd, Tb, etc.).

(ii) Polarization of Particles by Small-Angle Scattering

M. Kaminsky

A new program has been initiated to determine if energetic ions (even heavy ions!) can be polarized by traversing a set of parallel small capillaries drilled through a foil of a magnetizable, monocrystalline material. The direction of the collimated primary ion beam is held nearly parallel to the long axis of the small capillaries, so the ions can experience a series of near-glancing collisions with the capillary walls. The monocrystalline foil is magnetized to saturation, with the axis of easy magnetization parallel to a low-index direction in the monocrystal and perpendicular to the long axis of the capillaries.

In a certain favorable range of primary-ion energies, the collision processes between the traversing ions and the channel walls in the magnetically saturated monocrystalline material will lead to the capture of polarized electrons and subsequently to an output of collimated polarized atoms. These polarized atoms, in turn, travel through a weak uniform magnetic field for a long enough time that part of the electron polarization is transferred to the nucleus of the moving atom by hyperfine interaction.

In comparison with polarization by channeling [Sec. IV. 5a(i)], this method promises to yield higher beam intensities and appears to facilitate the polarization of heavy ions. A U.S. patent has been applied for.

(iii) Effect of Foil Texture (Partial Lattice Order) on the Degree of Particle Channeling and on Particle Polarization

M. Kaminsky

This program, which was started early in 1970, deals with measurements of the degree of particle channeling and the degree of polarization for particles which have traversed either cold-rolled polycrystalline foils with various degrees of texture or monocrystalline foils with various types and degrees of lattice disorder (e.g., twinning, astigmatism, mosaic spread, etc.). Preliminary results indicate that a significant fraction of ions penetrating through cold-rolled polycrystalline foils with a certain degree of texture are being channeled, and that this leads to a significant reduction in the mean energy loss of the emerging particles.

Systematic studies of the influence of the degree of foil texture on the yields of channeled particles and the yields of polarized particles should reveal if it is possible to replace the high-quality monocrystalline foils used in polarizing a beam by channeling [Sec. IV. 5a(i)] with considerably less expensive, highly textured, cold-rolled polycrystalline foils. Furthermore, it appears that studies of transmission channeling (e.g., measurements of angular and energy distributions) can lead to the development of a very sensitive analytical tool which, used separately or in conjunction with more standard techniques (such as x-ray diffraction, electron scattering, etc.), will permit better characterization of the structural quality of solids.

(iv) Charge Distribution of Energetic Particles Emerging from Coated Foils

M. Kaminsky and K.-O. Groeneveld

A new program to study the charge distribution of energetic particles emerging from metal foils onto which impurity layers have been deposited under controlled conditions was initiated in 1969. These studies with coating layers of known thickness and composition

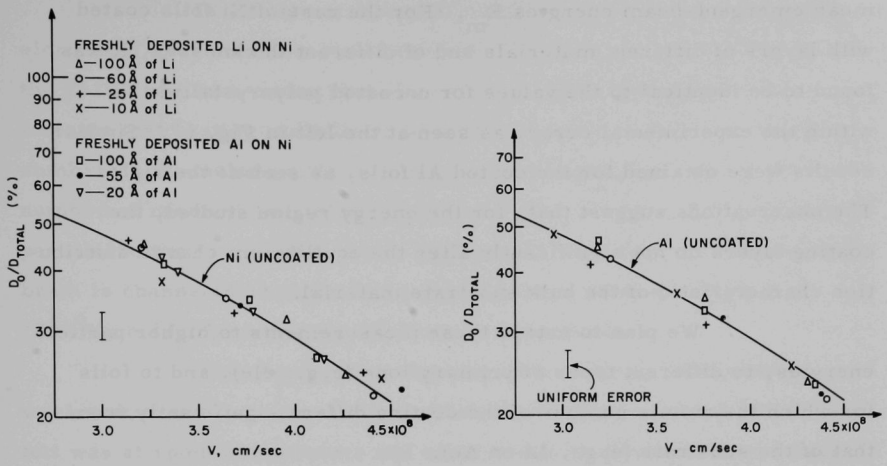

Fig. 67. Neutral fractions D_0 / D_{total} of deuterium particles emerging from uncoated foils and from foils freshly coated with metallic layers of different thicknesses, plotted as a function of the velocity v of the emergent particles. Left: Nickel substrates either uncoated (curve) or coated with a lithium layer of thickness 100 Å (•), 60 Å (o), 25 Å (+), or 10 Å (×) or with an aluminum layer of thickness 100 Å (□), 55 Å (Δ), or 20 Å (▽). Right: Aluminum substrates either uncoated (curve) or coated with a lithium layer of thickness 110 Å (□), 20 Å (Δ), or 15 Å (•) or with an aluminum layer of thickness 525 Å (×), 20 Å (+), or 10 Å (o). The curves for the two uncoated substrates are virtually identical.

are designed to resolve an existing controversy over the question whether or not "impurity" layers on target foils can influence the equilibrium charge states of the emerging particles.

In a first set of experiments, the equilibrium charge distribution of deuterium particles emerging from polycrystalline Ni or Al foils coated with Li or Al or KCl layers has been measured for average emergent-beam energies $\overline{E}_m$ = 100—200 keV under high-vacuum conditions. The thickness of the layers which were vacuum deposited onto the exit side of the foils ranged from approximately 20 Å to 1200 Å. The emergent particles were analyzed electrostatically and R(emergent beam) = $D^0 / (D^0 + D^+)$ was determined for different

mean emergent-beam energies $\overline{E}_m$. For the case of Ni foils coated with layers of different materials and of different thicknesses, R was found to be identical to the values for uncoated polycrystalline Ni within the experimental error, as seen at the left in Fig. 67. Similar results were obtained for the coated Al foils, as seen at the right. The observations suggest that, for the energy region studied, the coating layers do not significantly alter the equilibrium charge distribution characteristic of the bulk substrate material.

We plan to extend these measurements to higher particle energies, to different types of primary ions (e.g., He), and to foils for which the atomic number of the coating differs significantly from that of the substrate (e.g., Li on Au).

(v) Effect of Foil Temperature on Channeling Phenomena

M. Kaminsky

Studies of the influence of thermal vibrations of lattice atoms on the trajectories of axial- or planar-channeled particles in monocrystalline metal foils were started in 1969 in order to elucidate some of the basic processes underlying the channeling mechanism. The experiments are being conducted for a range of ion energies and foil temperatures in which the value of the root-mean-square displacement of the vibrating lattice atoms is nearly equal to or larger than the distance of closest approach of the ion to a particular "channel wall." (In axial channeling, this wall would be a continuous "row potential wall"; in planar channeling, it would be a continuous "planar potential wall.") Under these conditions, the trajectories of the channeled particles appear to be significantly influenced by the vibration of the lattice atoms; and these alterations in the trajectories are reflected in changes in the transmission of channeled ions and in the charge-changing collisions and the angular distributions of both channeled and randomly scattered particles. Little or no information had been available on such effects.

In a first set of experiments, deuterons were channeled along the [111] axis in a monocrystalline Mo foil and protons along the [110] axis in a monocrystalline W foil. Preliminary results indicate that heating the foils results in a significant decrease in the number of channeled particles and a corresponding increase in the number of randomly scattered particles. For example, for D^+ incident parallel to the [111] axis in Mo, approximately 80% of the transmitted beam is channeled when the foil temperature is about 300°K; but at 1700°K, only approximately 8% remained channeled.

The angular distributions of the transmitted particles were also measured at a number of foil temperatures. Both when the foil was at room temperature and when it was at elevated temperatures, the angular distributions of randomly scattered particles closely approximated a Gaussian. For channeled particles emerging from a foil at room temperature, the angular distribution was almost Gaussian except for a slight deviation near zero scattering angle; but as the foil temperature was raised, the distribution became increasingly non-Gaussian.

These transmission and angular-distribution experiments and the more recent investigations of charge-changing collisions are being continued vigorously. Such measurements will be facilitated by the purchase of position-sensitive detectors, the conversion of an existing multichannel analyzer into a two-dimensional analyzer, and the link-up to an on-line computer.

(vi) Effect of Channeling on Charge-Changing Collisions

M. Kaminsky

This program, which was started in 1968, deals with measurements of the equilibrium charge distribution of energetic ions penetrating through polycrystalline or monocrystalline metal foils. In the past, most studies of charge-changing collisions were conducted in gaseous targets and in a few polycrystalline solid targets. Information

on light ions ($Z \leq 2$) penetrating through metal monocrystalline foils was completely lacking, though such studies promise to yield information on the way in which the electron density distribution in the lattice (and especially along certain lattice channels) affects the process of electron capture and electron loss by the penetrating ions. The development of an adequate energy-loss theory for energetic ions would be greatly aided by such information.

In recent experiments, the distribution of charge states of hydrogen particles emerging from monocrystalline or polycrystalline W foils of various thicknesses was measured under ultrahigh-vacuum conditions for particles emerging with energies in the range 0.10—0.40 MeV. For example, (1) the particles emerging from a W(110) foil were electrostatically analyzed according to their charge state and (2) in order to study the channeling effect on the electron-capture reaction $H^+ + e \rightarrow H^0$, the ratio R^*(emergent beam) = $H^0/(H^0 + H^+)$ was determined. While the values of R^* (normalized to equal emergent energy) for the randomly scattered beam are nearly identical to those for a polycrystalline foil, they are larger than those obtained for the channeled beam. This result is in qualitative agreement with our previous observation of a channeling effect on the electron-capture process $D^+ + e \rightarrow D^0$ in Ni(110) and suggests a lower electron-capture probability for ions traversing and escaping from regions of lower electron density (e.g., the centers of lattice channels).

This program will be continued. The projected studies include measurements of the formation of negative ions (important for operation of the tandem Van de Graaff), the dependence of R^* on the crystallographic orientation of the monocrystalline foil (e.g., on the angle of incidence and on the exposure of different axial channels by using foils whose surfaces are parallel to different crystal planes), on the target material, on impurity layers (electron donor materials) deposited on monocrystalline foils, on the type of incident ion, on the foil temperature, and on the scattering angle of the emergent particles.

Planned improvements of the apparatus include construction of a better electrostatic analyzer (with well-regulated power supplies) and modification of the vacuum system to facilitate opening and closing the system.

(vii) Preparation of Thin Monocrystalline Metal Foils

M. Kaminsky, K. -O. Groeneveld, and R. Waldhauser

In order to provide the monocrystalline target foils needed for the measurements listed in this Sec. IV. 5a, we have continued with an extensive development program.

Thin wafers ($\frac{1}{2} \times \frac{1}{2} \times 0.001$ in.) were cut from monocrystalline blocks of Ni, Mo, and W by eloxing (done in Metallurgy) and were further thinned by repeated electropolishing and etching. Many of the well known etching solutions could not be used to thin our monocrystalline wafers because of preferential etching along certain crystallographic planes, leading often to pinholes. Therefore different polishing and etching solutions were developed for the various materials, and thinning procedures were established in order to obtain thin homogeneous foils with the desired high degree of monocrystallinity. We were able to obtain foils with usable areas of approximately 10 mm^2 and a thickness of approximately 0.00 008 in.

Since thinner foils could not readily be obtained by this method, we started a new program of growing thin monocrystalline films epitaxially. We are in the process of installing a 270° electron beam gun, a film-thickness monitor, and a deposition-rate meter in our ultrahigh-vacuum bell jar. With this new equipment we plan to start our research on the epitaxial growth of monocrystalline metal films and on the production of "sandwich foils" (in which impurity layers of, say, donor materials are deposited on thin metal foils).

b. Emission of Secondary Particles from Metal Surfaces under Energetic Neutron and Photon Impact

M. Kaminsky

Our studies of various phenomena associated with secondary-particle emission from metal surfaces under energetic ion impact will be extended to the cases of energetic neutron and photon impact. Such studies are fundamental for a better understanding of the production mechanism of internal secondary particles (e.g., the displacement collisions are caused primarily by inelastic collisions in the case of MeV ions but by elastic collisions in the case of MeV neutrons); and they are also of central importance in evaluating the feasibility of large D-T fusion reactors.

Much of this essential information is completely lacking. For example, the sputtering yields for 14-MeV neutrons incident on materials suggested for use as vacuum walls for fusion reactors (e.g., such metals as Nb, Ta, and Be) have not been measured experimentally. Rough theoretical estimates indicate that these yields could easily range from 0.001 to 0.010 atom/neutron. Since the vacuum wall is expected to be exposed to neutron fluxes as high as 4×10^{14} neutrons/cm^2/sec, the sputtering by neutrons alone could lead to intolerable contamination of the plasma and erosion of the vacuum wall—and this would be accompanied, of course, by the sputtering by deuterium, tritium, and α particles.

There is a similar lack of information on the extent of secondary processes occurring under the extreme conditions envisioned during operation of the fusion reactor. These processes would include the simultaneous impact of large fluxes of energetic neutral atoms, neutrons, and photons (from bremsstrahlung and synchrotron radiation) on vacuum walls at operating temperatures in the neighborhood of 1000°C.

It is anticipated that during the next year a significant amount of time will have to be devoted to the design and construction of new equipment for this work, and to extensive modifications of existing experimental equipment. Examples are the design of an intense source of 14-MeV neutrons and of massive shielding around the target chamber.

c. Operation of the 2-MeV Van de Graaff Accelerator

Jack R. Wallace

The 2-MeV Van de Graaff accelerator has operated 1202 hours from 1 April 1969 to 20 March 1970. It is operated only one shift per day, 5 days per week. It was not used in the period from September to December because of the lack of a trained technician. No major changes in the facility have been made during this period.

V. PUBLICATIONS FROM 1 APRIL 1969 THROUGH 31 MARCH 1970

The papers listed here are those whose publication was noted by the reporting unit of the Laboratory in the 1-year period stated above. The dates on the journals therefore often precede this period, and some dated within the period will be listed subsequently. The list of "journal articles and book chapters," which also includes letters and notes, is classified by topic; the arrangement is approximately that followed in the Table of Contents of this Annual Review. The "reports at meetings" include abstracts, summaries, and full texts in volumes of proceedings; they are listed chronologically.

A. PUBLISHED JOURNAL ARTICLES AND BOOK CHAPTERS

1. SEARCH FOR CHEMICALLY BOUND NEUTRONS
   V. E. Krohn, G. J. Perlow, G. R. Ringo, and S. L. Ruby
   Phys. Rev. Letters 23, 1475-1476 (29 December 1969)

2. DELBRÜCK SCATTERING OF 10.8-MeV γ RAYS
   H. E. Jackson and K. J. Wetzel
   Phys. Rev. Letters 22, 1008-1010 (12 May 1969)

3. RECOIL BROADENING OF SECONDARY TRANSITIONS IN NEUTRON-CAPTURE GAMMA-RAY CASCADES
   K. J. Wetzel
   Phys. Rev. 181, 1465-1476 (20 May 1969)

4. ABSENCE OF RECOIL DOPPLER BROADENING OF THE 3367-keV TRANSITION FOLLOWING THE REACTION $^{9}Be(n_{th},\gamma)^{10}Be$
   K. J. Wetzel
   Phys. Rev. 186, 1292-1293 (20 October 1969)

5. PRECISION DETERMINATION OF THE D-T NEUTRON SEPARATION ENERGY
   W. V. Prestwich and G. E. Thomas
   Phys. Rev. 180, 945-947 (20 April 1969)

6. NEUTRON RESONANCES OF Mo ISOTOPES
   Hla Shwe and R. E. Coté
   Phys. Rev. 179, 1148-1153 (20 March 1969)

7. $Ge^{73}(n,\gamma)Ge^{74}$ GAMMA-RAY SPECTRUM AND ENERGY LEVELS OF Ge^{74}
   A. P. Magruder and R. K. Smither
   Phys. Rev. 183, 927-944 (20 July 1969)

8. NEUTRON-CAPTURE GAMMA-RAY STUDIES OF THE LEVEL STRUCTURE OF THE Te^{124} NUCLEUS
   D. L. Bushnell, R. P. Chaturvedi, and R. K. Smither
   Phys. Rev. 179, 1113-1133 (20 March 1969)

9. LEVEL SCHEME OF ^{153}Sm BASED ON (n,γ), (n,e^-), AND β-DECAY EXPERIMENTS
   R. K. Smither, E. Bieber, T. von Egidy,* W. Kaiser,* and K. Wien†
   Phys. Rev. 187, 1632-1671 (20 November 1969)

10. REVIEW OF "I. I. GUREVICH AND L. V. TARASOV, LOW-ENERGY NEUTRON PHYSICS"‡
    Roy Ringo
    Am. Scientist 57, 239A (Autumn 1969)

11. ELECTROMAGNETIC TRANSITION STRENGTHS IN Pb^{206}, Pb^{207}, AND Pb^{208} FROM THRESHOLD PHOTONEUTRON CROSS-SECTION MEASUREMENTS
    C. D. Bowman,§ B. L. Berman,§ and H. E. Jackson
    Phys. Rev. 178, 1827-1836 (20 February 1969)

12. POLARIZATION AND DIFFERENTIAL CROSS SECTION FOR NEUTRONS SCATTERED FROM ^{12}C
    R. O. Lane, R. D. Koshel,‖ and J. E. Monahan
    Phys. Rev. 188, 1618-1625 (20 December 1969)

13. LIFETIMES OF EXCITED STATES OF V^{51}, Ni^{61}, Ga^{69}, As^{75}, Br^{79}, Rb^{85}, AND Sb^{123}
    E. N. Shipley, R. E. Holland, and F. J. Lynch
    Phys. Rev. 182, 1165-1168 (20 June 1969)

---

*Physik-Department der Technischen Hochschule München, Germany.

†Institut für Technischen Kernphysik der Technischen Hochschule Darmstadt, Germany.

‡Interscience Publishers, New York, 1968.

§Lawrence Radiation Laboratory, University of California, Livermore, California.

‖Ohio University, Athens, Ohio.

14. OPTICAL-MODEL ANALYSIS OF NUCLEON SCATTERING FROM 1p-SHELL NUCLEI BETWEEN 10 AND 50 MeV
B. A. Watson, P. P. Singh,* and R. E. Segel
Phys. Rev. 182, 977-989 (20 June 1969)

15. INELASTIC SCATTERING OF PROTONS FROM B^{10} BETWEEN 5 AND 16.5 MeV
B. A. Watson, R. E. Segel, J. J. Kroepfl,* and P. P. Singh*
Phys. Rev. 187, 1351-1364 (20 November 1969)

16. DISTORTED-WAVE ANALYSIS OF THE $^{11}B(d,p)$ REACTION LEADING TO THE LOWEST UNBOUND LEVEL IN ^{12}B
H. T. Fortune and C. M. Vincent
Phys. Rev. 185, 1401-1403 (20 September 1969)

17. PROPERTIES OF THE 3.39-MeV STATE IN B^{12}
F. P. Mooring, J. E. Monahan, and R. E. Segel
Phys. Rev. 178, 1612-1615 (20 February 1969)

18. STUDY OF THE $Al^{27}(He^3,p)Si^{29}$ AND $Al^{27}(He^3,p\gamma)Si^{29}$ REACTIONS
L. Meyer-Schützmeister, D. S. Gemmell, R. E. Holland, F. T. Kuchnir, H. Ohnuma, and N. G. Puttaswamy
Phys. Rev. 187, 1210-1219 (20 November 1969)

19. ENERGY LEVELS IN ^{33}P
G. Hardie, R. E. Holland, L. Meyer-Schützmeister, F. T. Kuchnir, and H. Ohnuma
Nucl. Phys. A134(3), 673-685 (1969)

20. COULOMB ENERGIES—AN ANOMALY IN NUCLEAR MATTER RADII
J. A. Nolen, Jr., and J. P. Schiffer
Phys. Letters 29B(7), 396-398 (23 June 1969)

21. ON COULOMB ENERGIES, THE ANOMALOUS ISOTOPE SHIFT OF NUCLEAR RADII, AND CORE POLARIZATION BY THE NEUTRON EXCESS
J. P. Schiffer, J. A. Nolen, Jr., and N. Williams
Phys. Letters 29B(7), 399-401 (23 June 1969)

22. COULOMB ENERGIES
J. A. Nolen, Jr.,† and J. P. Schiffer
Ann. Rev. Nucl. Sci. 19, 471-526 (1969)

---

*Indiana University, Bloomington, Indiana.

†University of Maryland, College Park, Maryland.

23. POSSIBLE SPIN DEPENDENCE IN PROTON INELASTIC SCATTERING
J. C. Legg* and J. L. Yntema
Phys. Rev. Letters 22, 1005-1008 (12 May 1969)

24. OBSERVATION OF THE $(g_{9/2})^2$ MULTIPLET IN Nb^{90} VIA THE (He^3,t) REACTION
R. C. Bearse, J. R. Comfort, J. P. Schiffer, M. M. Stautberg, and J. C. Stoltzfus
Phys. Rev. Letters 23, 864-866 (13 October 1969)

25. MULTIPOLE ANALYSIS OF PARTICLE-PARTICLE OR PARTICLE-HOLE MULTIPLETS
M. Moinester,† J. P. Schiffer, and W. P. Alford†
Phys. Rev. 179, 984-995 (20 March 1969)
Erratum: Phys. Rev. 185, 1598 (20 September 1969)

26. REVIEW OF "R. S. NELSON, THE OBSERVATION OF ATOMIC COLLISIONS IN CRYSTALLINE SOLIDS"‡
R. E. Holland
Am. Scient. 57 (No. 3), 253A (1969)

27. TEST OF THE BARSHAY-TEMMER THEOREM FOR THE REACTION $^{10}B + \alpha \rightarrow {}^7Li + {}^7Be$
H. T. Fortune, A. Richter, and B. Zeidman
Phys. Letters 30B(3), 175-178 (29 September 1969)

28. $B^{11}(He^3,\alpha)B^{10}$ REACTION AT 33 MeV
D. Dehnhard, N. Williams, and J. L. Yntema
Phys. Rev. 180, 967-970 (20 April 1969)

29. STUDY OF THE $^{39}K(d,t)^{38}K$ REACTION AT E_d = 23 MeV
H. T. Fortune, N. G. Puttaswamy, and J. L. Yntema
Phys. Rev. 185, 1546-1552 (20 September 1969)

30. (d,t) AND (d,He^3) REACTIONS ON THE CALCIUM ISOTOPES
J. L. Yntema
Phys. Rev. 186, 1144-1160 (20 October 1969)

31. STUDY OF THE $Zr^{94}(He^3,d)Nb^{95}$ REACTION
H. Ohnuma and J. L. Yntema
Phys. Rev. 179, 1211-1213 (20 March 1969)

---

*Kansas State University, Manhattan, Kansas.

†Nuclear Structure Research Laboratory, University of Rochester, Rochester, New York.

‡North-Holland Publishing Company and John Wiley & Sons, 1969.

32. STUDY OF THE J DEPENDENCE IN THE (d, He^3) REACTION
H. Ohnuma and J. L. Yntema
Phys. Rev. 178, 1654-1662 (20 February 1969)

33. EXPERIMENTAL STUDY OF THE (d,t) REACTION ON EVEN-MASS Mo ISOTOPES
H. Ohnuma and J. L. Yntema
Phys. Rev. 178, 1855-1863 (20 February 1969)

34. (d,p) AND (d,t) REACTION STUDIES OF THE ACTINIDE ELEMENTS. I. U^{235}
T. H. Braid, R. R. Chasman (Chemistry), J. R. Erskine, and A. M. Friedman (Chemistry)
Phys. Rev. C1, 275-289 (January 1970)

35. LIFETIME OF THE 11-keV LEVEL IN Cs^{134}
F. J. Lynch and L. E. Glendenin (Chemistry)
Phys. Rev. 186, 1250-1252 (20 October 1969)

36. LEVEL STRUCTURE OF LOW-LYING EXCITED STATES OF Ga^{66} POPULATED BY THE DECAY OF 2.2-h Ge^{66}
H. H. Bolotin and D. A. McClure
Phys. Rev. 180, 987-996 (20 April 1969)

37. DISTRIBUTION OF CHARGE IN Th^{232} AND U^{238} DETERMINED BY MEASUREMENTS ON MUONIC x RAYS
R. E. Coté, W. V. Prestwich, A. K. Gaigalas,* S. Raboy,* C. C. Trail,† R. A. Carrigan, Jr.,‡ P. D. Gupta,‡ R. B. Sutton,‡ M. N. Suzuki,‡ and A. C. Thompson‡
Phys. Rev. 179, 1134-1147 (20 March 1969)

38. SHELL-MODEL MATRIX ELEMENTS FROM A REALISTIC POTENTIAL
R. D. Lawson and J. M. Soper§
Nucl. Phys. A133(2), 473-480 (1969)

39. AN APPROXIMATION SCHEME FOR CONTINUUM SHELL-MODEL CALCULATIONS
William Romo
Nucl. Phys. A142, 300-320 (1970)

---

*State University of New York at Binghamton, New York.

†Brooklyn College, The City University of New York, Brooklyn, New York.

‡Carnegie-Mellon University, Pittsburgh, Pennsylvania.

§Weizmann Institute of Science, Rehovoth, Israel and U.K.A.E.A., Harwell, Didcot, Berks., England.

40. TWO-NUCLEON TRANSFER IN THE 1p SHELL
S. Cohen and D. Kurath
Nucl. Phys. A141(1), 145-157 (1970)

41. ANALOGS AND THE RESONANCE RENAISSANCE
M. H. Macfarlane and J. P. Schiffer
Comments on Nuclear and Particle Physics 3(5), 141-146 (September-October 1969)

42. NUCLEAR MODELS
David R. Inglis
Phys. Today 22(6), 29-40 (June 1969)

43. A DIELECTRIC FLUID DROP IN AN ELECTRIC FIELD
C. E. Rosenkilde
Proc. Roy. Soc. (London) A312, 473-494 (1969)

44. THEORY OF NUCLEAR LEVEL DENSITY FOR PERIODIC INDEPENDENT-PARTICLE ENERGY-LEVEL SCHEMES
Peter B. Kahn* and Norbert Rosenzweig
Phys. Rev. 187, 1193-1200 (20 November 1969)

45. LEVEL DENSITY OF A FERMI SYSTEM: NONPERIODIC PERTURBATIONS OF THE ENERGY-LEVEL SCHEME
Peter B. Kahn† and N. Rosenzweig
J. Math. Phys. 10, 707-715 (April 1969)

46. DISPERSION OF ATOMIC GYROMAGNETIC RATIOS—APPROACH TO STATISTICAL EQUILIBRIUM
N. Rosenzweig and B. G. Wybourne (Chemistry)
Phys. Rev. 180, 33-44 (5 April 1969)

47. CORRECTIONS TO THE HARTREE-FOCK APPROXIMATION FOR HOMOGENEOUS NUCLEAR MATTER
James J. MacKenzie
Phys. Rev. 179, 1002-1010 (20 March 1969)

48. FOUR-HOLE-LINE DIAGRAMS IN NUCLEAR MATTER
B. D. Day
Phys. Rev. 187, 1269-1302 (20 November 1969)

49. PRESYMMETRY. II
H. Ekstein
Phys. Rev. 184, 1315-1337 (25 August 1969)

---

*State University of New York, Stony Brook, New York.

†State University of New York, Stony Brook, New York and Weizmann Institute of Science, Rehovoth, Israel.

50. MAGNETIC CHARGE QUANTIZATION AND ANGULAR MOMENTUM
H. J. Lipkin,* W. I. Weisberger,* and M. Peshkin
Ann. Phys. (N.Y.) 53, 203-214 (June 1969)

51. GRAVITY-INDUCED ELECTRIC FIELD NEAR A CONDUCTOR
Murray Peshkin
Phys. Letters 29A(4), 181-182 (5 May 1969)

52. REVIEW OF "J. E. LYNN, THE THEORY OF NEUTRON RESONANCE REACTIONS"†
J. E. Monahan
Science Progress 57, 278-279 (Summer 1969)

53. CONDUCTIVITY AND MÖSSBAUER MEASUREMENTS IN DOPED ICE
I. Pelah (Solid State Science) and S. L. Ruby
J. Chem. Phys. 51, 383-387 (1 July 1969)

54. MÖSSBAUER EFFECT OF ^{129}I IN PYRIDINE COMPLEXES OF IODINE MONOHALIDES
C. I. Wynter,‡ J. Hill,‡ W. Bledsoe,‡ G. K. Shenoy (Solid State Science), and S. L. Ruby
J. Chem. Phys. 50, 3872-3874 (1 May 1969)

55. CHANGE IN NUCLEAR RADIUS UPON EXCITATION FOR ^{119}Sn, ^{121}Sb, ^{125}Te, ^{127,129}I, AND ^{129}Xe FROM MÖSSBAUER ISOMER SHIFTS
S. L. Ruby and G. K. Shenoy (Solid State Science)
Phys. Rev. 186, 326-331 (10 October 1969)

56. HYPERFINE ANOMALY IN ^{193}Ir BY THE MÖSSBAUER EFFECT, AND ITS APPLICATION TO DETERMINATION OF THE ORBITAL PART OF HYPERFINE FIELDS
G. J. Perlow, W. Henning, D. Olson, and G. L. Goodman (Chemistry)
Phys. Rev. Letters 23, 680-682 (29 September 1969)

57. THE COMPUTATION OF MÖSSBAUER SPECTRA, II
John R. Gabriel (Applied Mathematics) and Duane Olson
Nucl. Instr. Methods 70(2), 209-212 (15 April 1969)

---

*Weizmann Institute of Science, Rehovoth, Israel.

†Oxford University Press, New York, 1968.

‡A & T State University of North Carolina, Greensboro, North Carolina.

58. MAGNETIC MOMENT OF THE FIRST EXCITED STATE IN ^{83}Kr BY THE MÖSSBAUER EFFECT
L. E. Campbell, G. J. Perlow, and M. A. Grace*
Phys. Rev. 178, 1728-1731 (20 February 1969)

59. MÖSSBAUER EFFECT IN 7.2-yr Ba^{133}
A. J. F. Boyle and G. J. Perlow
Phys. Rev. 180, 625-626 (10 April 1969)

60. NUCLEAR GAMMA-RAY RESONANCE STUDY OF HYPERFINE INTERACTIONS IN ^{238}U
S. L. Ruby, G. M. Kalvius (Solid State Science), B. D. Dunlap (Solid State Science), G. K. Shenoy (Solid State Science), D. Cohen (Chemistry), M. B. Brodsky (Metallurgy), and D. J. Lam (Metallurgy)
Phys. Rev. 184, 374-380 (10 August 1969)

61. MÖSSBAUER ISOMER SHIFT IN ^{243}Am
G. M. Kalvius (Solid State Science), S. L. Ruby, B. D. Dunlap (Solid State Science), G. K. Shenoy (Solid State Science), D. Cohen (Chemistry), and M. B. Brodsky (Metallurgy)
Phys. Letters 29B(8), 489-490 (21 July 1969)

62. HYPERFINE STRUCTURE AND g_J VALUES OF LOW LEVELS OF ^{159}Tb
W. J. Childs and L. S. Goodman
J. Opt. Soc. Am. 59, 875 (July 1969)

63. HIGH-FREQUENCY FIELDS IN SOLENOIDAL COILS
N. Contaxes† and Albert J. Hatch
J. Appl. Phys. 40, 3548-3550 (August 1969)

64. PHOTOELECTRON SPECTROSCOPY OF AUTOIONIZATION PEAKS
J. Berkowitz and W. A. Chupka
J. Chem. Phys. 51, 2341-2354 (15 September 1969)

65. HIGH-RESOLUTION PHOTOIONIZATION STUDY OF THE H_2 MOLECULE NEAR THRESHOLD
W. A. Chupka and J. Berkowitz
J. Chem. Phys. 51, 4244-4268 (15 November 1969)

66. MASS-SPECTROMETRIC STUDY OF THE PHOTOIONIZATION OF C_2F_4 AND CF_4
T. A. Walter, C. Lifshitz, W. A. Chupka, and J. Berkowitz
J. Chem. Phys. 51, 3531-3536 (15 October 1969)

*Nuclear Physics Laboratory, Oxford University, England.

†Illinois Institute of Technology, Chicago, Illinois.

67. PHOTOIONIZATION OF HIGH-TEMPERATURE VAPORS. V. CESIUM HALIDES; CHEMICAL SHIFT OF AUTOIONIZATION
J. Berkowitz
J. Chem. Phys. 50, 3503-3512 (15 April 1969)

68. PHOTOIONIZATION OF HIGH-TEMPERATURE VAPORS. VI. S_2, Se_2, AND Te_2
J. Berkowitz and W. A. Chupka
J. Chem. Phys. 50, 4245-4250 (15 May 1969)

69. POLARIZATION OF CHANNELED PARTICLES
M. Kaminsky
Phys. Rev. Letters 23, 819-822 (13 October 1969)

B. PUBLISHED LECTURE SERIES

Boulder Summer School on "Quantum Liquids and Nuclear Structure," University of Colorado, Boulder, 8-19 July 1968

1. THE GROUND STATE OF HOMOGENEOUS NUCLEAR MATTER AND THE FOUNDATION OF THE NUCLEAR SHELL MODEL
F. Coester
Quantum Fluids and Nuclear Matter, edited by K. T. Mahanthappa and W. E. Brittin, Lectures in Theoretical Physics, Vol. XI-B (Gordon and Breach, Science Publishers, New York, 1969), pp. 157-186

International School of Physics "Enrico Fermi," Varenna, 26 June-15 July 1967

2. THE REACTION MATRIX IN NUCLEAR SHELL THEORY
Malcolm H. Macfarlane
Proceedings of the International School of Physics "Enrico Fermi," Course XL: Nuclear Structure and Nuclear Reactions, edited by M. Jean and R. A. Ricci (Academic Press, New York, 1969), pp. 457-510

C. PUBLISHED REPORTS AT MEETINGS

International Symposium on Contemporary Physics, Trieste, Italy, 7-28 June 1968

1. DISTRIBUTION OF ENERGY-LEVEL SPACINGS AND CONSERVATION LAWS
   N. Rosenzweig
   Contemporary Physics: Trieste Symposium 1968 (International Atomic Energy Agency, Vienna, 1969), Vol. II, pp. 381-390

Meteorite Research (proceedings of the IAEA symposium, Vienna, 7-13 August 1968), edited by Peter M. Millman (D. Reidel Publishing Company, Dordrecht, Holland, 1969)

2. MÖSSBAUER INVESTIGATION OF THE UNEQUILIBRATED ORDINARY CHONDRITES
   E. L. Sprenkel-Segel
   pp. 93-105

Proceedings for the Skytop Conference on Computer Systems in Experimental Nuclear Physics, Skytop, Pennsylvania, 3-6 March 1969 (Clearinghouse for Federal Scientific and Technical Information, Springfield, Virginia, 1969), CONF-690301, EANDC(U.S.) 121u, Physics (TID-4500)

3. AUTOMATIC COUNTING OF TRACKS IN NUCLEAR EMULSIONS
   John R. Erskine and Robert H. Vonderohe (Applied Mathematics Division)
   pp. 434-445

4. EXPERIENCE WITH A MULTI-COMPUTER MULTI-EXPERIMENT SYSTEM
   D. S. Gemmell
   pp. 37-53

5. ARGONNE COMPUTER-CONTROLLED SCATTERING CHAMBER
   J. L. Yntema
   pp. 321-325

1969 Particle Accelerator Conference—Accelerator Engineering and Technology, Washington, D.C., 5-7 March 1969

6. A LOW POWER MAGNETIC CHANNEL WITH DIPOLE COMPENSATION
   T. Khoe (Accelerator Division), R. Benaroya (Chemistry), J. J. Livingood, W. J. Ramler (Chemistry), and W. Wesolowski (Chemistry)
   IEEE Trans. Nucl. Sci. NS-16 (No. 3), Part I, 495-499 (June 1969)

Nuclear Isospin (Proceedings of the Conference, Asilomar, Pacific Grove, California, 13-15 March 1969), edited by John D. Anderson, Stewart D. Bloom, Joseph Cerny, and William W. True (Academic Press, Inc., New York, 1969)

7. CLOSING REMARKS
   David R. Inglis
   pp. 789-796

8. ANALOG RESONANCES IN HEAVIER NUCLEI (RAPPORTEUR'S REMARKS)
   Malcolm H. Macfarlane
   pp. 591-622

9. PROTON-INDUCED ANALOG RESONANCES
   George C. Morrison
   pp. 435-480

10. AN EXPERIMENTAL TEST OF THE BARSHAY-TEMMER THEOREM VIA THE REACTIONS $^{10}B(\alpha,{}^{7}Li_{gs})^{7}Be_{gs}$ AND $^{10}B(\alpha,{}^{7}Be_{gs})^{7}Li_{gs}$
    A. Richter, H. T. Fortune, and B. Zeidman
    pp. 825-830
    + Bull. Am. Phys. Soc. 14, 965 (October 1969)

11. COULOMB ENERGIES
    J. P. Schiffer
    pp. 733-755

12. SINGLE-PARTICLE ANALOG-STATE ANOMALIES IN THE SCATTERING OF PROTONS FROM Au^{197}, Pt^{196}, AND W^{184}
    J. P. Schiffer, P. Kienle, and G. C. Morrison
    pp. 679-684
    + Bull. Am. Phys. Soc. 14, 964 (October 1969)

Nuclear Isospin (cont'd.)

13. COMPARISON OF SPECTROSCOPIC FACTORS FROM (p,p_0) AND (d,p) REACTIONS ON BARIUM ISOTOPES
N. Williams, D. von Ehrenstein, J. A. Nolen, Jr., and G. C. Morrison
pp. 695-700
+ Bull. Am. Phys. Soc. 14, 964 (October 1969)

American Physical Society, Washington, D.C., 28 April-1 May 1969

14. DIRECT REACTIONS ON Be^{10}
D. L. Auton, B. Zeidman, H. T. Fortune, J. P. Schiffer, and R. C. Bearse
Bull. Am. Phys. Soc. 14, 489 (April 1969)

15. STATES OF Ho^{166} FROM AVERAGE RESONANCE CAPTURE IN $Ho^{165}(n,\gamma)Ho^{166}$
L. M. Bollinger and G. E. Thomas
Bull. Am. Phys. Soc. 14, 514-515 (April 1969)

16. ACCURATE METHOD OF DETERMINING COUNTING LOSSES IN NUCLEAR RADIATION DETECTION SYSTEMS
H. H. Bolotin, M. G. Strauss (Electronics), and D. A. McClure
Bull. Am. Phys. Soc. 14, 532 (April 1969)

17. PRIMARY GAMMA RAYS IN Sm^{150} FOLLOWING AVERAGE NEUTRON RESONANCE CAPTURE
D. J. Buss and R. K. Smither
Bull. Am. Phys. Soc. 14, 514 (April 1969)

18. HIGHLY EXCITED STATES IN C^{12}, N^{14}, AND O^{16} FROM Li-INDUCED REACTIONS ON B^{10} AND C^{12}
J. R. Comfort, H. T. Fortune, G. C. Morrison, and B. Zeidman
Bull. Am. Phys. Soc. 14, 507 (April 1969)

19. STUDY OF (α,t) REACTIONS ON 1p-SHELL NUCLEI
H. T. Fortune, D. Dehnhard, R. H. Siemssen, and B. Zeidman
Bull. Am. Phys. Soc. 14, 487 (April 1969)

20. DELBRÜCK EFFECT IN ELASTIC SCATTERING OF 10.8-MeV γ RAYS
H. E. Jackson and K. J. Wetzel
Bull. Am. Phys. Soc. 14, 607 (April 1969)

APS, Washington, D.C. (cont'd.)

21. ISOMER SHIFT OF THE NUCLEAR γ-RAY RESONANCE (NGR) IN ^{243}Am
G. M. Kalvius (Solid State Science), S. L. Ruby, B. D. Dunlap (Solid State Science), G. K. Shenoy (Solid State Science), D. Cohen (Chemistry), and M. B. Brodsky (Metallurgy)
Bull. Am. Phys. Soc. 14, 521 (April 1969)

22. LIFETIME OF THE 11-keV LEVEL IN Cs^{134m}
F. J. Lynch and L. E. Glendenin (Chemistry)
Bull. Am. Phys. Soc. 14, 629 (April 1969)

23. STUDY OF THE (He^3,d) REACTION FOR A ≈ 31
Richard A. Morrison
Bull. Am. Phys. Soc. 14, 567 (April 1969)

24. COULOMB ENERGIES AND NUCLEAR RADII
J. A. Nolen, Jr.,* and J. P. Schiffer
Bull. Am. Phys. Soc. 14, 584 (April 1969)

25. O^{16} ELASTIC SCATTERING FROM $Mg^{24,26}$ AND $Si^{28,30}$
R. H. Siemssen, H. T. Fortune, J. L. Yntema, and A. Richter
Bull. Am. Phys. Soc. 14, 548-549 (April 1969)

26. AVERAGE RESONANCE CAPTURE IN Cd^{113}
R. K. Smither, D. J. Buss, L. M. Bollinger, and G. E. Thomas
Bull. Am. Phys. Soc. 14, 513 (April 1969)

27. STATES OF Pd^{106} FROM AVERAGE RESONANCE CAPTURE IN $Pd^{105}(n,\gamma)Pd^{106}$
G. E. Thomas and L. M. Bollinger
Bull. Am. Phys. Soc. 14, 515 (April 1969)

28. COMPUTER-CONTROLLED MULTIPLE-DETECTOR SYSTEM FOR HEAVY-ION SCATTERING EXPERIMENTS
J. W. Tippie (Applied Mathematics), J. Bicek, H. T. Fortune, R. H. Siemssen, and J. L. Yntema
Bull. Am. Phys. Soc. 14, 533 (April 1969)

29. METHOD FOR DWBA CALCULATION OF STRIPPING TO UNBOUND STATES
C. M. Vincent and H. T. Fortune
Bull. Am. Phys. Soc. 14, 572 (April 1969)

*University of Maryland, College Park, Maryland.

APS, Washington, D.C. (cont'd.)

30. METHOD FOR DETERMINING SPINS OF NEUTRON RESONANCES
K. J. Wetzel, G. E. Thomas, L. M. Bollinger, and H. E. Jackson
Bull. Am. Phys. Soc. 14, 513 (April 1969)

31. ANGULAR DISTRIBUTIONS OF HEAVY IONS PRODUCED BY ^{3}He BOMBARDMENT OF ^{12}C
B. Zeidman and H. T. Fortune
Bull. Am. Phys. Soc. 14, 507 (April 1969)

Proceedings of the International Conference on Hypernuclear Physics, edited by A. R. Bodmer and L. G. Hyman (High Energy Physics Division, Argonne National Laboratory, Argonne, Illinois, 5-7 May 1969)

32. Λ-PARTICLE BINDING IN NUCLEAR MATTER
A. R. Bodmer and D. M. Rote*
Vol. II, pp. 521-597

Fifteenth Annual Meeting of the American Nuclear Society, Mathematics and Computation Division, Seattle, Washington, 15-19 June 1969

33. A SYSTEMS APPROACH TO THE NUCLEAR SHELL MODEL
Stanley Cohen
Trans. Am. Nucl. Soc. 12(1), 147 (June 1969)

Conference on Computational Physics, Culham Laboratory, Abingdon, Berkshire, England, 28 July-1 August 1969

34. A SYSTEMS APPROACH TO THE NUCLEAR SHELL MODEL
S. Cohen
Computational Physics, Vol. 1: Invited Papers (UKAEA Culham Laboratory, Abingdon, Berkshire, England, 1969), Report No. CLM-CP (1969), Session VII, pp. H1-H17

Physics and Chemistry of Fission, Proceedings of the Second IAEA Symposium, Vienna, 28 July-1 August 1969 (International Atomic Energy Agency, Vienna, 1969)

35. SHORT-LIVED SPONTANEOUSLY FISSIONING ISOMERS IN NEUTRON-INDUCED FISSION
A. J. Elwyn and A. T. G. Ferguson†
pp. 457-460

---

*University of Illinois, Chicago, Illinois.

†A. E. R. E., Harwell, Berks., England.

Sixth International Conference on the Physics of Electronic and Atomic Collisions, Cambridge, Massachusetts, 28 July-2 August 1969, Abstracts of Papers (Massachusetts Institute of Technology, Cambridge, Massachusetts, 1969)

36. PHOTOELECTRON SPECTROSCOPY OF AUTOIONIZATION PEAKS
J. Berkowitz and W. A. Chupka
p. 192

37. A STUDY OF SOME REACTIONS OF H_2^+ IN SELECTED VIBRATIONAL STATES
W. A. Chupka, J. Berkowitz, and M. E. Russell
p. 71

Neutron Capture Gamma-Ray Spectroscopy, Proceedings of the International Symposium, Studsvik, Sweden, 11-15 August 1969 (International Atomic Energy Agency, Vienna, 1969)

38. THERMAL-NEUTRON CAPTURE GAMMA-GAMMA COINCIDENCE STUDIES AND TECHNIQUES
H. H. Bolotin
pp. 15-34

39. LEVEL STRUCTURE OF LOW-LYING EXCITED STATES OF ^{187}W
H. H. Bolotin and D. A. McClure
pp. 389-402

40. USE OF AVERAGE-RESONANCE-CAPTURE MEASUREMENTS FOR NUCLEAR SPECTROSCOPY
R. K. Smither and L. M. Bollinger
pp. 601-605

41. RECENT IMPROVEMENTS IN THE ARGONNE 7.7-m BENT-CRYSTAL SPECTROMETER
R. K. Smither and D. J. Buss
pp. 55-63

42. LOW-LYING ROTATIONAL BANDS IN ^{153}Sm
R. K. Smither and T. von Egidy*
pp. 355-358

---

*Physikdepartment der Technischen Hochschule, München, Germany.

American Physical Society, Hawaii, 2-4 September 1969

43. EFFECT OF CHANNELING ON THE CHARGE-CHANGING COLLISIONS OF ENERGETIC DEUTERONS PENETRATING THROUGH Ni(110) MONOCRYSTALS
M. Kaminsky
Bull. Am. Phys. Soc. 14, 846 (August 1969)

158th American Chemical Society Meeting, New York, 8-12 September 1969

44. A SURVEY OF SINGLE PARTICLE AND COLLECTIVE STATES IN THE ACTINIDES BY USE OF TRANSFER REACTIONS
A. M. Friedman (Chemistry), J. R. Erskine, T. H. Braid, and R. R. Chasman (Chemistry)
Abstracts of Papers, NUCL-77

1969 Meeting of the Division of Nuclear Physics of the American Physical Society, Boulder, Colorado, 30 October-1 November 1969

45. ASSIGNMENT OF $J^{\pi} = \frac{3}{2}^{-}$ FOR THE 8.1-MeV STATE IN ^{11}C
J. R. Comfort, H. T. Fortune, J. V. Maher, and B. Zeidman
Bull. Am. Phys. Soc. 14, 1213 (December 1969)

46. COMPARISON OF SPECTROSCOPIC FACTORS FOR MIRROR STATES POPULATED IN THE (d,t) AND (d,He^3) REACTIONS ON Si^{28}
H. T. Fortune, J. V. Maher, G. C. Morrison, and B. Zeidman
Bull. Am. Phys. Soc. 14, 1201 (December 1969)

47. CHARGE DISTRIBUTION OF DEUTERIUM PARTICLES EMERGING FROM COATED FOILS
K. O. Groeneveld and M. Kaminsky
Bull. Am. Phys. Soc. 14, 1246 (December 1969)

48. Mg^{26}(d,He^3)Na^{25} REACTION AT 23 MeV
J. V. Maher, G. C. Morrison, H. T. Fortune, and B. Zeidman
Bull. Am. Phys. Soc. 14, 1200-1201 (December 1969)

49. INFLUENCE OF THE ^{7}Be FORM FACTOR ON CALCULATIONS OF ANGULAR DISTRIBUTIONS FOR THE $^{12}C(^3He,^7Be)^8Be$ REACTION
P. Neogy,* H. T. Fortune,* W. Scholz,* and B. Zeidman
Bull. Am. Phys. Soc. 14, 1226 (December 1969)

*University of Pennsylvania, Philadelphia, Pennsylvania.

Nuclear Physics Division, APS (cont'd.)

50. ACTIVATION CROSS SECTIONS FOR THE REACTIONS $^{19}F(\pi^-,\pi^-n)^{18}F$ AND $^{31}P(\pi^-,\pi^-n)^{30}P$ AT THE (3,3) RESONANCE
H. S. Plendl,* K. A. Eberhard,* D. Burch,* M. Kirby,* C. J. Umbarger,* A. Richter, and W. P. Trower†
Bull. Am. Phys. Soc. 14, 1241 (December 1969)

51. ENERGY DEPENDENCE OF ^{3}He-^{58}Ni INELASTIC SCATTERING BETWEEN 27 AND 84 MeV
B. W. Ridley,‡ T. H. Braid, and T. W. Conlon‡
Bull. Am. Phys. Soc. 14, 1219 (December 1969)

52. THE $Ti^{46,48}(He^3,p\gamma)V^{48,50}$ REACTIONS
J. W. Smith, L. Meyer-Schützmeister, G. Hardie,§ and P. P. Singh‖
Bull. Am. Phys. Soc. 14, 1233 (December 1969)

53. STATES OF $^{156,158}Gd$ FROM AVERAGE RESONANCE CAPTURE IN $^{155,157}Gd(n,\gamma)^{156,158}Gd$
G. E. Thomas and L. M. Bollinger
Bull. Am. Phys. Soc. 14, 1237 (December 1969)

54. NUCLEON PICKUP REACTIONS ON ^{46}Ca
J. L. Yntema
Bull. Am. Phys. Soc. 14, 1201 (December 1969)

55. $Al^{27}(d,p)Al^{28}$ REACTION AT 23 MeV
B. Zeidman, J. V. Maher, H. T. Fortune, and G. C. Morrison
Bull. Am. Phys. Soc. 14, 1201 (December 1969)

1969 Meeting of the Division of Plasma Physics of the American Physical Society, Los Angeles, California, 12-15 November 1969

56. COMPUTER SIMULATION OF RADIOFREQUENCY CONFINEMENT OF A CHARGED PARTICLE
Albert J. Hatch and J. L. Shohet
Bull. Am. Phys. Soc. 14, 1024 (November 1969)

---

*The Florida State University, Tallahassee, Florida.

†Virginia Polytechnic Institute, Blacksburg, Virginia.

‡A. E. R. E., Harwell, England.

§Western Michigan University, Kalamazoo, Michigan.

‖Indiana University, Bloomington, Indiana.

American Physical Society, Chicago, 26-29 January 1970

57. HYPERFINE AND ZEEMAN STUDIES OF THE $4f^{10}6s^2$ ^5I GROUND TERM OF $Dy^{161-164}$
W. J. Childs and L. S. Goodman
Bull. Am. Phys. Soc. 15, 46 (January 1970)

58. T=1 STATES IN THE MASS-12 SYSTEM
H. T. Fortune, J. E. Monahan, C. M. Vincent, and R. E. Segel
Bull. Am. Phys. Soc. 15, 35 (January 1970)

59. ISOMER SHIFTS OF ROTATIONAL STATES OF THE $K=\frac{1}{2}^-$, [521] BAND IN ^{171}Yb
W. Henning, G. M. Kalvius (Solid State Science), and G. K. Shenoy (Solid State Science)
Bull. Am. Phys. Soc. 15, 107 (January 1970)

60. SCATTERING OF N FROM ^{16}O
R. Malmin,* P. P. Singh,* and R. H. Siemssen
Bull. Am. Phys. Soc. 15, 36 (January 1970)

61. AN INTRASHELL COLLECTIVE STATE ABOVE THE PAIRING GAP IN ^{136}Ba
R. A. Meyer,† G. C. Morrison, and R. D. Griffioen†
Bull. Am. Phys. Soc. 15, 74-75 (January 1970)

62. THE RELATIVE GAMMA-RAY STRENGTH FUNCTIONS OF ^{199}Au AND Ta
W. V. Prestwich and L. M. Bollinger
Bull. Am. Phys. Soc. 15, 87 (January 1970)

63. RADIATIVE CAPTURE THROUGH THE ^{38}Ar GIANT DIPOLE RESONANCE
R. E. Segel, L. Meyer-Schützmeister, D. S. Gemmell, R. C. Bearse, N. G. Puttaswamy, H. T. Fortune, J. V. Maher, and E. L. Sprenkel-Segel
Bull. Am. Phys. Soc. 15, 47 (January 1970)

64. ENERGY LEVELS IN ^{148}Sm AND ^{150}Sm
R. K. Smither and D. J. Buss
Bull. Am. Phys. Soc. 15, 86 (January 1970)

---

*Indiana University, Bloomington, Indiana.

†Lawrence Radiation Laboratory, Livermore, California.

Symposium on Reactions of Organic Ions in a Mass Spectrometer, American Chemical Society, Houston, Texas, 22-27 February 1970

65. STUDIES OF ION-MOLECULE REACTIONS BY PHOTOIONIZATION TECHNIQUES
W. A. Chupka, J. Berkowitz, and M. E. Russell
Abstracts of Papers, PETR-105

American Physical Society, Dallas, 23-26 March 1970

66. HYPERFINE MAGNETIC FIELDS IN USb FROM MÖSSBAUER SPECTROSCOPY
S. L. Ruby, G. K. Shenoy (Solid State Science), B. D. Dunlap (Solid State Science), G. M. Kalvius (Solid State Science), Moshe Kuznietz (Solid State Science), and F. P. Campos (Materials Science)
Bull. Am. Phys. Soc. 15, 261 (March 1970)

D. ANL TOPICAL REPORTS

1. MIDWEST TANDEM CYCLOTRON—a Proposal for a Regional Accelerator Facility
Chemistry and Physics Staff
Argonne National Laboratory Topical Report ANL-7582 (June 1969)

2. HARTREE-FOCK SELF-CONSISTENT FIELD CALCULATIONS FOR IRIDIUM
L. W. Panek and G. J. Perlow
Argonne National Laboratory Topical Report ANL-7631 (November 1969)

E. PHYSICS DIVISION INFORMAL REPORTS

1. AN INTRODUCTION TO SPEAKEASY
   S. Cohen and C. M. Vincent
   Physics Division Informal Report PHY-1968E (December 1968)

2. PROTON-INDUCED ANALOG RESONANCES
   George C. Morrison
   Physics Division Informal Report PHY-1969C (April 1969)

3. ANALOG RESONANCES IN HEAVIER NUCLEI
   Malcolm H. Macfarlane
   Physics Division Informal Report PHY-1969D (June 1969)

4. LOW-LYING LEVELS IN SOME SPHERICAL AND ROTATIONAL NUCLIDES BY COULOMB EXCITATION AND RADIATIVE CAPTURE OF THERMAL NEUTRONS
   Donald A. McClure
   Physics Division Informal Report PHY-1969E (August 1969)
   Ph.D. Thesis, University of Missouri - Rolla (August 1969)

5. AN AUTOMATIC NUCLEAR-EMULSION SCANNER
   John R. Erskine and R. H. Vonderohe (Applied Mathematics Division)
   Physics Division Informal Report PHY-1969F (December 1969)

VI. STAFF MEMBERS OF THE PHYSICS DIVISION

The Physics Division staff for the year ending 31 March 1970 is listed below. Although the members are classified by programs, it must be understood that many of them work in two or more of the areas. In such cases, the classification indicates only the current primary interest.

In the period from 1 April 1969 through 31 March 1970, there were 34 temporary staff members and visitors (20 staff members from universities and other laboratories and 14 postdoctoral fellows), 17 graduate students (including 13 doing thesis research), and 29 undergraduates (2 Senior Thesis Students, 5 in the Argonne Semester program of the Associated Colleges of the Midwest, 5 co-op technicians, 10 CSUI-ANL Honor Students, and 7 on summer appointments).

SLOW-NEUTRON PHYSICS

Permanent Scientific Staff

†Lowell M. Bollinger, Ph. D., Cornell University, 1951

Herbert H. Bolotin, Ph. D., Indiana University, 1955

S. Bradley Burson, Ph. D., University of Illinois, 1946

Harold E. Jackson, Jr., Ph. D., Cornell University, 1959

Victor E. Krohn, Ph. D., Case-Western Reserve University, 1952

G. R. Ringo, Ph. D., University of Chicago, 1940

Robert K. Smither, Ph. D., Yale University, 1956

George E. Thomas, Jr., B. A., Illinois Wesleyan University, 1943

Temporary Scientific Staff

*Duane J. Buss, Ph. D., University of Notre Dame, 1966

*Karl J. Wetzel, Ph. D., Yale University, 1965

---

*No longer at Argonne as of 31 March 1970.

†Director of Physics Division.

Technical Staff

Charles H. Batson

*Jeanette M. Ebl

Visitors

*David L. Bushnell, Ph. D., Virginia Polytechnic Institute, 1961
(On leave from Northern Illinois University, DeKalb, Illinois)

Harry G. Miller, Ph. D., Ohio State University, 1963
(On leave from Defiance College, Defiance, Ohio)

Graduate Students

*Paul J. Dawson (RSA, summer, Illinois Institute of Technology)

*Donald A. McClure (AUA-ANL Predoctoral Fellow, University of Missouri at Rolla)

FAST-NEUTRON REACTIONS

Permanent Scientific Staff

Alexander J. Elwyn, Ph. D., Washington University, 1956

†Carl T. Hibdon, Ph. D., Ohio State University, 1944

Alexander Langsdorf, Jr., Ph. D., Massachusetts Institute of Technology, 1937

F. P. Mooring, Ph. D., University of Wisconsin, 1951

Temporary Scientific Staff

W. Gene Stoppenhagen, Ph. D., Ohio University, 1968

CHARGED-PARTICLE REACTIONS

Permanent Scientific Staff

*Robert C. Bearse, Ph. D., Rice University, 1964

---

*No longer at Argonne as of 31 March 1970.

†Retired on 31 August 1969.

Thomas H. Braid, Ph. D., Edinburgh University, 1950

John R. Erskine, Ph. D., University of Notre Dame, 1960

Donald S. Gemmell, Ph. D., Australian National University, 1960

Robert E. Holland, Ph. D., University of Iowa, 1950

Frank J. Lynch, B. S., University of Chicago, 1944

Luise Meyer-Schützmeister, Ph. D., Technical University of Berlin, 1943

George C. Morrison, Ph. D., University of Glasgow, 1957

†John P. Schiffer, Ph. D., Yale University, 1954

‡Ralph E. Segel, Ph. D., Johns Hopkins University, 1955

Rolf H. Siemssen, Ph. D., University of Hamburg, 1963

J. L. Yntema, Ph. D., Free University of Amsterdam, 1952

Benjamin Zeidman, Ph. D., Washington University, 1957

Temporary Scientific Staff

*Donald R. Abraham, M. S., University of Wyoming, 1963
(On leave from Kansas State University)

George B. Beard, Ph. D., University of Michigan, 1955
(On leave from Wayne State University, Detroit, Michigan)

Joseph R. Comfort, Ph. D., Yale University, 1968

*H. T. Fortune, Ph. D., Florida State University, 1967

James V. Maher, Jr., Ph. D., Yale University, 1969

Achim Richter, Ph. D., University of Heidelberg, 1967
(On leave from Max-Planck-Institut für Kernphysik, Heidelberg)

James W. Smith (AUA-ANL Predoctoral Fellow, Indiana University)

*Joseph C. Stoltzfus, Ph. D., University of Iowa, 1961
(On leave from Beloit College)

Technical Staff

John Bicek

William F. Evans

Elliot S. Silber

Elizabeth A. Sutter

---

*No longer at Argonne as of 31 March 1970.

†Associate Director of Physics Division. Joint appointment with University of Chicago.

‡Joint appointment with Northwestern University.

*Rosemary Sutter

James N. Worthington

Visitors

*Paul Kienle, Ph. D., Technische Hochschule München, 1957
(On leave from Technische Hochschule München, Germany)

*James C. Legg, Ph. D., Princeton University, 1962
(On leave from Kansas State University)

*Roeland O. Roos
(On leave from University of Mexico, Mexico City, D. F.)

Margaret M. Stautberg, Ph. D., University of Colorado, 1966
(Research participant from DePaul University, Chicago, Illinois)

Graduate Students

*David L. Auton (SA, thesis, University of Chicago)

Douglas J. Crozier (AUA-ANL Predoctoral Fellow, University of Chicago)

Hsiang Fan (RSA, University of Chicago)

Ronald E. Malmin (AUA-ANL Predoctoral Fellow, Indiana University)

Jeffrey M. Moller (RSA, University of Chicago)

*Richard A. Morrison (SA, thesis, University of Chicago)

Richard Rapids (RSA, University of Chicago)

George H. Wedberg, Jr. (AUA-ANL Predoctoral Fellow, Indiana University)

Abdelhadi S. Yousef (Guest Fellow, thesis, Illinois Institute of Technology)

DEVELOPMENT OF EQUIPMENT AND ACCELERATORS

Permanent Scientific Staff

David C. Hess, Ph. D., University of Chicago, 1949

†John J. Livingood, Ph. D., Princeton University, 1929

---

*No longer at Argonne as of 31 March 1970.

†Emeritus.

[†] Dieter von Ehrenstein, Ph. D., University of Heidelberg, 1960

Jack R. Wallace, B.A., College of Wooster, 1942

GAMMA- AND BETA-RAY SPECTROSCOPY

Permanent Scientific Staff

[‡] G. T. Wood, Ph. D., Washington University, 1956

ATOMIC-BEAM STUDIES

Permanent Scientific Staff

William J. Childs, Ph. D., University of Michigan, 1956

Leonard S. Goodman, Ph. D., University of Chicago, 1952

Henry E. Stanton, Ph. D., University of Chicago, 1944

Technical Staff

John A. Dalman

MÖSSBAUER STUDIES

Permanent Scientific Staff

Gilbert J. Perlow, Ph. D., University of Chicago, 1940

Richard S. Preston, Ph. D., Yale University, 1954

Stanley Ruby, B.A., Columbia University, 1947

[†] Joint appointment with Northern Illinois University, DeKalb, Illinois.

[‡] Resident Associate since October 1969.

Technical Staff

Bruce J. Zabransky

Visitors

*Lawrence E. Conroy, Ph. D., Cornell University, 1955
(On leave from University of Minnesota)

*Hendrik DeWaard, Ph. D., University of Groningen, Netherlands, 1954
(On leave from University of Groningen)

Esther L. Segel, Ph. D., University of Rochester, 1959
(Research participant from Illinois Institute of Technology)

*John G. Stevens, Ph. D., North Carolina State University, 1969
(On leave from University of North Carolina at Asheville)

THEORETICAL PHYSICS

Permanent Scientific Staff

†Arnold R. Bodmer, Ph. D., Manchester University, 1953

‡Fritz Coester, Ph. D., University of Zurich, 1944

Stanley Cohen, Ph. D., Cornell University, 1955

Benjamin Day, Ph. D., Cornell University, 1963

Hans Ekstein, Ph. D., University of Berlin, 1934

*David R. Inglis, Ph. D., University of Michigan, 1931

§Dieter Kurath, Ph. D., University of Chicago, 1951

Robert D. Lawson, Ph. D., Stanford University, 1953

‖Malcolm H. Macfarlane, Ph. D., University of Rochester, 1959

James E. Monahan, Ph. D., St. Louis University, 1953

---

*No longer at Argonne as of 31 March 1970.

†Joint appointment with University of Illinois, Chicago Circle Campus.

‡Joint appointment with University of Iowa, Iowa City, Iowa.

§On leave at State University of New York at Stony Brook (September 1969—July 1970).

‖Joint appointment with University of Chicago.

†Murray Peshkin, Ph. D., Cornell University, 1951

Norbert Rosenzweig, Ph. D., Cornell University, 1951

Temporary Scientific Staff

Alan L. Goodman, Ph. D., University of California, Berkeley, 1969

William J. Romo, Ph. D., University of Wisconsin, 1967

*Agam P. Shukla, Ph. D., Princeton University, 1967

C. Martin Vincent, Ph. D., University of the Witwatersrand, 1966

Visitors

*Thomas T. S. Kuo, Ph. D., University of Pittsburgh, 1964
(On leave from State University of New York at Stony Brook)

*Kiuck Lee, Ph. D., Florida State University, 1955
(On leave from Marquette University, Milwaukee, Wisconsin)

*Harry J. Lipkin, Ph. D., Princeton University, 1950
(On leave from Weizmann Institute of Science)

*Igal Talmi, Dr. Sc. Nat., Swiss Federal Institute of Technology, Zurich, 1952 (On leave from Weizmann Institute of Science)

Graduate Students

Peter Chien (Guest Fellow, thesis, University of Illinois, Chicago Circle Campus)

David H. Gloeckner (AUA-ANL Predoctoral Fellow, University of Chicago)

Richard N. Kimmel (AUA-ANL Predoctoral Fellow, University of Chicago)

Nimai C. Mukhopadhyay (RSA, thesis, University of Chicago)

Stanley Skupsky (Guest Fellow, thesis, University of Chicago)

INTERACTION OF ELECTRONS AND PHOTONS WITH GASES

Permanent Scientific Staff

Joseph Berkowitz, Ph. D., Harvard University, 1955

---

*No longer at Argonne as of 31 March 1970.

†Associate Director of Physics Division.

William A. Chupka, Ph. D., University of Chicago, 1951

Temporary Scientific Staff

David Gutman, Ph. D., University of Illinois, 1965
(On leave from Illinois Institute of Technology)

Paul-Marie Guyon, Ph. D., Faculté des Sciences Orsay, 1969
(On leave from Laboratoire de Collisions Electroniques, Orsay, Essone, France)

Reimar N. Spohr, Ph. D., The Swedish Filosofie Licentiat, 1968

*Theodore A. Walter, Ph. D., Harvard University, 1967

Technical Staff

Warren T. Jivery

INTERACTION OF PARTICLE BEAMS WITH SOLIDS

Permanent Scientific Staff

Manfred S. Kaminsky, Ph. D., University of Marburg, Germany, 1957

Temporary Scientific Staff

Karl-Ontjes E. Groeneveld, Ph. D., University of Frankfurt, 1966
(On leave from Institut für Kernphysik Frankfurt, Germany)

PLASMA PHYSICS

Permanent Scientific Staff

Albert J. Hatch, M. S., University of Illinois, 1947

---

*No longer at Argonne as of 31 March 1970.

ADMINISTRATIVE

Permanent Scientific Staff

†Charles Eggler, B.S., Virginia Polytechnic Institute, 1944

†Francis E. Throw, Ph.D., University of Michigan, 1940

---

†Assistant Director of Physics Division.